

POLITECNICO DI TORINO

Corso di Laurea Magistrale
In Ingegneria Biomedica

Tesi di Laurea Magistrale

Assessing the performance of community face coverings



Relatore

Prof. Paolo Tronville

Correlatore

Prof.ssa Valeria Chiono

Candidato

Jesús Alejandro Marval Díaz

Anno Accademico 2019/2020

Table of Contents

DEDICATIONS.....	8
1. ABSTRACT.....	9
2. INTRODUCTION.....	10
2.1. Transmission of infectious diseases by virus.....	11
2.1.1. How does a virus spread?	11
2.1.2. Risk factors enhancing disease emergence and transmission	14
2.1.3. Preventing the transmission of infectious diseases.....	15
2.1.4. Droplet and airborne particle transmission and its prevention by face masks .	16
2.2. Face masks to prevent airborne infectious disease transmission.....	18
2.2.1. Types of face masks and their properties	18
2.3. Particle size distribution of bioaerosol produced by humans.....	23
2.4. Test methods for face masks for controlling airborne contamination	29
2.4.1. Surgical masks	30
2.4.2. Personal protective equipment for respiratory tract	32
2.4.3. Community face coverings.....	35
2.5. Aim of the work.....	35
3. MATERIAL AND METHODS.....	37
3.1. Innovative test method for assessing performance of community face coverings..	37
3.1.1. Description of the test rig	37
3.1.2. Qualification tests of the test rig.....	45
3.1.3. Resistance to airflow	46
3.1.4. Size-resolved efficiency	47
3.2. Tested samples description	49
4. EXPERIMENTAL DATA AND DISCUSSION	51
4.1. Comparison of performance of woven vs non-woven.....	52
4.2. Correlation between resistance to airflow and filtration efficiency	54
4.3. Proposed classification	58
4.4. Rating by using a reference particle size distribution	61
5. CONCLUSIONS.....	62
6. ACKNOWLEDGMENTS.....	63
7. REFERENCES.....	64
Appendix A. AIRBORNE PARTICLE CHARACTERIZATION	71

A.1. Particle size, shape, and density.....	71
A.2. Optical, aerodynamic, electrical diameter.	73
A.3. Aerosol concentration	73
Appendix B. PARTICLE SIZE STATISTICS.....	74
B.1. Properties of size distributions.....	74
Appendix C. AIR FILTRATION.....	77
C.1. Surface filtration vs. Deep filtration	77
C.2. Quality factor	77
C.3. Deposition mechanisms	77
C.3.1. Interception.....	77
C.3.2. Inertial impaction	78
C.3.3. Diffusion	78
C.3.4. Electrostatic attraction.....	78
Appendix D. Scanning electron microscope figures of layers of face masks made up of woven and non-woven materials.....	80

Table of Figures

Figure 1. SARS-CoV-2. Note the spikes that adorn the outer surface of the virus, which impart the look of a corona surrounding the virion. Image created at the Centers for Disease Control and Prevention (CDC) [6].	10
Figure 2. Possible transmission routes of respiratory viral infection between an infected individual and a susceptible host [17].	12
Figure 3. Settling of droplets under different respiratory patterns [24].	13
Figure 4. Different transmission routes of infectious diseases [14].	13
Figure 5. Potential types of aerosol-generating medical procedures (AGMP). AGMPs are classified in two types: (1) procedures that induce the patient to produce aerosols and (2) procedures that mechanically generate aerosols by themselves [44].	17
Figure 6. Face masks reduce airborne transmission. No masking maximizes exposure, while universal masking results in lower exposure [47].	17
Figure 7. Surgical mask made up of three layers of material (the two external ones of spunbond material and the inner one of meltblown material).	18
Figure 8. Scanning electron microscope images (SEM) of Non-woven (at the left) vs. Woven (at the right) materials at different magnifications. (A) and (B) at 50X, (C) and (D) at 100X, (E) and (F) at 250X, and (G) and (H) at 250X.	19
Figure 9. Typical surgical mask.	21
Figure 10. Typical respirator with (A) and without (B) exhalation valve.	21
Figure 11. Cloth mask. Note the similitude with surgical mask.	22
Figure 12. Community mask after full processing cleaning cycle (washing and drying).	23
Figure 13. Average number concentrations of aerosol generated by 15 individuals in the particle size range from 0.3 μm to 20 μm during different activities (see below legend) [72].	24
Figure 14. Number particle size distribution of the particles generated during different respiratory activities. Particle size distribution measured with an optical particle counter [68].	26
Figure 15. Number particle size distributions for: (a) breathing (b) speaking (c) sustained vocalization and voluntary cough. Particle size distribution measured with an aerodynamic particle sizer [71]. The vertical red line represents the size of 1 μm and it was added to help the reader to appreciate that majority of generated particles are in the submicron size range.	27
Figure 16. Number particle size distributions corrected for dilution to represent concentrations in the respiratory tract. The size distribution is represented in both linear and a log scaling of the vertical axis [72].	28
Figure 17. Comparison between droplet transmission (red dots) and aerosol transmission (yellow dots). Once inhaled, very small particles can go deeper into the lung region, while larger particles are captured in the nasopharyngeal region in the upper respiratory system [78].	29
Figure 18. Comparison of two particle size distribution withing limits of EN 14683. Fractional efficiency curve is represented as a trend.	31
Figure 19. Count efficiency as a function of count median diameter and geometric standard deviation within limits of EN 14683.	31

Figure 20. Limits of particle size distribution of paraffin oil aerosol within limits of EN 149. Fractional efficiency is represented as a trend.	33
Figure 21. Mass efficiency as a function of count median diameter and geometric standard deviation within limits of EN 149 for paraffin oil aerosol.	33
Figure 22. Limits of particle size distribution of NaCl aerosol within limits of EN 149. Fractional efficiency is represented as a trend. Notice that dashed blue line is present but with a very low height.....	34
Figure 23. Mass efficiency as a function of count median diameter and geometric standard deviation within limits of EN 149 for NaCl aerosol.	34
Figure 24. Schematic representation of the test rig used to perform fractional efficiency tests.	37
Figure 25. Test rig used to perform fractional efficiency tests	38
Figure 26. HEPA filter placed just downstream of the upstream fan.	39
Figure 27. Plenum of test rig.	39
Figure 28. Representation of a mixing plate.	40
Figure 29. DEHS aerosol generator.	40
Figure 30. DEHS aerosol generator of test rig.....	41
Figure 31. From left to right, isokinetic, subisokinetic and superisokinetic sampling.	42
Figure 32. Aerosol sampling system.....	42
Figure 33. PMS LAS-X II, also known as TSI OPS 3340.....	44
Figure 34. TSI OPS 3330.....	44
Figure 35. Single OPC counting cycle with five sampling cycles.	47
Figure 36. Pie chart of received and tested samples.	49
Figure 37. Surgical mask samples fixed to an adapter plate.....	50
Figure 38. Respirators samples fixed to adapter plates.....	50
Figure 39. Fractional efficiency curves of all the tested samples.	51
Figure 40. Fractional efficiency curves of tested surgical masks.	52
Figure 41. Fractional efficiency curves of tested respirators.....	52
Figure 42. Fractional efficiency curve of samples made up of non-woven and woven materials.	53
Figure 43. Reference number particle size distribution used to integrate surgical masks fractional efficiency curves. Count media diameter equal to 3.0 μm , geometric standard deviation equal to 1.89 and particle count equal to 10 000 particles.	55
Figure 44. Quality factors of tested surgical masks.	56
Figure 45. Number and volume particle size distribution used to integrate respirators fractional efficiency curves with paraffin oil aerosol. Count media diameter equal to 0.37 μm and geometric standard deviation equal to 1.9.....	56
Figure 46. Number and volume particle size distribution used to integrate respirators fractional efficiency curves with NaCl aerosol. Count media diameter equal to 0.08 μm and geometric standard deviation equal to 2.5.....	57
Figure 47. Quality factors of tested respirators.	57
Figure 48. From top to bottom number, surface, and volume reference particle size distribution of UNI PdR 90:2020.	59

Figure 49. From top to bottom number, surface, and volume reference particle size distribution of UNI PdR 90:2020 represented till 3.0 μm	60
Figure 50. eCFC rating for all tested samples.....	61
Figure 51. Legend of Figure 50.....	61
Figure 52. Particle size range of different substances [94]. Particle size expressed in μm	72
Figure 53. Histogram of frequency vs. particle size.	75
Figure 54. Histogram of frequency normalized by width of intervals vs. particle size.	75
Figure 55. Probability density function.	76
Figure 56. Scheme of deposition mechanism by representing the effect of a single fiber.	78
Figure 57. How deposition mechanism impacts the fractional efficiency curve?	79
Figure 58. SEM figure of first layer of sample (A) at 100X.	80
Figure 59. SEM figure of second layer of sample (A) at 100X.	81
Figure 60. SEM figure of third layer of sample (A) at 100X.....	81
Figure 61. SEM figure of first layer of sample (B) at 100X.	82
Figure 62. SEM figure of second layer of sample (B) at 100X.	82
Figure 63. SEM figure of third layer of sample (B) at 100X.....	83
Figure 64. SEM figure of first layer of sample (C) at 100X.	83
Figure 65. SEM figure of second layer of sample (C) at 100X.	84
Figure 66. SEM figure of third layer of sample (C) at 100X.....	84
Figure 67. SEM figure of sample (D) at 100X.	85
Figure 68. SEM figure of sample (E) at 100X.	85
Figure 69. SEM figure of transversal section of sample (E) at 30X.	86
Figure 70. SEM figure of sample (F) at 100X.	86
Figure 71. SEM figure of first layer of sample (G) at 100X.....	87
Figure 72. SEM figure of second layer of sample (G) at 100X.....	87
Figure 73. SEM figure of third layer of sample (G) at 100X.	88

DEDICATIONS

Quiero dedicar esta tesis a toda mi familia, en especial a mi mamá y a mi papá. Siempre han creído en mí, en mis conocimientos y se han esforzado por darme todo lo mejor del mundo y de brindarme todas las posibilidades para hacerme una mejor persona y profesional.

Además, dedico esta tesis a mis amigos, en especial a Victor, Luis y Veronica porque fueron un gran apoyo para mí desde el primer día en el que emprendimos este camino de dejar todo atrás y de venir a un país desconocido.

Como última persona, dedico esta tesis al amor de mi vida, Scarlett. Eres un pilar fundamental en mi vida porque siempre me apoyas incondicionalmente. Tú siempre has creído en mí y se que podemos llegar muy lejos tanto profesional como sentimentalmente.

Este título también es de ustedes... Sin su ayuda no habría podido llegar a donde estoy hoy en día.

1. ABSTRACT

The World Health Organization (WHO) has found that coronavirus disease 2019 (COVID-19) is transmitted via droplets and fomites during unprotected exposure in the immediate environment of those infected. Several studies concluded that wearing facemasks reduces virus transmission. Most national strategies to respond to the Severe Acute Respiratory Syndrome coronavirus 2 (SARS-CoV-2) pandemic included, among others, the use of face masks to reduce the infection propagation. For this reason, just a few weeks after the COVID-19 epidemic started, there was a massive increase in face masks demand, and a shortage occurred.

Major providers of facemasks increased their production as much as four times their typical output, but this was not enough to fulfill the market demand. Moreover, facemask-manufactures faced a lack of non-woven material, which is a vital component of most face masks.

Some other companies modified their original production and, to try to meet consumer demand, started to producing face masks made up of other available materials, like cotton. These products do not guarantee the minimum performance requirements of medical masks or personal protective equipment (PPE) for the respiratory tract. In Italy, this third category is called “community masks” and was lacking a specific test method and rating system to regulate its presence on the market.

Current standards test methods to assess the performance of medical masks (EN 14683) and PPE for the respiratory tract (EN 149) prescribe complicated and lengthy test methods using equipment out-of-date, i.e., challenging to find in the market. For example, the Bacterial Filtration Efficiency (EN 14683) takes at least two days to be measured, and it requires the use of the pathogenic *Staphylococcus aureus*. Moreover, the uncertainty of the reported data of these two standards is not clearly defined.

We developed an innovative test method to measure the filtration performance of the “community masks”. In this way, we can provide more useful and complete performance assessments in a much shorter time and with a defined uncertainty. Furthermore, this new test method can be performed in a typical laboratory by using instrumentation commonly used for assessing the performance of air filtering media and devices and without using a biological test aerosol.

We compare the data obtained with current standardized test methods with those provided by the innovative test method. This comparison was performed by testing the three categories of protective devices mentioned above (medical masks, PPE for the respiratory tract, and “community masks”).

Our analysis shows that the performance of “community masks” covers a vast range of removal efficiency, starting from almost zero and reaching efficiencies like the ones of certified medical masks. We also analyze the breathability of all those products.

Finally, we propose a new approach to classify the “community masks” and to provide solid ground for ensuring their minimum performance requirements.

2. INTRODUCTION

From conception to death, humans are targeted by a large number of other microorganisms, all of them fighting for a place in the shared environment. Infectious diseases are process caused by this microorganism (infectious agent including bacteria, viruses, fungi, parasites, and prions) that harms people [1].

Such diseases are a severe public health concern because they can cause a large number of human deaths and have a substantial economic and social impact in the world [2], [3]. For instance, the estimated direct cost of the ongoing pandemic of coronavirus disease 2019 (COVID-19) caused by Severe Acute Respiratory Syndrome coronavirus 2 (SARS-CoV-2) has been around \$ 11 trillion [4]. It has caused around 560 thousand deaths worldwide at the time of writing [5].

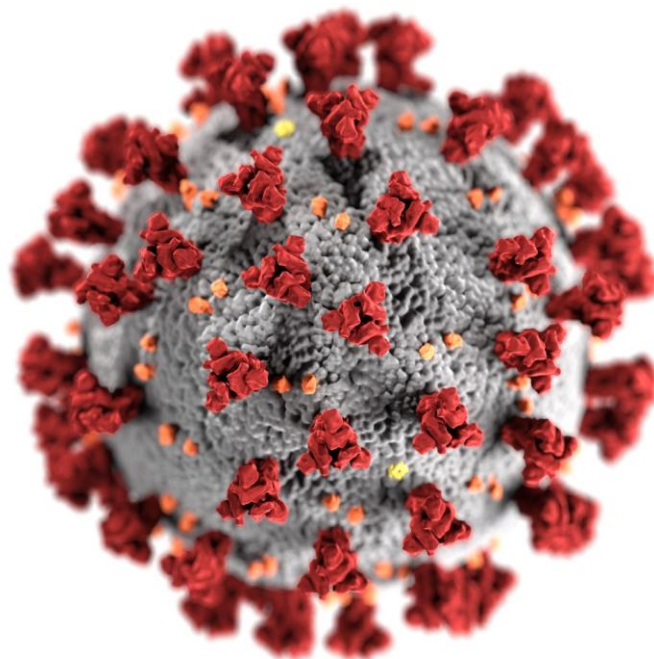


Figure 1. SARS-CoV-2. Note the spikes that adorn the outer surface of the virus, which imparts the look of a corona surrounding the virion—image created at the Centers for Disease Control and Prevention (CDC) [6].

Viruses pose a severe threat to human health. During the past century, viruses were responsible for far more deaths than all the armed conflicts that took place during that period [7], [8]. In modern societies, with people in better health, viruses are also a significant cause of morbidity and loss of productivity. Therefore, viruses impose a cost on society, due to (1) premature deaths, (2) long-term morbidity, (3) increased use of healthcare system, and (2) loss of schooling and working hours [7].

There are three theories for the emergence of pandemic viruses: (1) genetic reassignment between human and animal viruses, (2) direct transfer of viruses between animals and humans, and (3) the reappearance of viruses from unrecognized or unsuspected reservoirs [9].

Despite significant public health efforts, epidemics based on viral-respiratory-tract infections continue to be very frequent among health populations and can have fatal consequences, especially in the most susceptible individuals [10].

In response to epidemic and pandemic situations, like the ongoing COVID-19 pandemic, many countries have used a combination of restraint and mitigation activities. The fundamental approaches are delaying large waves of patients and level the demand for available hospital beds while protecting the most vulnerable from infection. To achieve these goals, national risk assessments base the activities on that usually include estimation of patient numbers requiring hospitalization and availability of hospital beds [11].

In details, most national response strategies include:

1. Varying levels of contact tracking and self-isolation or quarantine.
2. Promotion of public health measures, such as hand washing, respiratory etiquette, and social distancing.
3. Preparing health systems for a wave of critically ill patients requiring isolation, oxygen, and mechanical ventilation.
4. Strengthen the prevention and control of infections in health centers, with particular attention to nursing homes and the rescheduling or cancellation of large-scale public meetings.

2.1. Transmission of infectious diseases by virus

New types of viruses that could lead to infectious diseases emerge regularly. In many cases, these viruses “jump” from animals (i.e., bats, pigs, primates, and others) to humans. Usually, this happens when a person is in close contact with an animal that carries the virus. Then the virus evolves to become transmissible between humans [1].

In the last century, there are many examples of the virus originated from animals that originated epidemics and pandemics including human immunodeficiency virus (HIV/AIDS), ebolaviruses, SARS coronavirus, influenza A H1N1, and the last one SARS-CoV-2.

Most people spend 90% of their lives in indoor microenvironments [12]–[14], which implies that the vast majority of person-to-person transmission events occur indoors.

2.1.1. How does a virus spread?

The transmission of viruses can occur by four exposure routes, through direct or indirect contact, by droplets in short-range transmission, or by aerosol in long-range transmission [10], [15]–[17].

The transmission modes vary by organism type, and usually, more than one route can transmit the infectious agents. Furthermore, each infectious disease has specific properties [15], like the median infectious dose (ID_{50}) defined as dose infective agents that produces infection in 50% of the test objects [18].

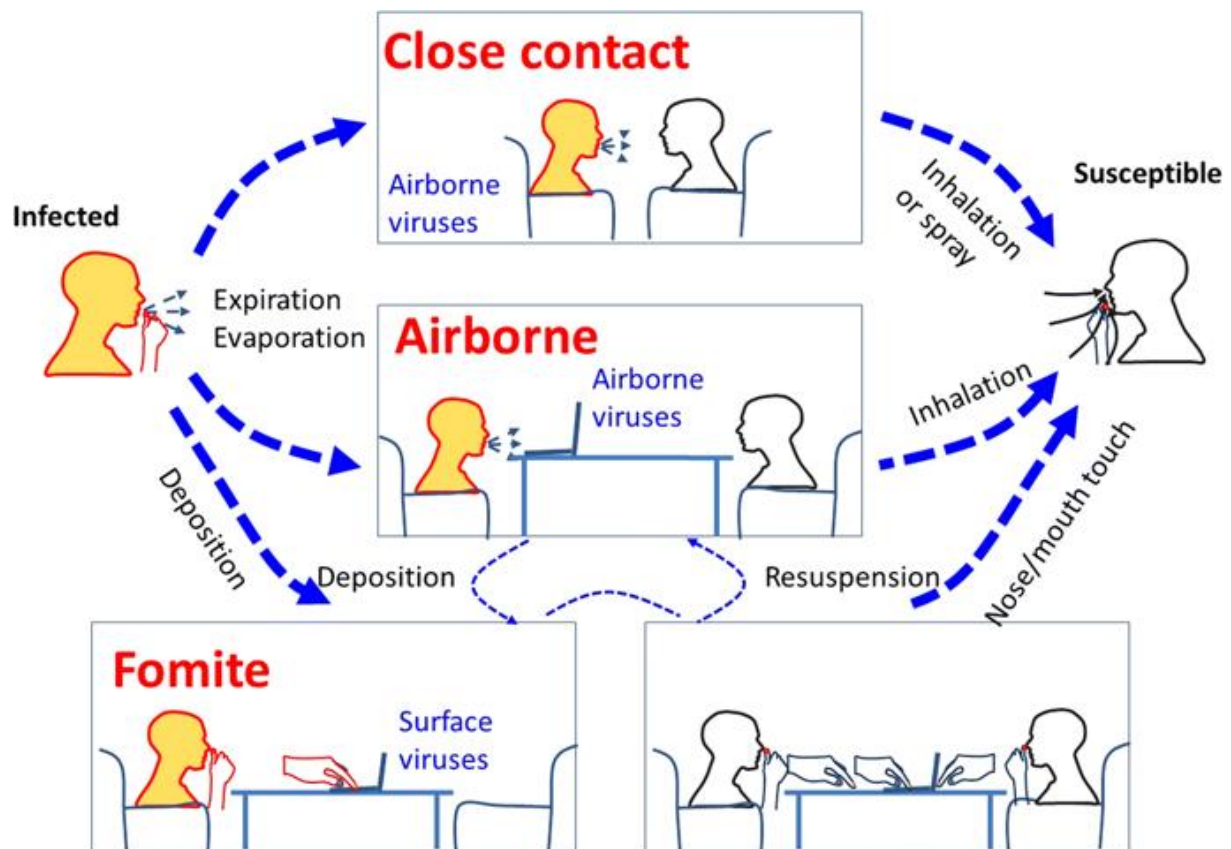


Figure 2. Possible transmission routes of respiratory viral infection between an infected individual and a susceptible host [17].

2.1.1.1. Direct contact

Transmission of the virus occurs by direct physical contact between an infected individual and a susceptible host [15], [19].

2.1.1.2. Indirect contact

Transmission of the virus occurs by passive contact between an infected individual and a susceptible host through an intermediate object, such as contaminated instruments or the hands of a third person [15], [19]. An object carrying infections is denominated as “fomite,” for example, handkerchief, drinking glass, door handle, and clothing [20].

2.1.1.3. Droplet (short-range transmission)

Transmission of the virus occurs through large droplets (particles with a size larger than $5\ \mu\text{m}$) generated by the infected person from its respiratory tract during sneezing, coughing, talking, breathing, or during medical procedures, such as bronchoscopy (see Figure 5). Such drops being relatively heavy can travel a maximum distance of around 1-2 m through the air till settling [21], [22], sometimes depositing on the nasal or oral mucosa of a susceptible host [15], [19].

This type of transmission is technically a form of direct contact. However, in this case, the virus travels directly from the respiratory tract of the infected person to the mucosal surfaces of a susceptible host [15].

The distance that droplets travel depends on different variables, including the mechanics generating droplets (i.e., a respiratory pattern like coughing or sneezing), the air velocity, particle density, and air humidity and temperature [23]. Figure 3 shows how respiratory pattern can “shoot” particles over 6 meters when sneezing.

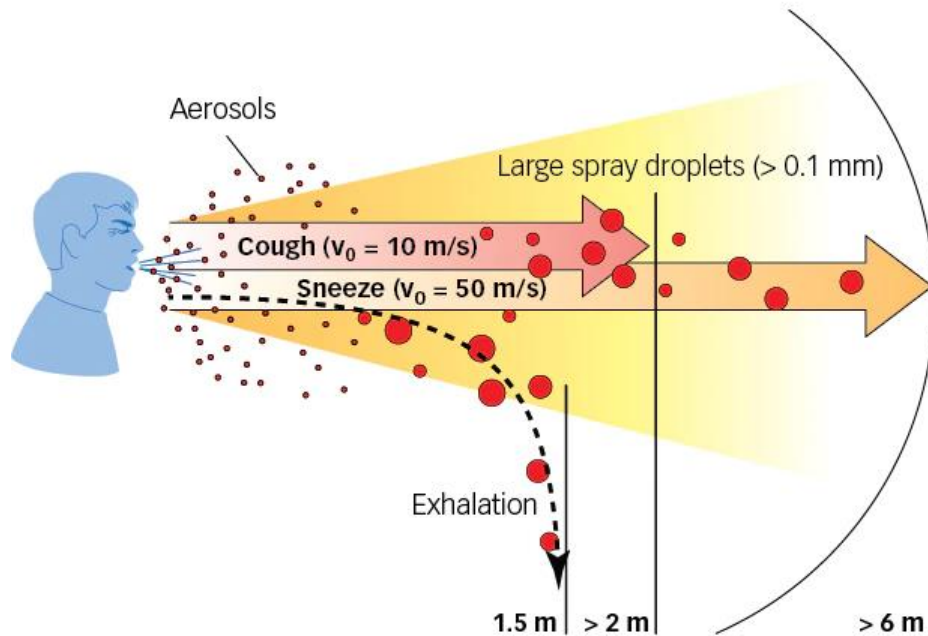


Figure 3. Settling of droplets under different respiratory patterns [24].

2.1.1.4. Airborne particles (long-range transmission)

Transmission occurs through the spread of the virus by aerosolization, usually generated by the same actions described in the above section. Therefore, the virus is enclosed in particle nuclei (particles with a size smaller than $5\ \mu\text{m}$). These particles are dispersed by air streams and inhaled by susceptible hosts that can be at large distances from an infected individual, even in different rooms [15], [19], [22].

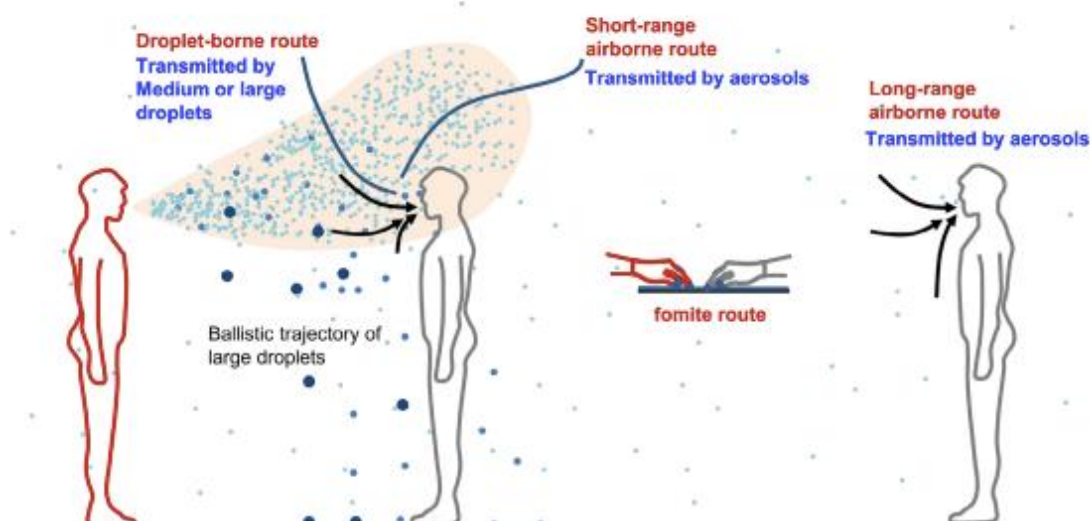


Figure 4. Different transmission routes of infectious diseases [14].

Just a few weeks ago, the WHO concluded that available studies are consistent with the potential aerosol spread of SARS-CoV-2. Hence, transmission occurs not only through coughing and sneezing (i.e., droplet transmission), but by normal breathing [25], [26].

Control of transmission through airborne particles is the most difficult. It requires control of airflow through select ventilation units with adequate filtration systems like high-efficiency particulate air (HEPA) filters [14], [15], [27], [28].

2.1.2. Risk factors enhancing disease emergence and transmission

The factors that enhance viral-respiratory-tract based infection diseases are principally related to human behavior and environmental parameters, being the first one the most important [3], [10].

Family patterns and social habits: Humans are social animals, and their social habits can influence the spread of infectious agents. Human behavior patterns affect contact rates between infected and susceptible individuals [10]. In families with infants, infectious diseases spread more readily. Principal reasons are (1) children are usually more susceptible to infections, and (2) children usually have undeveloped hygiene habits in comparison with adults [1].

Population density: Population density does not increase infection spreading by itself. The real problem shows when the population becomes so dense as to cause overcrowding. Since living quality and sanitation conditions often decrease in overcrowded areas, densely populated cities can potentially facilitate the dispersion of infection diseases [1]. Furthermore, it is necessary to consider only the population density of susceptible individuals and not the entire population density [3].

Temperature and humidity: In a social gathering, the human density can be much higher than in any home, causing air humidity and temperature to rises to levels uncomfortable for humans, but ideal for microbes [1]. Studies found that temperatures in the thermal comfort zone, and low relative humidity conditions, typical characteristics of interior winter in temperate climates, slow down the inactivation of some viruses [10]. Other studies have revealed that environments with high relative humidity (> 60%) and low relative humidity (<40%) seem to allow the transformation of viruses into droplets. In contrast, in environments with intermediate relative humidity (40% to 60%), the viruses are inactivated [29]–[31].

Movement: an outbreak of infectious disease often follows the movement in a new environment. People entering into isolated communities can carry new diseases, and these can spread astonishingly quickly [1]. Humans are the animals that most moves through the earth. Due to intense human trafficking, the spread of infectious diseases can be brought to new areas at any time. Viruses present in rural areas of the world, such as rural Africa or Asia, can arrive in more developed areas, such as Europe or the United States, in just hours [3].

Route of transmission: The transmission route of infectious agents is an essential factor in how fast an infectious agent can spread through a population. An infectious agent that can spread through the air has a more significant potential to infect more individuals than a one that spreads through direct contact [32].

Survival time: An agent that survives only a few seconds between hosts will not be able to infect as many individuals as a one that can survive in the environment for hours, or days [32].

2.1.3. Preventing the transmission of infectious diseases

When a virus invaded a person, there is a wide range of possible outcomes. From the clinical (observable) point of view, some people would never develop any symptoms (a process called subclinical infection). In contrast, others would become severely ill and even could die [15].

Each animal species has a specific natural resistance to disease. The dependency of this resistance is not well understood. In the case of viruses, resistance is often related to the presence of protein receptors on the cell surface that binds to the virus, allowing it to enter the cell and therefore cause infection. There may be apparent racial differences in humans. However, it is always essential to unravel factors such as climate, nutrition, and economics that could be genetically determined [33].

The resistance to a disease, known as immunity, can be naturally or clinically acquired [33].

In the first case, immunity is acquired by repeated exposure to the infectious agent after a complicated series of physiological events (the article “immune system” [33] describes these events in detail). When unvaccinated individuals are exposed to an infectious disease, there are two possible alternatives. (1) Active immunization can be started immediately with the expectation that immunity can develop during the incubation period. (2) The passive immunity process will start during the transition period. Then the active immunization will start at the right time [1].

In the second case, the immunization is acquired by vaccines (exposing the individual to an attenuated version of the virus that generally does not cause alteration in the health state). Similarly, by passing antibodies from one person to another (the recipient eventually eliminate the antibody and is from, and therefore, protection is short-lived) [10].

In many cases, acquired immunity is lifelong, but it may be short-lived (not more than a few months). The durability of acquired immunity is related not only to the level of circulating antibodies but also to sensitized T cells (cell-mediated immunity). Although cell-mediated immunity and humoral B-cell immunity are essential, their relative importance in protecting a person against disease varies with microorganisms. For instance, antibodies are of great importance for protection against common bacterial infections, while cellular immunity is of greater importance for protection against viruses [1], [33], [34].

When possible, vaccination is the most important strategy to control outbreaks of epidemic-prone and pandemic infectious respiratory diseases. However, the mutational ability of most viral pathogens often makes vaccines ineffective or delays their use until a clear identification of the genetic makeup has been made, allowing precious time for the microorganism to spread [9].

Access to the vaccine against the new strain of the virus represents a challenge for countries around the world. In particular, countries with limited resources are incredibly concerned about being left unprotected to deal with the flu pandemic [35]. Besides, in the case of a pandemic virus, particular problems arise regarding the composition and packaging of

vaccines that must be addressed before vaccine production can be completed. The time between the identification of a new strain and the start of vaccine production is usually 2-3 months, and vaccine batches are available after 4-5 months. Thus, in the face of a pandemic threat, it is expected that at least eight months will elapse before manufacturers begin to distribute the new vaccine [9].

Consequently, WHO and other agencies continue to recommend application and adherence to necessary infection control precautions known as non-pharmaceutical interventions (NPIs). This approach is considered as a keystone to preventing transmission of epidemic-prone diseases [36]–[41]. Dependence on NPIs, such as the cough etiquette, calls for more research into the efficacy of blocking cough drops and stopping the spread of outbreaks provided by these interventions [35], [42].

There is no agreement on the best description of respiratory hygiene and cough etiquette among health agencies. However, it appears that: *“Cover your mouth and nose with a tissue when you cough or sneeze. Properly dispose of the used tissue in a garbage can. If you do not have a tissue, cough, or sneeze into your elbow or sleeve, not in your hands”* is the most appropriate recommendation [35], [39], [40].

The most common elements of cough etiquette include: (1) people’s education; (2) placement of signs in a language appropriate to the population; (3) source control measures (i.e., covering the mouth and nose with a tissue when coughing and quick and proper disposal of used tissues, using masks on the coughing person when possible); (4) hand hygiene after contact with respiratory secretions; and (5) spatial separation of people by at least 1-2 meters [15].

2.1.4. Droplet and airborne particle transmission and its prevention by face masks

Carl Flügge was a German bacteriologist and hygienist. He conducted extensive research on the transmission of infectious diseases by expiratory aerosols. In the 1890s, he showed that even during “quiet speech,” small drops (also known as “Flügge drops”) are sprayed into the air. His research laid the basis for the current concept of droplet transmission [43].

Naturally produced aerosols (droplets and airborne particles) from humans, produced by coughing, sneezing, talking and breathing, contains various cell types (e.g., epithelial cells and immune system cells), physiological electrolytes presented in the mucosa and saliva (e.g., Na^+ , K^+ , Cl^-), as well as, potentially various infectious microorganisms (e.g., bacteria, fungi, and viruses) [28].

Artificially generated aerosols in a healthcare environment (e.g., respiratory tract suction) are primarily constituent of sterile water with various electrolytes (e.g., normal or physiological saline, including Na^+ , Cl^-) and often pharmacological molecules [28].

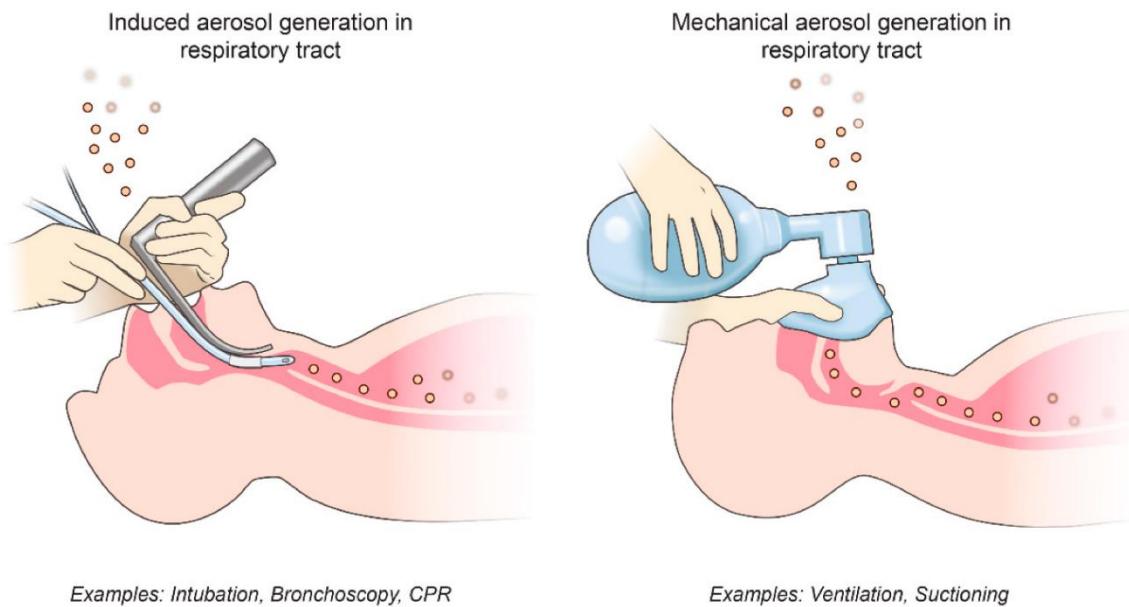


Figure 5. Potential types of aerosol-generating medical procedures (AGMP). AGMPs are classified into two types: (1) procedures that induce the patient to produce aerosols and (2) procedures that mechanically generate aerosols by themselves [44].

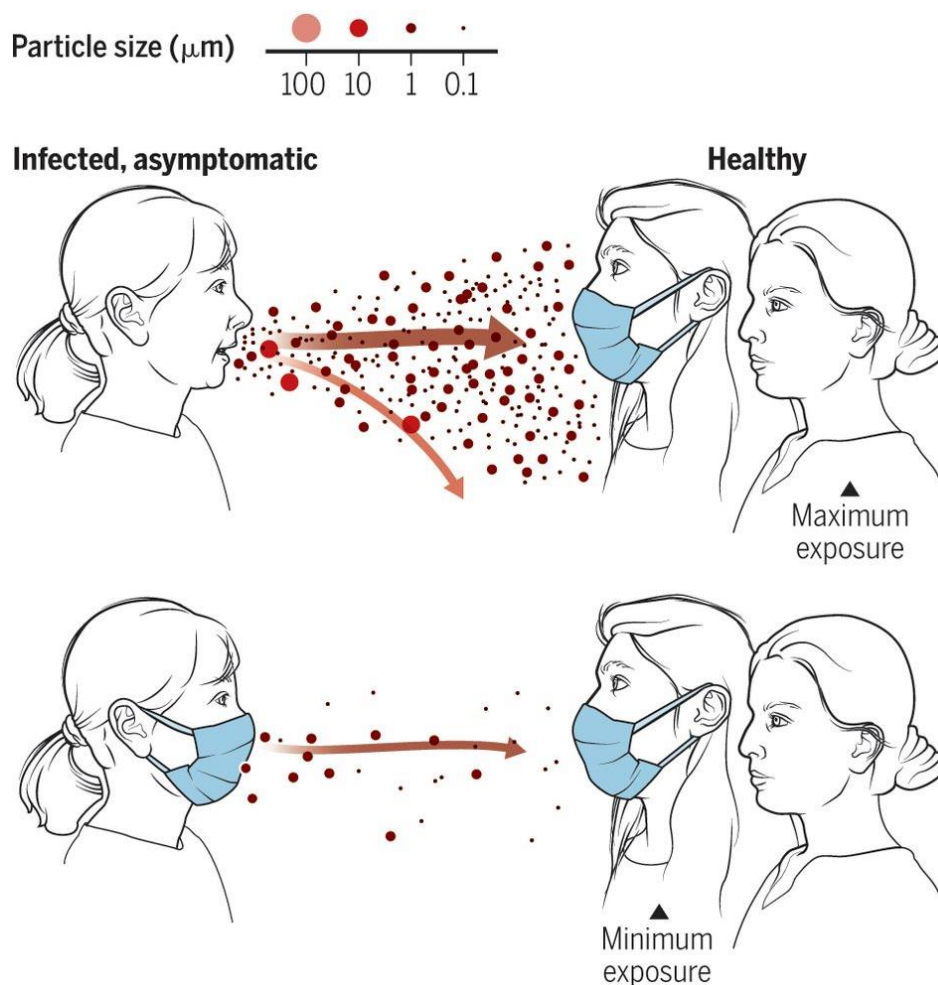


Figure 6. Face masks reduce airborne transmission. No masking maximizes exposure, while universal masking results in lower exposure [47].

Both naturally and artificially produced aerosols will contain a range of particle sizes. Their movement will depend significantly on various environmental factors. Such as the direction of local airflows, air temperature, and relative humidity, which affect the particle size due to evaporation [16], [28].

In order to reduce the disease spreading by droplet transmission, public health organizations call for universal use of face coverings (i.e., surgical masks, respiratory protective devices, and cloth masks) in public spaces [41], [45]–[47]. These devices act as a passive barrier to stop the microorganism spreading. It can also reduce fomite transmission, and are likely to be better than active practices (i.e., covering nose or mouth when sneezing and coughing) [46].

However, the effectiveness of face masks to reduce the transmission of diseases is not very clear [45], [46], [48]–[52].

2.2. Face masks to prevent airborne infectious disease transmission

2.2.1. Types of face masks and their properties

The use of face masks is part of a complete package of prevention and control measures to limit the spread of viral respiratory diseases. For protecting healthy people (worn by non-infected individuals to protect themselves of an infected individual) can use face masks. Additionally, it can be used for source control (worn by an infected person to prevent transmission) [45].

Face masks are made from a mixture combination of non-woven and woven materials, layering sequences of materials and available in different shapes. The unlimited combination of materials results in very-wide filtration efficiency and breathability (i.e., resistance to airflow) [45], [53].

Figure 7 shows an example of layered non-woven materials to form a surgical mask.



Figure 7. Surgical mask made up of three layers of material (the two external ones of spunbond material and the inner one of meltblown material).

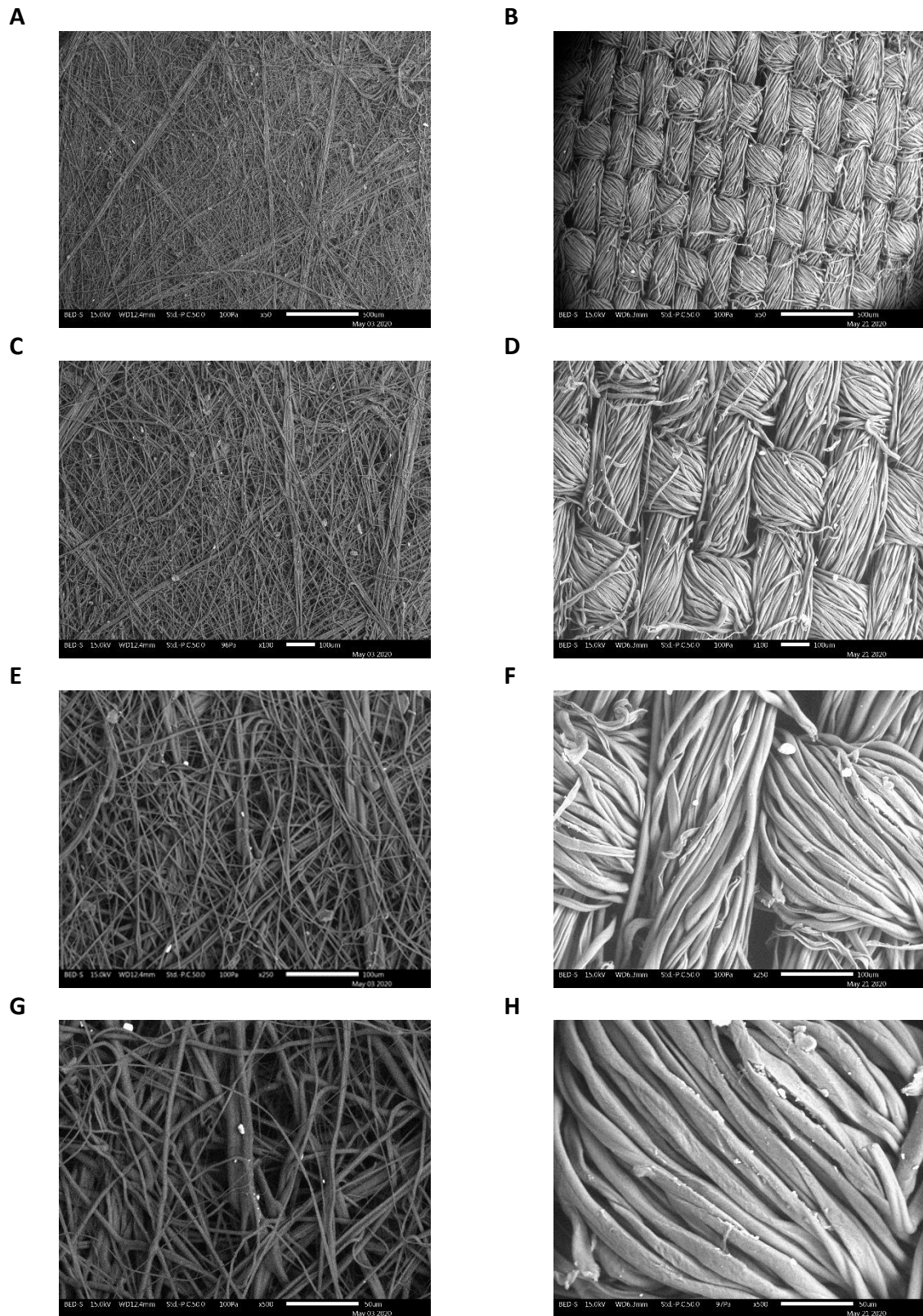


Figure 8. Scanning electron microscope images (SEM) of Non-woven (at the left) vs. Woven (at the right) materials at different magnifications. (A) and (B) at 50X, (C) and (D) at 100X, (E) and (F) at 250X, and (G) and (H) at 250X.

Figure 8 shows a comparison between non-woven and woven materials. In the case of non-woven, its fibers are longer but with a smaller diameter and follows a random pattern. Instead,

in the woven case, its fibers form yarns that then are weaving to structure a systematic pattern.

Note the particles captured by the fibers, because these images correspond to laboratory tested materials with an artificial aerosol. In the case of non-woven material, particles are much smaller than the gap between fibers. Instead, in the case of woven material, the particles have been captured by “sieving.” Please, see section C.1 of Appendix C for more information.

Filtration efficiency and resistance to airflow are dependent on the material type, more specifically on the tightness of the weave, fiber, or thread diameter, and in the manufacturing process (for non-woven materials: *spunbond*, *meltblown*, electrostatic charging) [45], [53].

Non-woven materials fibers are electrostatically charged through corona discharge, and triboelectric means into quasi-permanent dipoles [53], [54], allowing to improve their filtration efficiency while keeping the same resistance to airflow. Once the fibers are charged, the filtration efficiency can decrease when challenging the material to an aerosol, such as NaCl or dioctyl phthalate (DOP) [55].

The ongoing epidemic of COVID-19 has induced a rise in the demand for face masks. However, industrial face mask manufacturers faced a bottleneck of a critical component: the non-woven materials, which are made by smaller companies with capacity limited [53], [56].

Significant manufacturers of face masks, including 3M Co., Owens & Minor Inc, Cardinal Health Inc, and Medline Industries Inc., increased their productions up to four times their typical output, but this was not enough to satisfy the market demand [56].

The real boost to the global supply of face masks comes from China (the world’s most extensive face mask manufacturer), which produces more than half of the world’s production. However, due to the epidemic situation, their daily production dropped from 20 million to 15 million. In contrast, around 89 million face masks are the estimated worldwide demand [46], [56], [57].

2.2.1.1. *Surgical masks*

The European normative EN 14683:2019 “Medical face masks – Requirements and test methods” defines a surgical mask as a “*medical device for covering the mouth and nose providing a barrier to minimize the direct transmission of infective agents between staff and patient.*” Usually, surgical masks are intended for single shift use, and their initial filtration shall be higher than 95% for droplets of around 3 μm [58].

Surgical masks are primarily designed to prevent transmission of droplets from healthcare workers to patients, or blood-borne infection from patients to healthcare workers during medical procedures. This face mask is lacking air-tightness and generally considered ineffective in preventing airborne infection [46], [59]–[61].

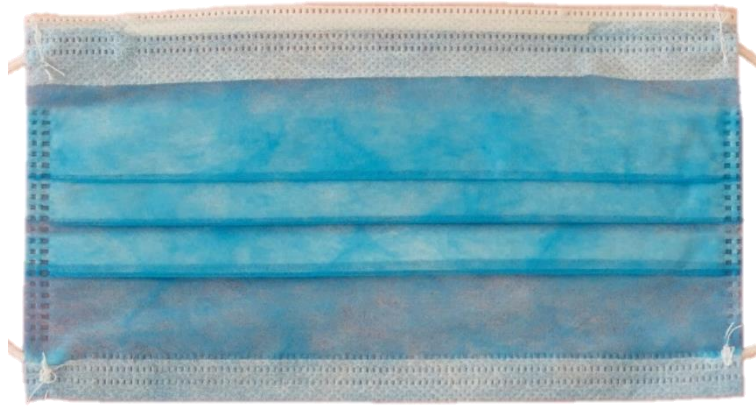


Figure 9. Typical surgical mask.

These facepieces usually are flat or pleated. These are attached with straps to the head that goes around the ears, the head, or both. Several tests determine Their performance according to a set of standardized test methods that seek to balance high filtration, adequate breathability, and optionally, resistance to fluid penetration. These must be certified per international or national standards to ensure that these offer minimal performance when used by healthcare workers, according to the risk and type of procedure performed in a healthcare setting [45].

2.2.1.2. Personal protective equipment for respiratory tract

PPE for the respiratory tract, also known as respiratory protective equipment (RPE) or simply “respirators,” is designed to reduce user exposure to airborne particles (e.g., fine dust generated from industrial processes or biological aerosols generated by sneezing) by forming a tight-fit seal around the face of the wearer [45].

A



B



Figure 10. Typical respirator with (A) and without (B) exhalation valve.

As for the surgical mask, respirators also offer a balance of filtration and breathability. However, while surgical masks shall filter 3 μm drops, respirators must filter much smaller particles (for instance, the particle size of 0.075 μm) and shall guarantee proper sealing.

2.2.1.3. Community face coverings

To face the emergency of COVID-19, in addition to considering respiratory protective equipment (RPE) and medical devices, Decree-Law 18/2020 established other protection

measures in favor of the community. In paragraph 2 of article 16 is reported that: “Until the state of emergency ends [...], people present throughout the national territory may use filter masks without the CE mark, and that has been manufactured as an exception to the current marketing standards”.

In Italy, the term “community masks” was introduced in the Prime Ministerial Decree (DPCM in Italian) April 26, 2020, referring to the objects mentioned by Decree-Law 18/2020. These objects were introduced without specifying any minimum requirements in art. 16, comma 2, of the Law Decree 18/2020, and stating that the manufacturer is the responsibility for guaranteeing their efficacy. Furthermore, Decree-Law 18/2020 establishes that community masks may not be used for the workers' protection in workplaces but may be used by the civil population for the sole purpose of containing the spread of the COVID-19.

The term “community face coverings” is the European equivalent for the Italian term community masks and was introduced by the CEN Workshop Agreement (CWA) 17553:2020 “Community face coverings – Guide to minimum requirements, methods of testing and use” [62].

Such a document defines community face coverings as “*facepiece covering the mouth, nose, and chin fitted with the head harness which can be head or ears attachment*” and specifies that these devices “*shall not incorporate any inhalation or exhalation valve(s)*” [62].

Community face coverings do not fall inside the bounds of a medical device (MD) within the meaning of Directive 93/42 /CEE, nor as personal protective equipment (PPE) for the respiratory tract within the meaning of Regulation EU/2016/425 [45], [62].



Figure 11. Cloth mask. Note the similitude with a surgical mask.

Community face coverings are usually made up of one or more layers of materials (e.g., woven, knitted, non-woven, fabric, and others) and can be reusable or disposable [62]. These devices are also known as “cloth face masks” because they are often made up of fabrics.

As to surgical masks, community face coverings are recommended as a simple barrier to help prevent the spreading of respiratory droplets, but with lower requirements of filtration efficiency and breathability, and are not intended to be used by health care workers. For this reason, it should be considered only for source control in community locations, and formally diagnosed infected individuals shall not use it [62].

Community face coverings are intended to be used by people who do not have clinical symptoms of infectious disease and who do not encounter people with such symptoms [62].

These facepieces can also limit the particle penetration of external origin into the nose and mouth of users without claiming the users' protection [62].

Cloth masks are generally highly breathable but offer lower filtration. Some studies have demonstrated that the particle filtration efficiency of cloth fabrics vary widely between 0.7% to 60% [53], [63]–[65].



Figure 12. Community mask after full processing cleaning cycle (washing and drying).

2.3. Particle size distribution of bioaerosol produced by humans

To understand whether face masks are adequate to protect individuals from droplets and airborne particles, it is required to analyze the particle size distribution of the aerosol challenging these devices. For more information regarding how aerosol characteristics and properties impact filtering performance of materials, see Appendix C.

There have been numerous studies on the number and size of droplet secretions from respiratory activities, and a few overall reviews were published. These studies and reviews indicate that the size of the droplet and particles due to sneezing, coughing, talking, and breathing is likely to be a function of the generation process and environmental conditions. The actual droplet size also depends on parameters such as exhaled air velocity, fluid viscosity, and flow path (i.e., through the nose, mouth, or both). There is also immense person-to-person variability [16], [22], [66]–[72].

The generation of bioaerosols is not clearly understood. However, some studies have found that could be generated by warm and moist gas in the alveolar region passing from the lungs into the upper respiratory tract, where the gas cools till condensing to form liquid particles. The high-speed turbulent airflow expels these particles during exhalation. More outstanding particle atomization also occurs during the speech, sneezing, and coughing, due to increased turbulent airflows that expel particles faster. The vigorous vibration and energetic movement of the vocal cords during speech and cough are responsible for the majority of particle generated [22].

There is natural physiological variation in the volume and composition of aerosols generated between people and even within the same person during any of these activities. An infection is likely to increase this variability, which in turn can vary as the host's immune system begins to respond to the infection over time. For example, a patient will not have specific antibodies against the virus at the infection beginning. Therefore, the viral particle load is much higher and, consequently, potentially more transmissible during the acute, febrile, cough phase of infection than later, when the specific antibody response begins to develop [28], [72].

Figure 13 shows a comparison of the count particle concentration of aerosol generated during different activities. These results correspond to the Morawska et al. study, and their findings suggested even tidal breathing through the nose can generate particles. Being a count particle concentration(i.e., number of particles present in a fixed volume), this data by itself does not represent a useful parameter to establish the diffusion of an infectious disease by airborne transmission because it does not take into account the particle mass. For instance, the case “cough” seems to generate a lower number of particles than the case “aah-v-p,” but in the former, the particles can be much larger in diameter and represent much more amount of mass.

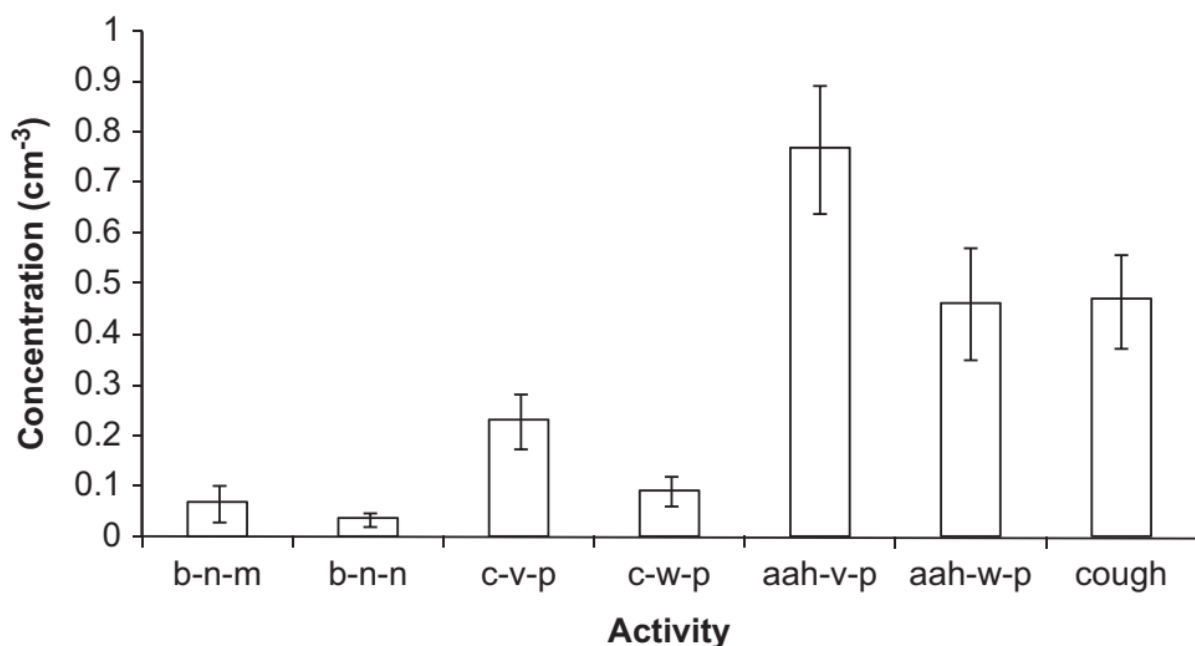


Figure 13. Average number concentrations of aerosol generated by 15 individuals in the particle size range from $0.3 \mu\text{m}$ to $20 \mu\text{m}$ during different activities (see below legend) [72].

Legend of Figure 13 and Figure 16:

- **b-n-m**: natural paced breathing, in through the nose and out through the mouth
- **b-n-n**: natural paced breathing, in through the nose and out through the nose
- **c-w-p**: alternately 10 s of whispered counting and 10 s of naturally paced breathing
- **c-v-p**: alternately 10 s of voiced counting and 10 s of naturally paced breathing
- **aah-v-p**: alternately 10 s of un-modulated vocalization (voiced “aah”) and 10 s of naturally paced breathing
- **aah-w-p**: alternately 10 s of un-modulated whisper (whispered “aah”) and 10 s of naturally paced breathing for recovery to prevent drying of the mouth or labored breathing
- **cough**: repeated coughing at an intensity and frequency which the volunteer felt comfortable. In practice, for most volunteers, the resulting cough intensity can be best described as a mild throat-clearing cough

Size differences are due to variations in pressure and air velocity in different parts of the respiratory tract. The importance of each of these activities in the spread of infection depends on several factors, including: (1) the number of droplets it produces, (2) its particle size, (3) the content of infectious agents, and (4) the frequency of their performance. For example, sneezing and coughing may produce more droplets than talking, laughing, and breathing. However, the latter activities are performed more frequently [16], [28], [72].

Studies conducted between 1920 to 1940 concluded that the vast majority of droplets generated by expiratory human activities are more extensive than 1 μm and concluded that 95% of the particles were smaller than 100 μm . Most were in the range of 4 to 8 μm [73], [74], because the techniques they had available at the time to conduct such studies were not suitable for smaller droplets [72].

Contrary to previous studies, a more recent study, which included optical particle detection techniques (i.e., Optical particle counter – OPC) capable of measuring down to 0.3 μm , suggests that most of these particles are in the submicron size range [68]. Another study using a particle detection instrument based on aerodynamic properties (i.e., Aerodynamic particle sizer – APS) confirmed these results [71]. Figure 14 and Figure 15 show the results of these studies.

These studies showed that 80-90% of the particles from human expiratory activities are smaller than 1 μm and showed that during coughing commonly generates peak droplet concentrations and lowest droplets during nasal breathing [68], [71]. However, this does not mean that there are not larger particles. Figure 16 shows the comparison of the same particle size distributions using both linear and a vertical log scale in which it is possible to see also massive particles with a size of 10 μm .

Besides, there was significant variability between subjects in the particle concentration generated during various activities [68], [71]. Another study obtained results with the same variability [75].

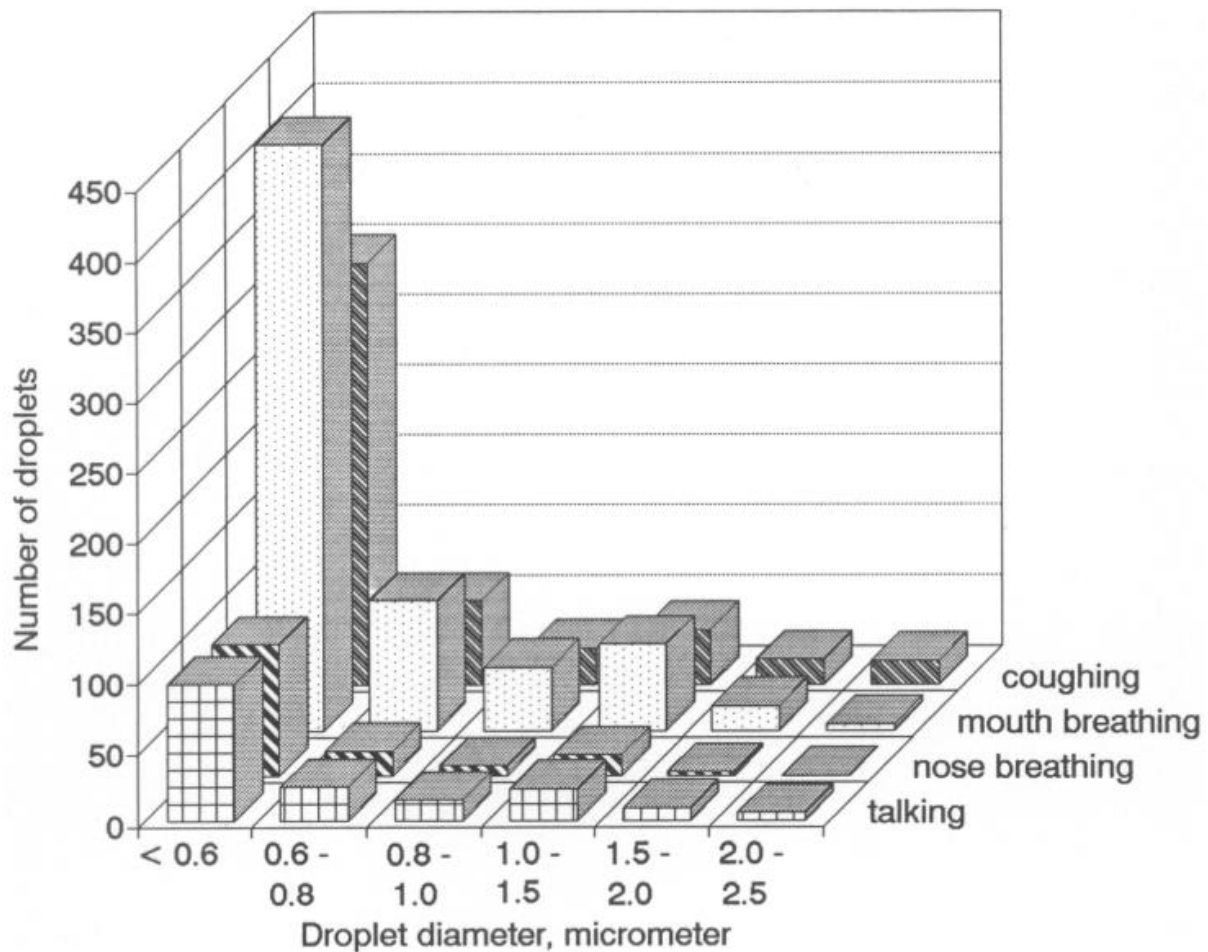


Figure 14. Number particle size distribution of the particles generated during different respiratory activities. Particle size distribution measured with an optical particle counter [68].

Published articles suggested that sneezing can produce up to 40,000 droplets with size between 0.5 and 12 μm that can be expelled at speeds of up to 100 m/s, while cough can produce up to 3,000 droplets, approximately the same number as talking for five minutes [76], [77].

Deposition models have concluded that particles with a size smaller than 10 μm are more likely to penetrate deeper into the respiratory tract on the upper airway surfaces of the airways, and particles larger than 10 μm in size are less likely to penetrate the lower lung region. However, small particles can also deposit in the upper respiratory tract [22]. Figure 17 shows a graphical representation of particle deposition in the respiratory system as a function of particle size.

To establish shedding infection for control measures can use particle size, but it is necessary to improve the understanding of some parameters. For instance: (1) the deposition site of infected particles, (2) the relationship between particle size and pathogenic load, and (3) the threshold of pathogenic particle load necessary for the establishment of infection in different regions of the airways[22], [75].

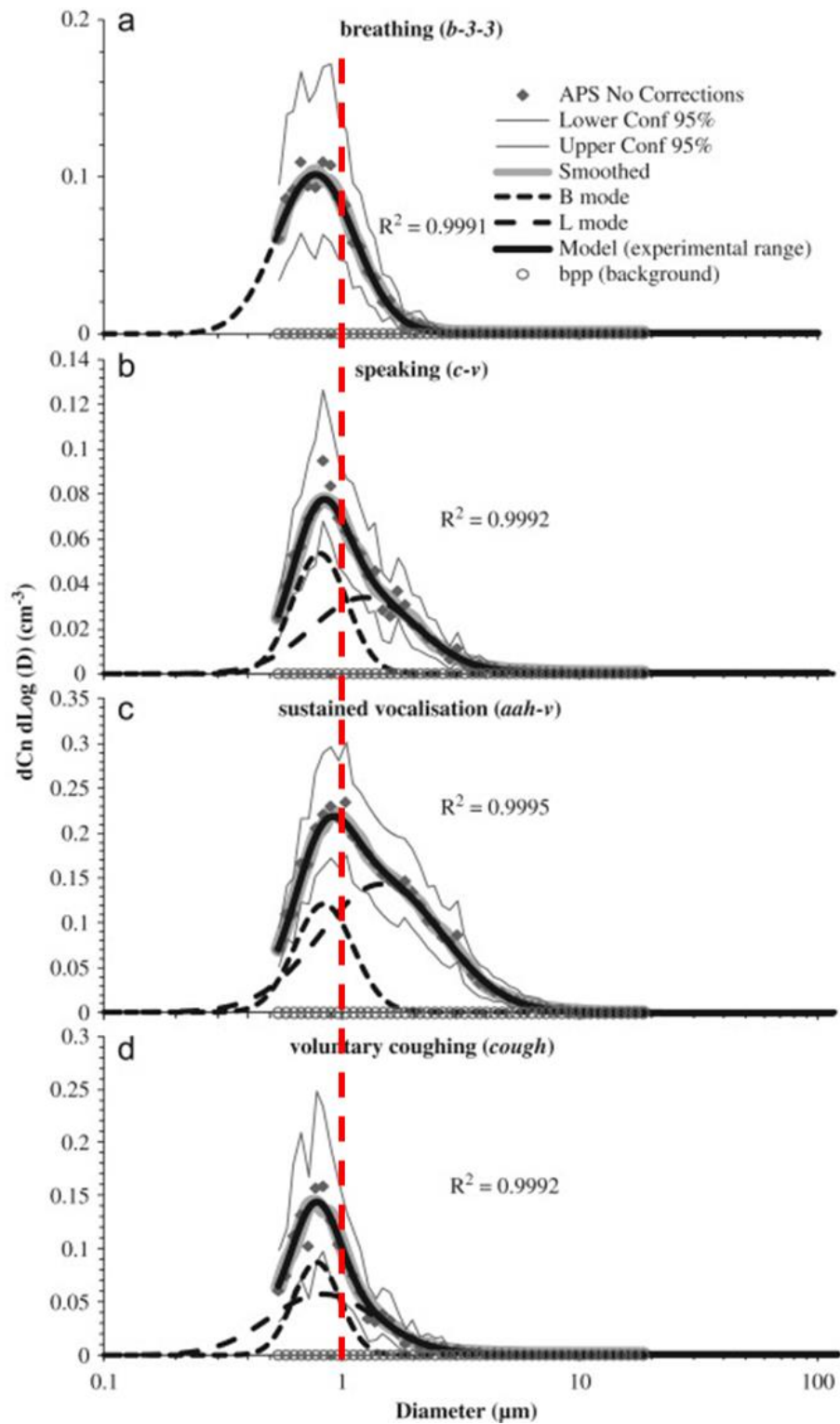


Figure 15. Number particle size distributions for (a) breathing (b) speaking (c) sustained vocalization and voluntary cough—particle size distribution measured with an aerodynamic particle sizer [71]. The vertical red line represents the size of 1 μm , and it was added to help the reader to appreciate that majority of generated particles are in the submicron size range.

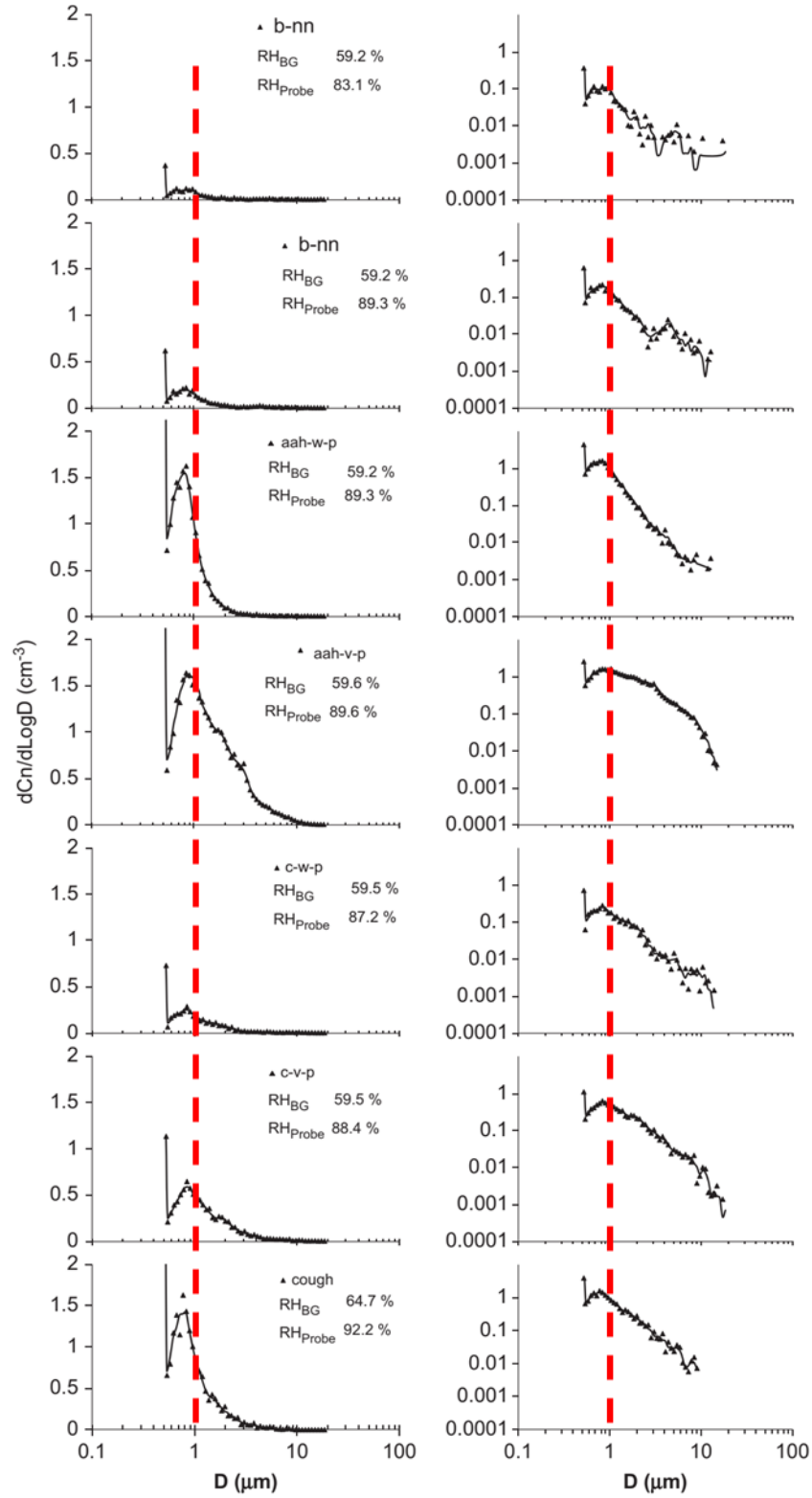


Figure 16. Number particle size distributions corrected for dilution to represent concentrations in the respiratory tract. The size distribution is represented in both linear and a log scaling of the vertical axis [72].

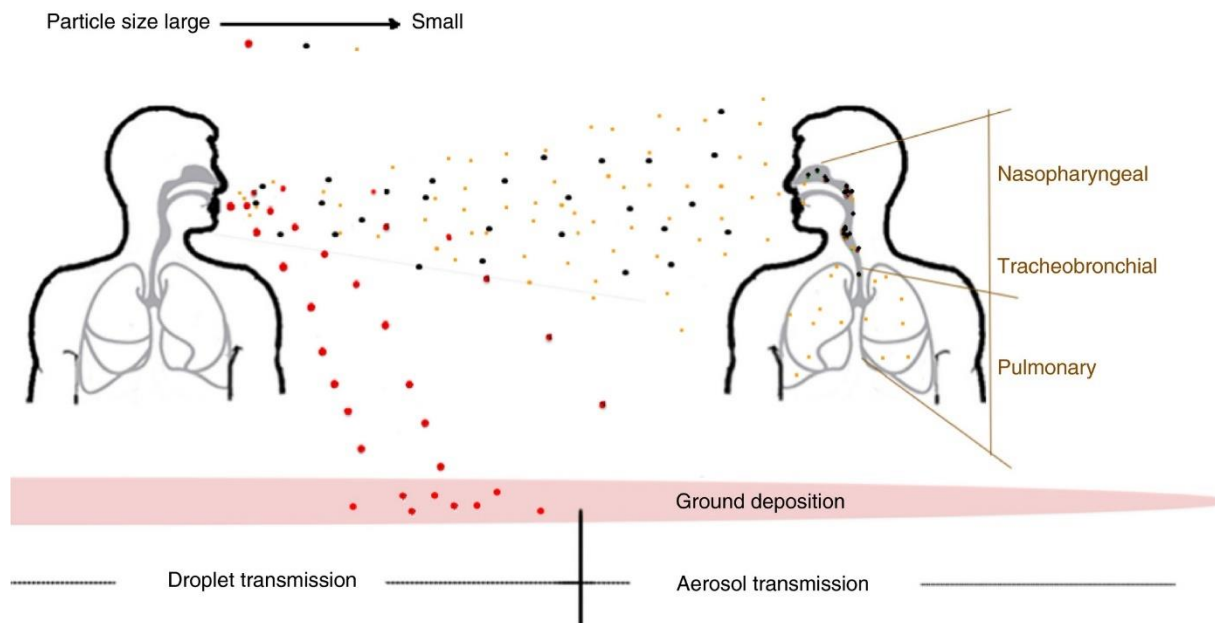


Figure 17. Comparison between droplet transmission (red dots) and aerosol transmission (yellow dots). Once inhaled, microscopic particles can go deeper into the lung region, while in the upper respiratory system, the nasopharyngeal region captures larger particles [78].

2.4. Test methods for face masks for controlling airborne contamination

The test methods are intended to guarantee minimum performance requirements for face masks following their specific intended use.

Like face masks, we studied three different types of devices: (1) surgical masks, (2) respiratory protective equipment, and (3) community face coverings. All of them have different intended use and are assessed with different test methods. However, their reference standards have the same main scope: a balance between filtration efficiency and resistance to airflow.

Table 1. Summarization of European test methods for face masks.

Test	Surgical mask	Respirator	Community face covering*
European test method	EN 14683:2019	EN 149:2001+A1:2009	CWA 17553:2020** and UNI PdR 90:2020**
Filtration efficiency	Measured count efficiency with bacterial aerosol	Measured mass efficiency with two aerosols by using a photometer	Calculated mass efficiency through integrating measured size-resolved efficiency
Resistance to airflow	Defined as "breathability."	Defined as "respiratory resistance."	Defined as "respiratory resistance."

*Per UNI PdR 90:2020

**Not mandatory

In the above section, we described the prescribed test of filtration efficiency and resistance to airflow for each face masks type. Table 1 summarizes the filtration efficiency and resistance to airflow test per current European standards.

The community face coverings being a new face mask type does not have to fulfill requirements of any specific standard. Just a few days ago, it was published the Italian regulatory practice called UNI PdR 90:2020 “Community face mask” [79], [80], and currently, its application is not mandatory at the national level.

2.4.1. Surgical masks

2.4.1.1. *Standardized test method*

Surgical masks, officially known as “Medical face masks,” are regulated in Europe by EN 14683:2019 “Medical face masks - Requirements and test methods” [58]. In the United States, these devices are regulated by a series of standards; the most important one is ASTM F2101 - 19 “Standard Test Method for Evaluating the Bacterial Filtration Efficiency (BFE) of Medical Face Mask Materials, Using a Biological Aerosol of *Staphylococcus aureus*” [81].

2.4.1.2. *Bacterial filtration efficiency*

Bacterial filtration efficiency (BFE) is a measure of the resistance of a material to bacterial penetration, specifically “*Staphylococcus aureus*.” The results are reported as a percentage of efficiency and correlate with the ability of the material to resist bacterial penetration. Higher numbers on this test indicate better barrier efficiency.

2.4.1.3. *Critical points*

The use of a bacterial aerosol denotes a series of problems without adding any value to the obtained results. The CDC states [82], “Whether the particle is alive or infectious plays no role in how well a filtering material will collect it. Once a particle is collected, it will remain bound by electrostatic forces and van der Waals”. Consequently, the use of *Staphylococcus aureus* requires to perform the test in special laboratories adequate to manipulate this pathogen. Furthermore, since colonies of bacterial must grow up to be count, the test takes at least two days to be performed.

Another weak point is that it provides, as a result, single efficiency value and not a full fractional efficiency curve. This single value is the combination between the fractional efficiency of material and the upstream particle size distribution. Therefore, the results are highly dependent on any variation of the test aerosol generator.

An additional weakness is that particle size distribution is not well defined because EN 14683 prescribes only a range for count median diameter and particle concentration but not specify any kind of limitation for the geometric standard deviation. Figure 18 shows two different numbers of particle size distribution within prescribed limits.

By taking a reference fractional efficiency curve of a typical material used to manufacture a surgical mask, we calculated the bacterial filtration efficiency that would be obtained by using particle size distributions within showed limits. Figure 19 shows the hypothetical results as a 3D chart. BFE values vary from 60% to 95%, which means that the same material tested by two different laboratories could lead to such different results.

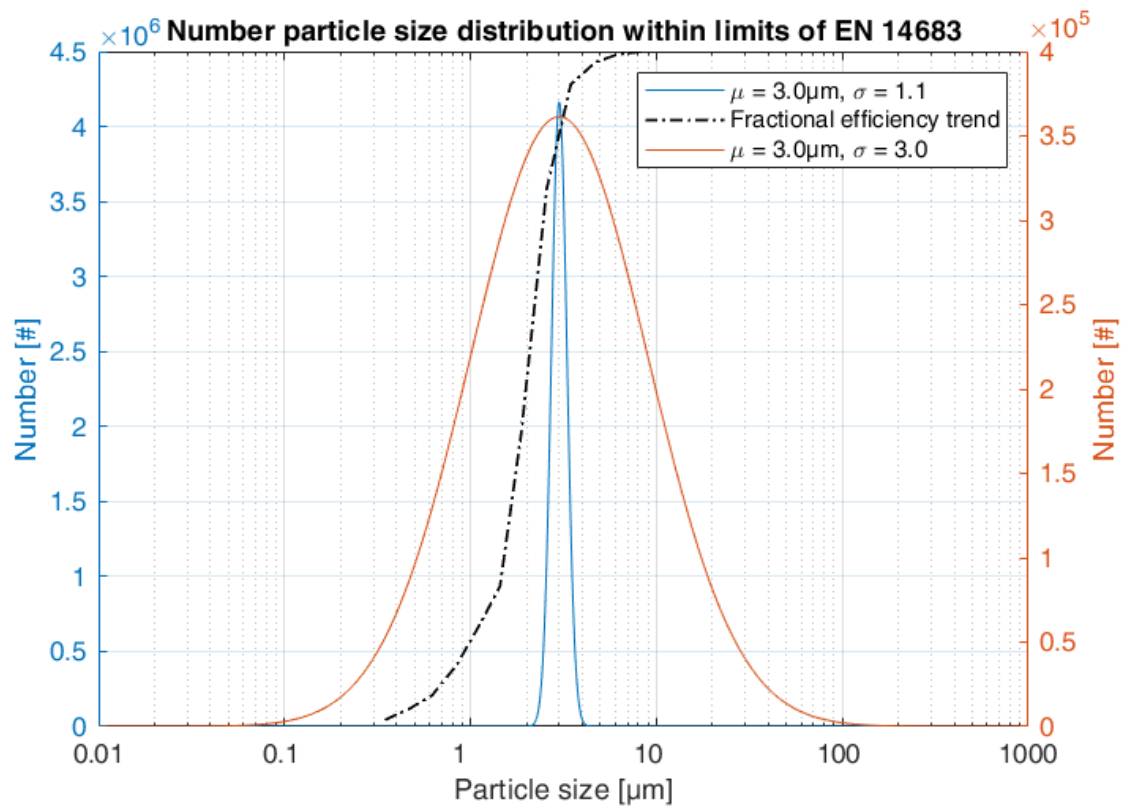


Figure 18. Comparison of two particle size distribution withing limits of EN 14683. The fractional efficiency curve is represented as a trend.

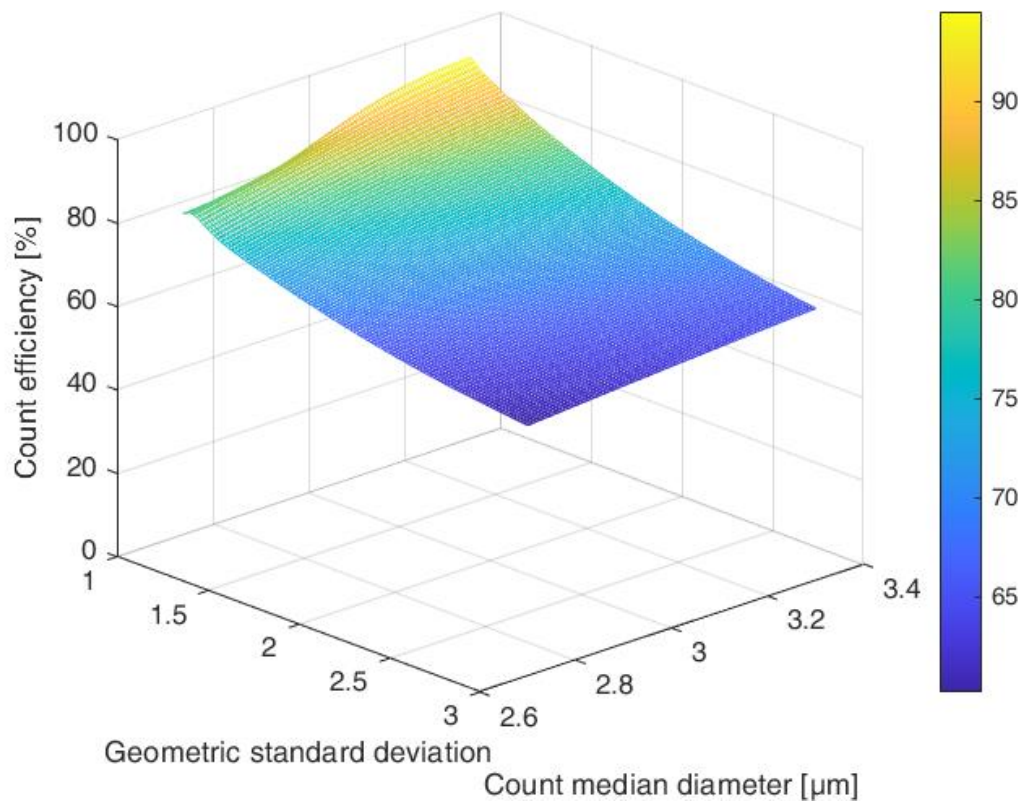


Figure 19. Count efficiency as a function of count median diameter and geometric standard deviation within limits of EN 14683.

2.4.2. Personal protective equipment for respiratory tract

2.4.2.1. *Standardized test method*

Personal protective equipment for respiratory tract (RPE) is regulated in Europe by EN 149 “Respiratory protective devices. Filtering half masks to protect against particles. Requirements, testing, marking” [83]. In the United States, these devices are regulated by NIOSH “42 CFR Part 84 Respiratory Protective Devices” and in China by GB2626-2019 “Respiratory protective equipment -- Non-powered air-purifying particle respirator.”

The most crucial difference between European standards and the other ones mentioned is that in Europe, RPE is tested by using two aerosols on the same device. One aerosol (NaCl aerosol) is intended to measure particle filtration efficiency by using a tiny particle of around $0.08\ \mu\text{m}$. The other one (Paraffin oil aerosol) is intended to assess how particle filtration efficiency decrease when removing electrostatic charges on the fibers of the tested material.

The non-European standards usually do not perform any test intended to discharge tested devices. For this reason, these test their devices with only one aerosol, usually NaCl aerosol. This is the case for the so-known N95 respirators and the KN95 respirators.

It represents a huge difference because it means that currently, respirators produced by following non-European standards cannot be compared with ones produced by following EN 149. So, N95 and KN95 respirators cannot be linked to FFP2 ones.

2.4.2.2. *Mass filtration efficiency*

To measure mass filtration efficiency, EN 149 prescribed the use of a photometer, which is a device that burns aerosol and determines mass particle concentration by comparing the color of the flame. Two different mass filtration efficiencies are prescribed, one for each of the described aerosol in the above section.

The results are reported as a percentage of efficiency and correlate with the ability of the material to resist particle penetration. Higher numbers on this test indicate better barrier efficiency.

2.4.2.3. *Critical points*

As for surgical masks, the provided results consist of a single efficiency value correlated with mass efficiency. Therefore, from these results, it is not possible to determine the fractional efficiency curve. Furthermore, mass filtration efficiency is highly dependent on the upstream particle size distribution. Furthermore, photometers are very-old instruments that are difficult to find in the market.

Another weak point is that limits of particle size distributions are substantial and can lead to an extensive range of possible results. Figure 20 shows the two boundaries for the case of paraffin oil.

Figure 21 shows the mass efficiency results that would be obtained by testing the same materials with aerosols having particle size distributions within limits of European standard. In this case, values vary from 49% to 94%. Consequently, within this range, the same face mask could be classified as FFP2 or FFP1 or could be classified as not adequate for EN 149.

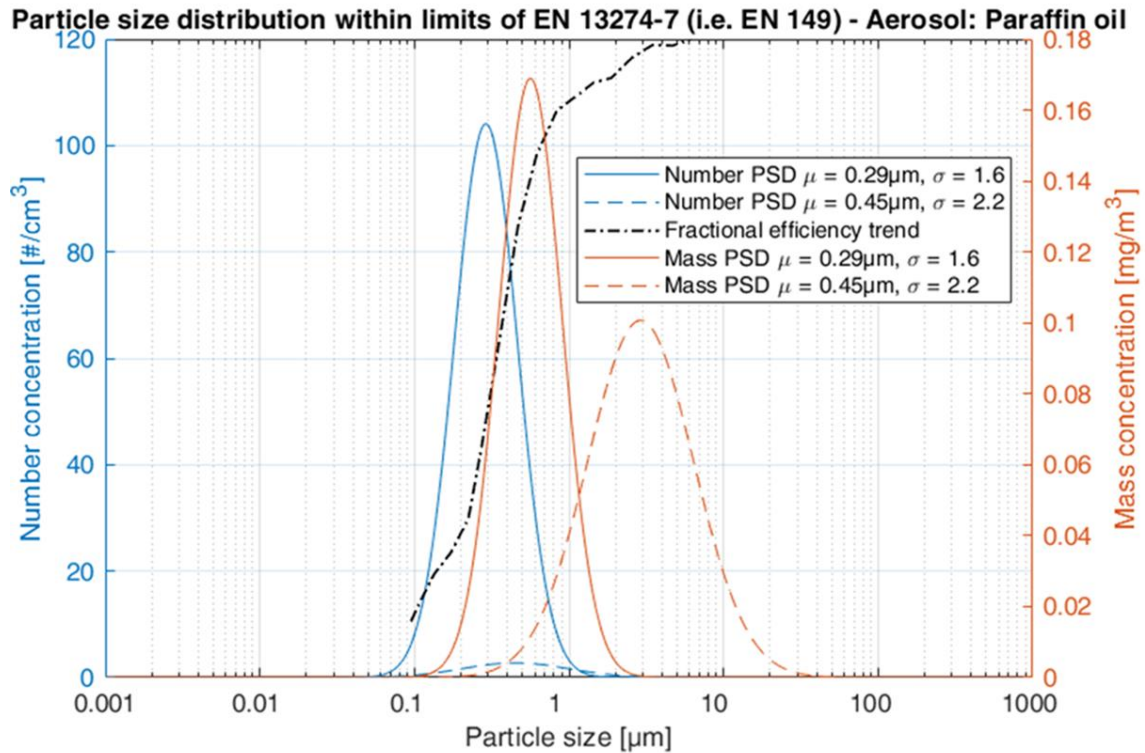


Figure 20. Limits of the particle size distribution of paraffin oil aerosol within limits of EN 149. Fractional efficiency is represented as a trend.

Mass efficiency (within allowed limits of EN 13274-7, i.e. EN 149) - Aerosol: Paraffin oil

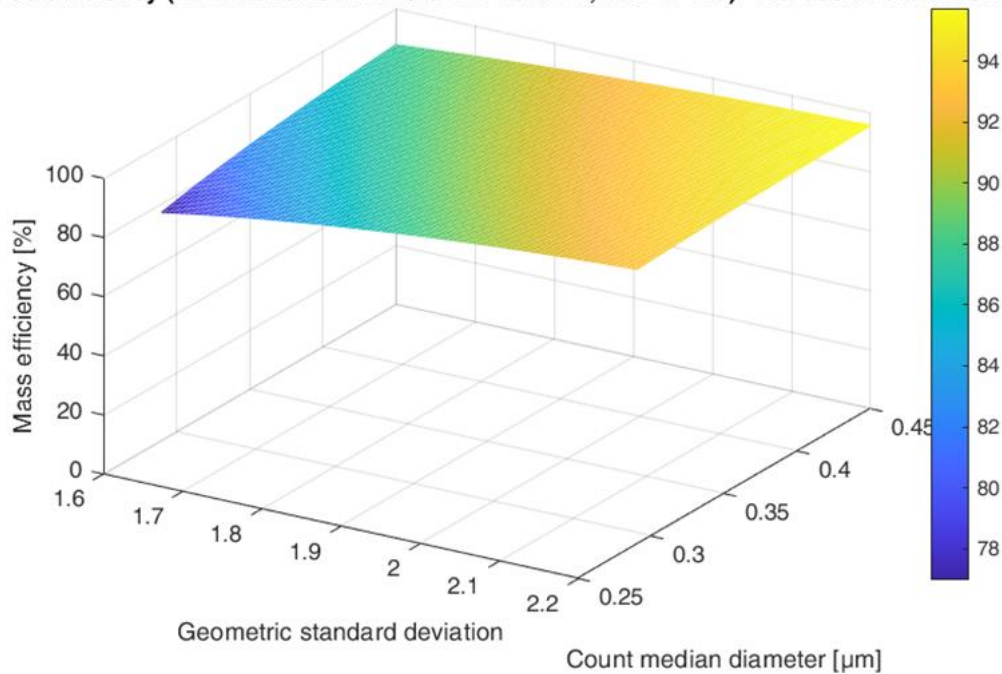


Figure 21. Mass efficiency as a function of count median diameter and geometric standard deviation within limits of EN 149 for paraffin oil aerosol.

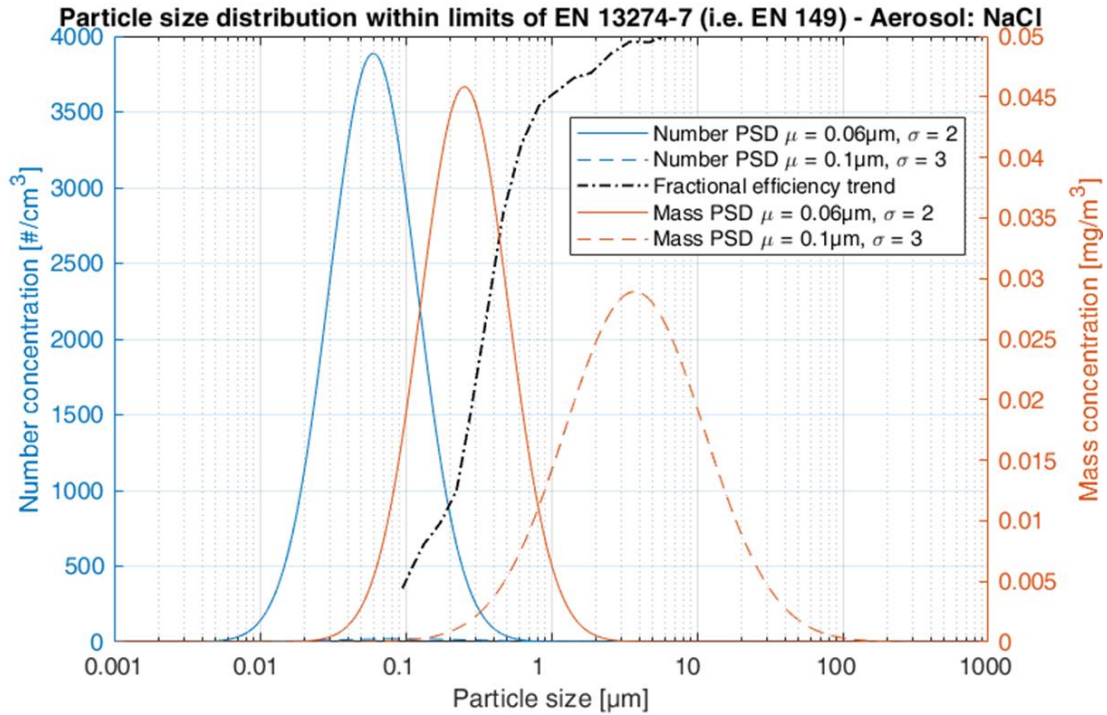


Figure 22. Limits of the particle size distribution of NaCl aerosol within limits of EN 149. Fractional efficiency is represented as a trend. Notice that the dashed blue line is present but with a shallow height.

Mass efficiency (within allowed limits of EN 13274-7, i.e. EN 149) - Aerosol: NaCl

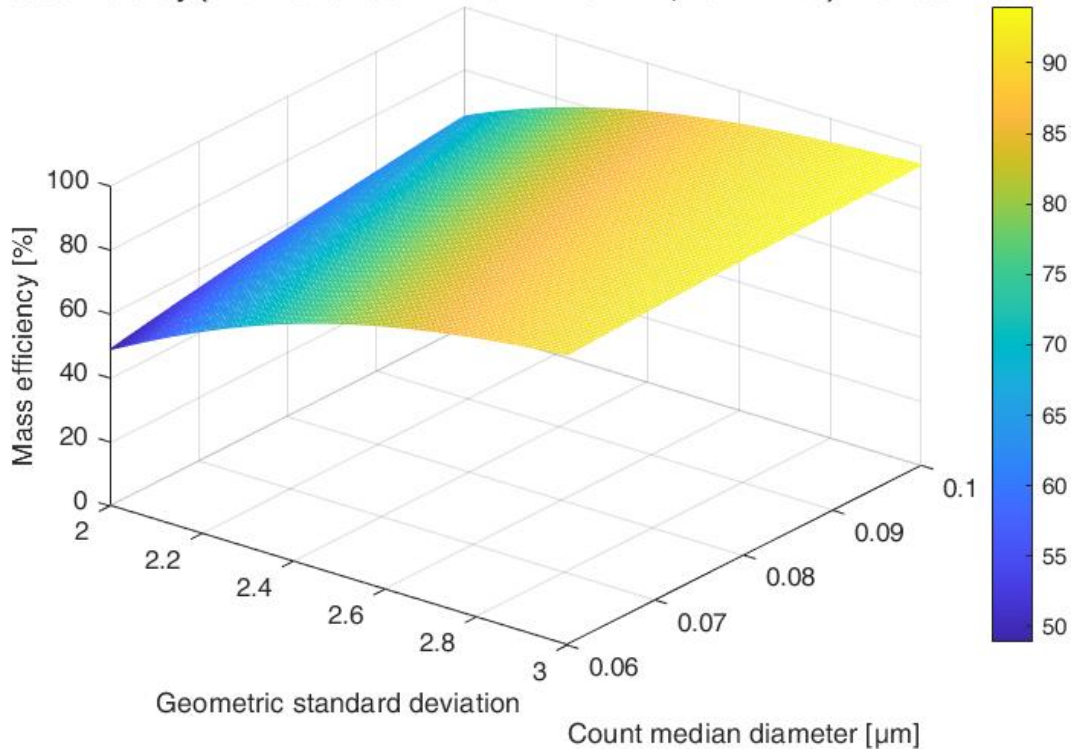


Figure 23. Mass efficiency as a function of count median diameter and geometric standard deviation within limits of EN 149 for NaCl aerosol.

With the same correspondence, Figure 22 and Figure 23 show the same comparison with NaCl aerosol. In this case, mass efficiency would vary between 77% and 96%, a smaller range, but producing the same results. The same face mask could be classified as FFP2 or FFP1 or could be classified as not adequate for EN 149.

2.4.3. Community face coverings

2.4.3.1. *Why is it necessary the use community face coverings?*

As shown before, the use of face masks seems to be very important to avoid the spreading of infectious diseases. Since the COVID-19 pandemic produces a shortage of regulated face masks, it was necessary to produce a new type of face mask made up of non-conventional materials.

Many products with very low efficiency arrive at the market without following any type of standard. Figure 40 and Figure 41 show the results of several face masks and compare them with typically standardized face masks. All the curves below the dashed reference lines would be classified into the same category, the so-called “community face coverings” without allowing to difference in any way their performance.

2.4.3.2. *How to assess their performance*

The recent reference procedure UNI PdR 90-1: 2020 specifies the performance requirements of the community mask. Instead, UNI PdR 90-2: 2020 specifies the test method to measure its performances (i.e., maximum resistance to airflow rate, minimum initial particle removal efficiency depending on the size of the particles).

It is essential to mention that two parts of UNI PdR 90:2020 are based on the results finds in this study.

2.5. Aim of the work

Some studies have demonstrated that cough etiquette, especially the use of face mask, is an appropriate approach to reduce the spreading of infectious diseases.

Unfortunately, the global market was not prepared to satisfy the demand increase of face masks, followed by the ongoing COVID-19 pandemic.

The Italian government, as well as other European nations, allowed the commercialization of face masks without the CE mark, with the aim of consenting. (1) Promoting the foundation of new face masks manufacturers in a shorter time. (2) Importation of face masks made in other countries produced by following non-European standards.

Unfortunately, this approach causes at least two problems: (1) the placement of products on the national market without any minimum performance (the so-called “community masks” in Italy or “community face coverings” in Europe) and (2) the use of fabrics to manufacture cloth masks due to the lacking of non-woven materials.

To make the situation worse, currently, in Italy, it is not possible to measure the face mask performances quickly and reliably. Current European test methods prescribe the use of instrumentation not readily available on the market and provide results without a well-defined and precise value of uncertainty.

For these reasons, in the Aerosol Technology Laboratory of Politecnico di Torino in the last months, we performed hundreds of measurements with the aim of. (1) Help new face mask manufacturers to understand the performance of their products. (2) Develop a reliable and repeatable method for assessing the performance of all types of face masks by employing state-of-the-art instrumentation available on the market.

The aim of this work is the validation of the proposed test method to evaluate the performance of all types of face masks produced in different parts of the world, even the ones produced by following non-European standards.

3. MATERIAL AND METHODS

3.1. Innovative test method for assessing performance of community face coverings

The basis for the development of UNI PdR 90:2020 is the results of this study. Therefore, referencing UNI PdR 90:2020 is just to avoid lengthy explanations of specific details of the test method.

3.1.1. Description of the test rig

Figure 24 shows a schematic representation of the test rig used to perform the tests.

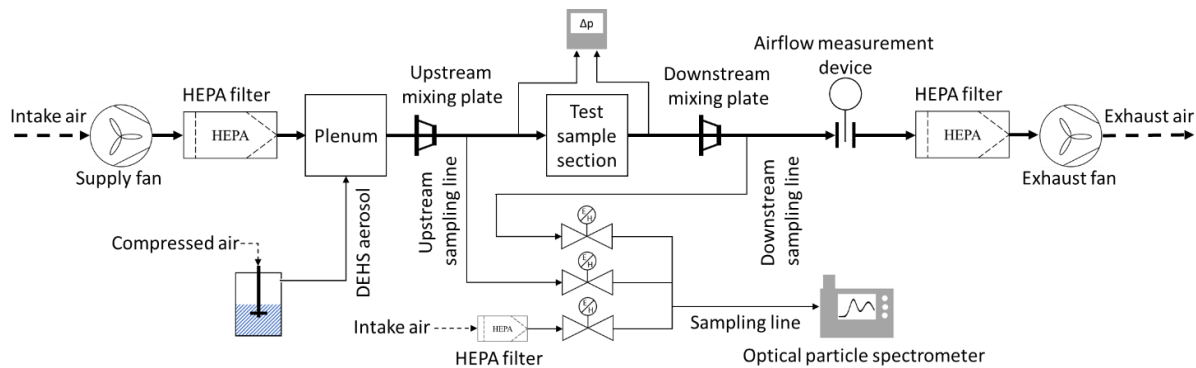


Figure 24. Schematic representation of the test rig used to perform fractional efficiency tests.

The test rig material is electrically conductive, electrically grounded, has a smooth interior finish, and is sufficiently rigid to maintain its shape at the operating pressure. This test rig was designed to meet the requirements of ISO EN 21083 “Test method to measure the efficiency of air filtration media against spherical nanomaterials — Part 1: Size range from 20 nm to 500 nm” [84]. Its dimensions are discretionary, but it meets all the requirements of qualification tests described in 3.1.2.

The test rig has two fans, one located upstream of the test sample section and the other one located downstream. Therefore, the test rig can be operated either in negative or positive pressure. All the tests were performed operating the test rig in an overpressure between 200 and 500 Pa to avoid the leaking of external particles into the duct.

A High-Efficiency Particulate Air (HEPA) filter is placed just downstream of the upstream fan to provide meager background particle count during a test. Another HEPA filter is located at the exhaust for the removal of any test aerosol that may be present in the exhaust air.



Figure 25. Test rig used to perform fractional efficiency tests



Figure 26. HEPA filter placed just downstream of the upstream fan.

A plenum of 600x600x600 mm is present to guarantee an adequate control volume to mix the test aerosol with the intake airflow. Furthermore, two mixing plates, like the shown in Figure 28, are located upstream and downstream of the test sample section to improve the mixing of test aerosol.



Figure 27. The plenum of the test rig.

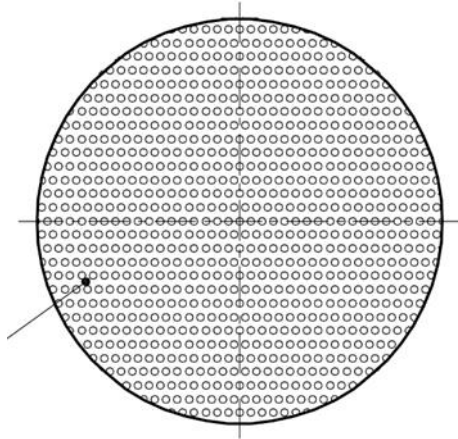


Figure 28. Representation of a mixing plate.

The airflow rate measurement was performed by using a Venturi accordance with ISO 5167-1 “Measurement of fluid flow by means of pressure differential devices inserted in circular cross-section conduits running full — Part 1: General principles and requirements” [85]. Measurement of pressure drop through the Venturi was performed at measuring points located in the test rig wall. The uncertainty of airflow rate measurement does not exceed 5 % of the measured value.

3.1.1.1. Aerosol generation system

We used a liquid phase aerosol of untreated and undiluted DiEthylHexylSebacate (DEHS) produced by a Laskin nozzle arrangement. This aerosol generator (shown in Figure 32) produces spherical particles with particle size distributions with one or more log-mean modes (Count Median Diameter – CMD – from 0.2 μm to 0.8 μm) [86], [87].

Such aerosol is intended primarily for filter efficiency measurements in the diameter range from 0.3 μm to 3.0 μm , but it also can be used up to 10.0 μm [88], [89].

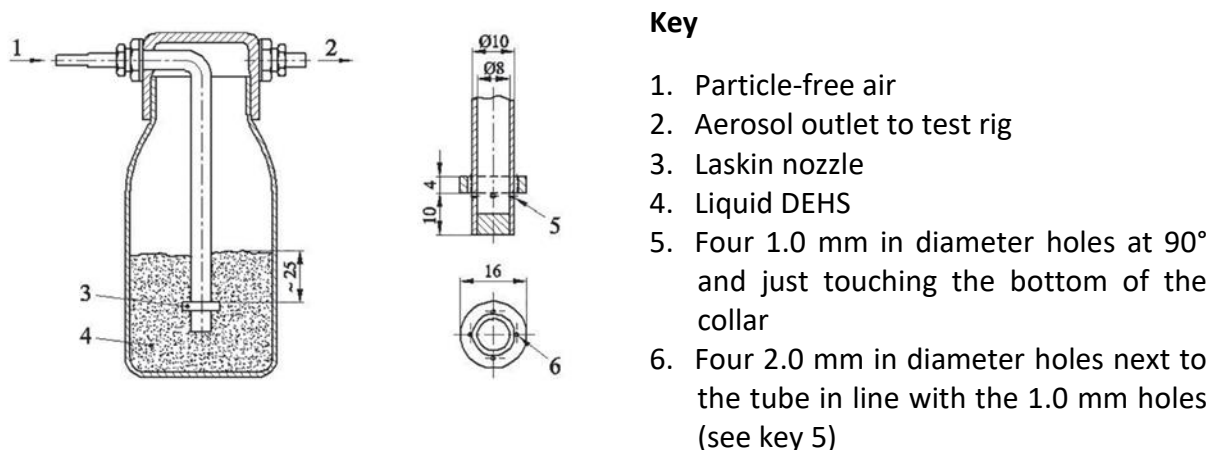


Figure 29. DEHS aerosol generator.

This aerosol generator has a single Laskin nozzle submerged below the free surface of liquid DEHS and is supplied with particle-free compressed air. The pressure of the air supply is

adjusted to yield enough particles in the test filter airflow to meet the data quality requirements specified in Section 10.3.4 of UNI PdR 90-2:2020.



Figure 30. DEHS aerosol generator of the test rig.

3.1.1.2. Aerosol sampling

The upstream and downstream sampling lines are made of rigid electrically conductive and electrically grounded tubing having a smooth inside surface and were rigidly secured to prevent movement during testing. Both sampling lines are nominally identical in geometry (bends and straight lengths) to guarantee identical particle losses by aerosol transportation.

Tapered sharp-edged sampling probes with a diameter of 9 mm are placed in the center of the upstream and downstream measuring sections. As shown in Figure 32, the sampling probes are parallel to the airflow with the inlet facing the airstream.

For sampling, a system with three one-way valves (see Figure 32) were used, because we were using a single optical particle spectrometer for sampling air from both upstream and downstream sections. The third valve is used to have particle-free air using a HEPA filter. The first measurement after a valve switched was ignored because particles could be released from the sampling system when commutating. An auxiliary pump was used to guarantee an isokinetic sampling within 10%.

Isokinetic sampling is a procedure to ensure that a representative aerosol sample enters the inlet of a sampling probe when a sample is taken from a moving gas stream. Sampling is

isokinetic when the sampling probe inlet axis is aligned parallel to the gas streams, and the gas velocity entering the tube is equal to the free flow velocity approaching the inlet. This condition is equivalent to taking a sample so that there is no distortion of aerodynamics. The isokinetic condition is essential because the concentration and size distribution of the aerosol entering the tube must be the same as those of the flowing stream.

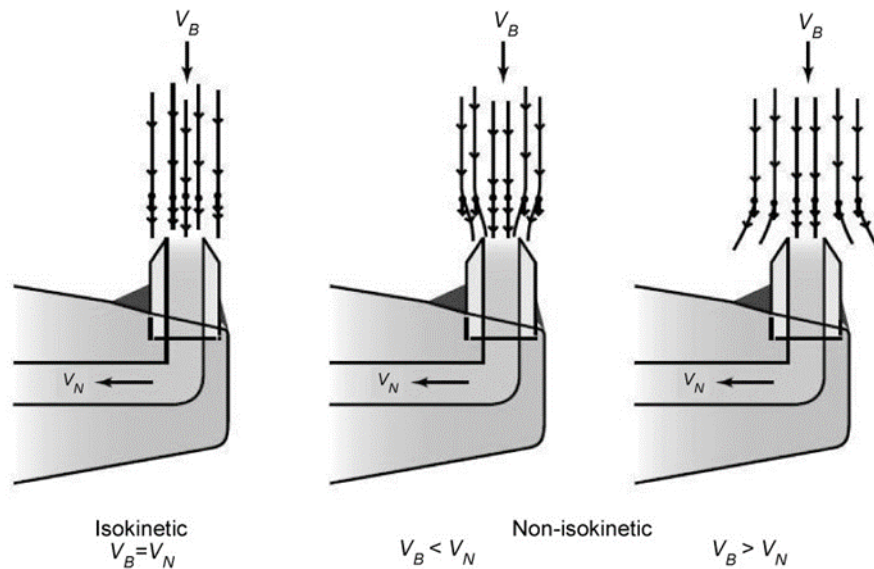
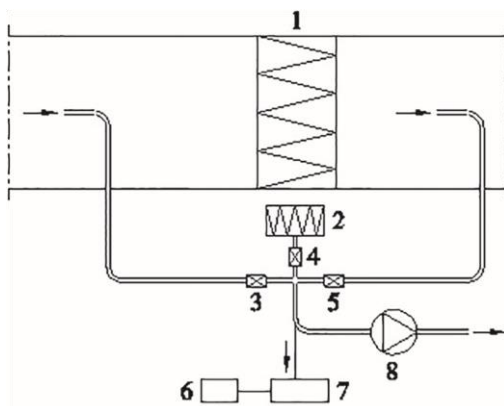


Figure 31. From left to right, isokinetic, subisokinetic, and supersokinetic sampling.



Key

- Test sample section
- HEPA filter
- Upstream valve
- Clean air valve
- Downstream valve
- Computer
- Optical particle spectrometer
- Auxiliary pump

Figure 32. Aerosol sampling system.

For all the fractional efficiency tests, we performed six sampling cycles of 45 seconds by following the procedure described below:

- 1) Installing the test sample
- 2) Starting the airflow and letting stabilize
- 3) Measuring the beginning background particle count
 - a) Purging the upstream sampling line for 45 seconds
 - b) Sampling the upstream ($B_{b,1}$) background particle count
 - c) Purging the downstream sampling line for 45 seconds
 - d) Sample the downstream (d_b) background particle count

- e) Purging the upstream sampling line for 45 seconds
- f) Sampling the upstream ($B_{b,2}$) background particle count
- 4) Starting the aerosol generator and letting stabilize
- 5) Measuring particle concentration upstream and downstream until six upstream and six downstream counts were sampled
 - a) Purging the upstream sampling line
 - b) Sampling the upstream (N_x) particle count
 - c) Purging the downstream sampling line
 - d) Sampling the upstream (D_x) particle count
- 6) Measuring the final upstream efficiency count
 - a) Purging the upstream sampling line
 - b) Sampling the final upstream (N_7) particle count
- 7) Stopping the aerosol generator and letting stabilize
- 8) Measuring the final background particle count
 - a) Purging the upstream sampling line for 45 seconds
 - b) Sampling the upstream ($B_{f,1}$) background particle count
 - c) Purging the downstream sampling line for 45 seconds
 - d) Sample the downstream (d_f) background particle count
 - e) Purging the upstream sampling line for 45 seconds
 - f) Sampling the upstream ($B_{f,2}$) background particle count
- 9) Checking the data quality requirements: Uncertainty lower than 5% and fractional efficiency curve trend following the theory (for more information, please see Appendix C)
- 10) If the data quality requirements were reasonable, stopping the airflow and remove the test device.
- 11) If the data quality requirements were not acceptable, repeating items 3) to 8)

3.1.1.3. Particle spectrometer and size distribution measurement

To perform the fractional efficiency measurements, we used two different models of optical particle spectrometers. These instruments count the particles and determine their optical diameter based on the phenomenon of light scattering. When an incident light beam illuminates a particle, the intensity of the light scattered from the particle at a given angle is calculable. It depends on its diameter and its refraction index [90].

Particle spectrometer divides the size spectrum into “channels” whose lower and upper limits are defined in Table 2 from 0.09 to 10.0 μm . The limits for each channel do not overlap with its neighbors. Hence the total number of counts output from a run matches the count, which would have been obtained if the lower size limit had been the minimum size and the upper size limit had been the maximum size the spectrometer can detect.

The instrument output is a histogram representing the particle size distribution subdivided into channels with user-defined boundaries.

- PMS LAS-X II [91]: It can be used to measure the particle size range from 0.09 μm to 7.5 μm , with a user-set sampling airflow rate in the range from 10 to 100 cm^3/min .
- TSI OPS 3330 [92]: It can be used to measure the particle size range from 0.30 μm to 10.0 μm , with a fixed sampling airflow rate of 1000 cm^3/min .

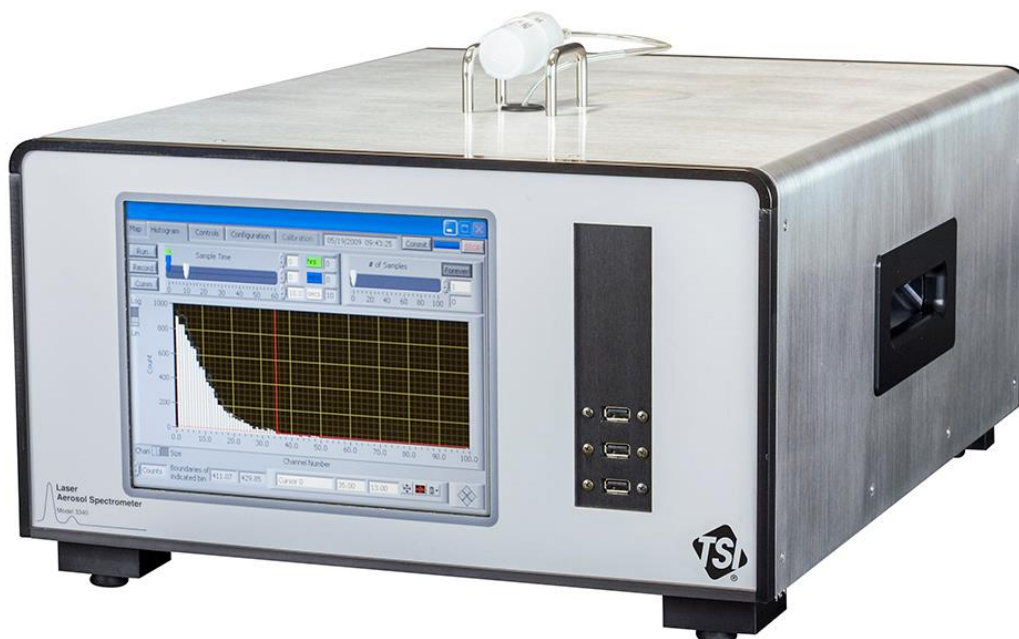


Figure 33. PMS LAS-X II, also known as TSI OPS 3340.



Figure 34. TSI OPS 3330.

For the particle size range, we used an arrangement like the prescribed by ISO 1690-2:2016, which has twelve logarithmically spaced particle size channels. However, we started at 0.09 μm to have a total of 18 logarithmically spaced particle size channels with the scope to study the behavior of filtering materials below 0.3 μm .

Table 2. Particle size range used during tests.

Size range	Lower limit [μm]	Upper limit [μm]	Geometric mean particle size limit [μm]
1	0.09	0.10	0.09
2	0.10	0.12	0.11
3	0.12	0.15	0.13
4	0.15	0.20	0.17
5	0.20	0.25	0.22
6	0.25	0.30	0.27
7	0.30	0.40	0.35
8	0.40	0.55	0.47
9	0.55	0.70	0.62
10	0.70	1.00	0.84
11	1.00	1.30	1.14
12	1.30	1.60	1.44
13	1.60	2.20	1.88
14	2.20	3.00	2.57
15	3.00	4.00	3.46
16	4.00	5.50	4.69
17	5.50	7.00	6.20
18	7.00	10.00	8.37

3.1.2. Qualification tests of the test rig

To ensure the reliability of data obtained by using the described test rig, we have run several qualification tests. The principal scope of this test is providing to the user a way to check the system regularly and keep it in good operating order.

Table 3 specifies a list of all the qualification tests that were performed. A detailed explanation of each of these is available on UNI PdR 90-2:2020. The following are the basic qualification test that shall be performed.

OPC — Overload test: OPCs may underestimate particle concentrations if their particle concentration limit is exceeded. Therefore, it is necessary to know the concentration limit of the OPC being used. The maximum aerosol concentration used in the tests shall then be kept sufficiently below the concentration limit so that the counting error resulting from coincidence does not exceed 5 %. To ensure that there is no overload when performing measurements, we carried out all the tests using an upstream particle concentration between 12% and 32% of the instrument overload.

Test rig — Correlation ratio: The correlation ratio is a test to correct any bias between the upstream and the downstream sampling system when performing a fractional efficiency measurement. This test consists of measuring the particle count upstream and downstream of the test device section with the aerosol generator turned on but without any filtering media in the test device section. In theory, without a device that removes particles in the test device section and if there are no leakages, the particle concentration upstream and downstream should be substantially the same. Section 10.3.3 of UNI PdR 90-2:2020 reports the maximum acceptable bias of the sampling system for each channel. We corrected the particle concentration of all the fractional efficiency measurements with correlation ratio values within the limits of UNI PdR 90-2:2020. The correlation ratio tests were performed with the same conditions and test rig configuration than the fractional efficiency test.

Table 3. Qualification tests performed.

Qualification testing	Subclause of UNI PdR 90-2:2020	Requirement
Test rig — Pressure system testing	8.2.1	No change in Pa
OPC — Airflow rate stability test	8.2.2	<5 % of the set sample air flow rate
OPC — Zero test	8.2.3	<2 % between U/S and D/S <10 counts per minute from 0,30 μm to 10,0 μm
OPC — Sizing accuracy	8.2.4	Relative to the max in the appropriate channel
OPC — Overload test	8.2.5	No predetermined level
Aerosol generator — Response time	8.2.6	No predetermined level
Test rig — Air leakage test	8.2.7	<1 %
Test rig — Aerosol uniformity	8.2.8	CV < 15 %
Test rig — Empty test device section pressure	8.2.9	<5 Pa
Test rig — 100 % efficiency test	8.2.10	>99 % for all particle sizes
Test rig — Correlation ratio	8.2.11	0.30 μm to 1.0 μm : 0.90 to 1.10 1.0 μm to 3.0 μm : 0.80 to 1.20 3.0 μm to 10.0 μm : 0.70 to 1.30

3.1.3. Resistance to airflow

Since the tested samples were fixed to an adapter, measuring the resistance to airflow was performed with another instrument to avoid any kind of bias that could be introduced by adapters. This instrument was the TEXTEST FX 3300 LabAir IV [93], which is usually used to measure the air permeability of flat sheets of materials.

For the case of surgical masks, we measured the resistance to airflow at 27,2 cm/s by using a head adapter with a surface of 5 cm², a procedure very similar to the one described by EN 14683 standard.

For the case of respirators, we tried to fulfill the requirements of EN 149 that prescribed a fixed airflow rate by estimating the surface of each sample. With these two values, we calculated the face velocity of each sample and measured this value to measure the resistance to airflow.

3.1.4. Size-resolved efficiency

The filtration efficiency as a function of the particle size of a filtering media is determined by measuring the number of particle concentration upstream and downstream of the sample. The fractional penetration P represents the fraction of aerosols that have passed through the filtering media:

$$P_{ps} = \frac{D_{ps}}{U_{ps}} \quad (1)$$

D_{ps} : is the downstream number particle concentration for particle size, ps ;

U_{ps} : is the upstream number particle concentration for particle size, ps .

Fractional efficiency E_{ps} is defined by:

$$E_{ps} = 1 - P_{ps} = 1 - \frac{D_{ps}}{U_{ps}} \quad (2)$$

When using a single OPC to sampling particle concentration by using the scheme showed in Figure 32, the count is made by alternating between upstream and downstream sampling probes with equal sampling time, as shown in Figure 35.

Background, beginning				Gen On	1	2	3	4	5	6	7	8	9	10	11	Gen Off	Background, final			
U/S	Purge	$B_{b,1,ps}$	Purge		Purge	$N_{1,ps}$	Purge	$N_{2,ps}$	Purge	$N_{3,ps}$	Purge	$N_{4,ps}$	Purge	$N_{5,ps}$	Purge		Purge	$B_{f,1,ps}$	Purge	$B_{f,2,ps}$
D/S			$d_{b,ps}$			$D_{1,ps}$		$D_{2,ps}$		$D_{3,ps}$		$D_{4,ps}$		$D_{5,ps}$					$d_{f,ps}$	

Figure 35. Single OPC counting cycle with five sampling cycles.

For a single OPC system, the upstream counts from two samples shall be averaged to obtain an estimate of the upstream counts that would have occurred at the same time as the downstream counts were taken.

For the upstream beginning and final background counts:

$$U_{B,b,ps} = \frac{B_{b,i,ps} + B_{b(i+1),ps}}{2} \quad (3)$$

$$U_{B,f,ps} = \frac{B_{f,i,ps} + B_{f(i+1),ps}}{2} \quad (4)$$

where

$U_{B,b,ps}$: is the beginning upstream background average count for particle size, ps ;

$U_{B,f,ps}$: is the final upstream background average count for particle size, ps ;

$B_{b,i,ps}$: is the measured beginning upstream background count for particle size, ps ;

$B_{f,i,ps}$: is the measured final upstream background count for particle size, ps .

The upstream background counts before and after the efficiency or correlation samples shall simply be averaged.

$$U_{B,c,ps} \text{ o } U_{B,ps} = \frac{U_{B,b,ps} + U_{B,f,ps}}{2} \quad (5)$$

where

$U_{B,ps}$: is the upstream background average count for efficiency sample, i , and for particle size, ps ;

$U_{B,c,ps}$: is the upstream background average count for correlation sample, i , and for particle size, ps ;

$U_{B,b,ps}$: is the beginning upstream background average count for sample, i , and particle size, ps ;

$U_{B,f,ps}$: is the final upstream background average count for sample, i , and particle size, ps .

The downstream background counts before and after the efficiency or correlation samples shall simply be averaged.

$$D_{B,c,ps} \text{ o } D_{B,ps} = \frac{d_{b,ps} + d_{f,ps}}{2} \quad (6)$$

where

$D_{B,ps}$: is the downstream background average count for efficiency sample, i , and for particle size, ps ;

$D_{B,c,ps}$: is the downstream background average count for correlation sample, i , and for particle size, ps ;

$d_{b,ps}$: is the beginning downstream background average count for particle size, ps ;

$d_{f,ps}$: is the final downstream background average count for particle size, ps .

For the upstream efficiency counts:

$$U_{i,ps} = \frac{N_{i,ps} + N_{(i+1),ps}}{2} \quad (7)$$

where

$U_{i,ps}$: is the upstream efficiency average for sample, i , and for particle size, ps ;

$N_{i,ps}$: is the measured upstream efficiency count for sample, i , and particle size, ps .

3.2. Tested samples description

Due to the COVID-19 pandemic, the task force of Politecnico di Torino designated the Aerosol technology lab of the Energy Department to help face mask manufacturers to assess the performance of their products. In this way, all the tested samples were treated as potential surgical masks or potential respirators.

Our measurements were not intended to certify face masks following current test methods, but to judge if a face mask could pass the prescribed tests to start the certification procedure in an accredited laboratory.

We receive a total of 424 samples, from which 21 were not tested because their resistance to airflow was too high. From the 403 tested samples, we will show the data of 348 ones of them. The refining was made by taking into account only the samples with both the fractional efficiency curve and the resistance to airflow values. This data set is form by 251 samples tested as surgical masks and 97 samples tested as respirators. Figure 36 shows a pie chart of received and tested samples.

In the case of surgical masks samples, we cut their strips to create a flat sheet sample. Then, treated samples were attached with tape to adapter plates, as shown in Figure 37.

In the case of respirators, we fixed the hole face mask to adapter plates by using either hot glue or mastic butilic, as shown in Figure 38.

Unfortunately, most of the manufactures did not provide any data on the characteristics of materials that compose their products. In some of the cases because they did not know any type of data more than the name of the material or the name of the final product.

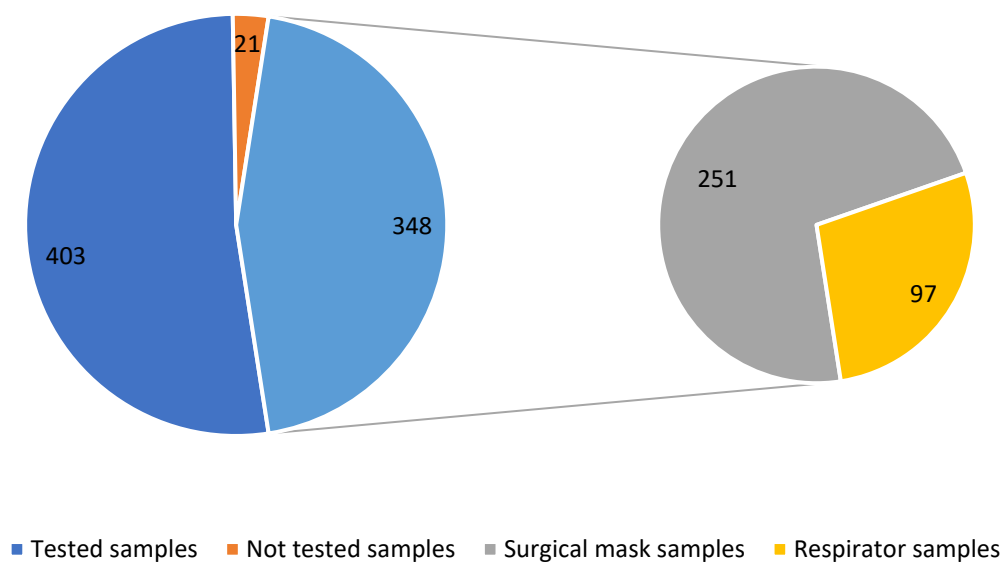


Figure 36. Pie chart of received and tested samples.

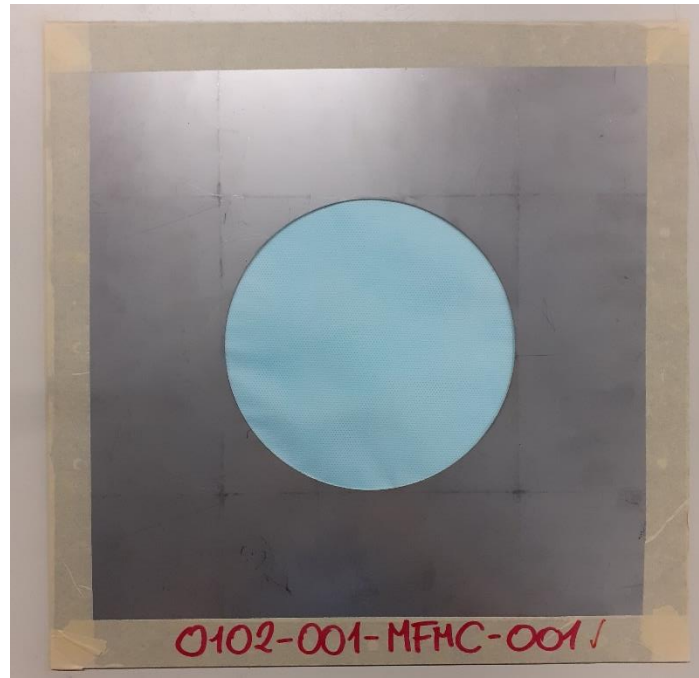


Figure 37. Surgical mask samples fixed to an adapter plate.



Figure 38. Respirators samples fixed to adapter plates.

4. EXPERIMENTAL DATA AND DISCUSSION

Figure 39 shows all the fractional efficiency curves that were measured during our study. There is a broad spectrum of filtration efficiency. For instance, at 1 μm , samples have an efficiency that varies from almost zero to 100%.

As described in Section 3.2, most tested samples correspond to surgical masks. Therefore, their fractional efficiency measurements started at 0.3 μm . Just a few samples of surgical masks were measured down to 0.09 μm .

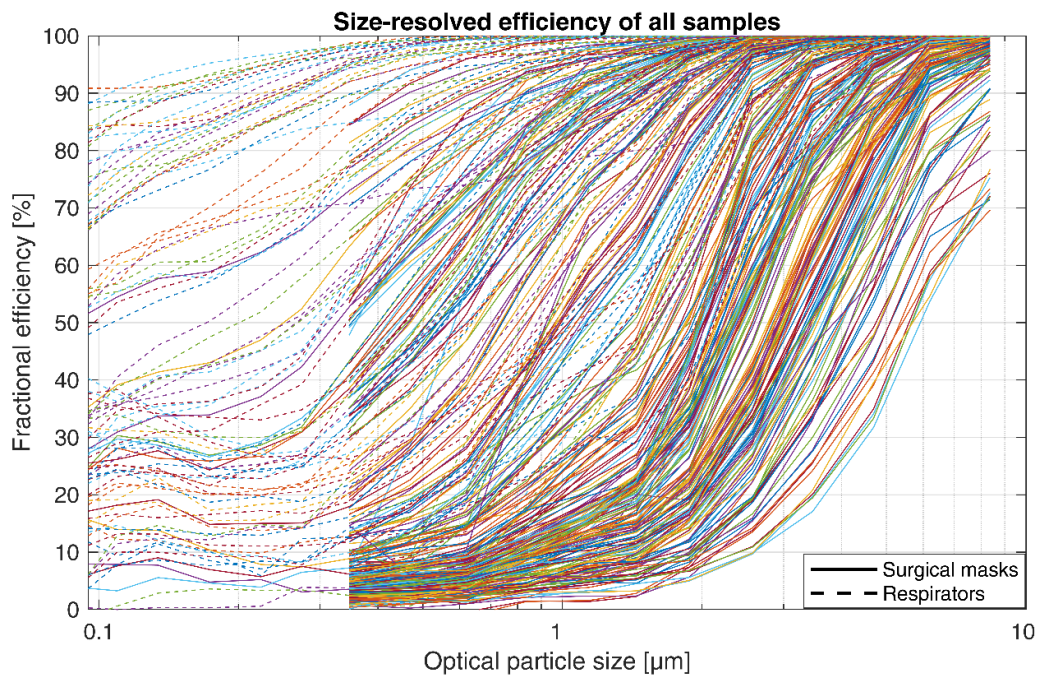


Figure 39. Fractional efficiency curves of all the tested samples.

To improve the understanding of the behavior of surgical masks and respirators, we subdivide the data showed in Figure 39 into two different figures.

Figure 40 shows the data corresponding to surgical masks, and Figure 41 shows the data corresponding to respirators. The dashed line on each figure corresponds to the fractional efficiency curve of typical surgical masks and respirators that fulfill all the prescribed requirements of European standards.

Comparing their behavior, the filtration performance of respirators seems to be higher than the one of surgical masks, as expected. For instance, at 3.0 μm , the filtration efficiency of respirators starts at around 45% in comparison to almost 15% of surgical masks. Furthermore, at 10.0 μm , almost all respirators samples achieve a filtration efficiency equal to 100%.

Viewing dashed lines, almost any of the samples could be classified as surgical masks per EN 14683 nor respiratory protective equipment per EN 149. Therefore, all these devices with a lower performance would be classified as “Community face coverings,” even if their performance varies so much, in some cases been almost zero.

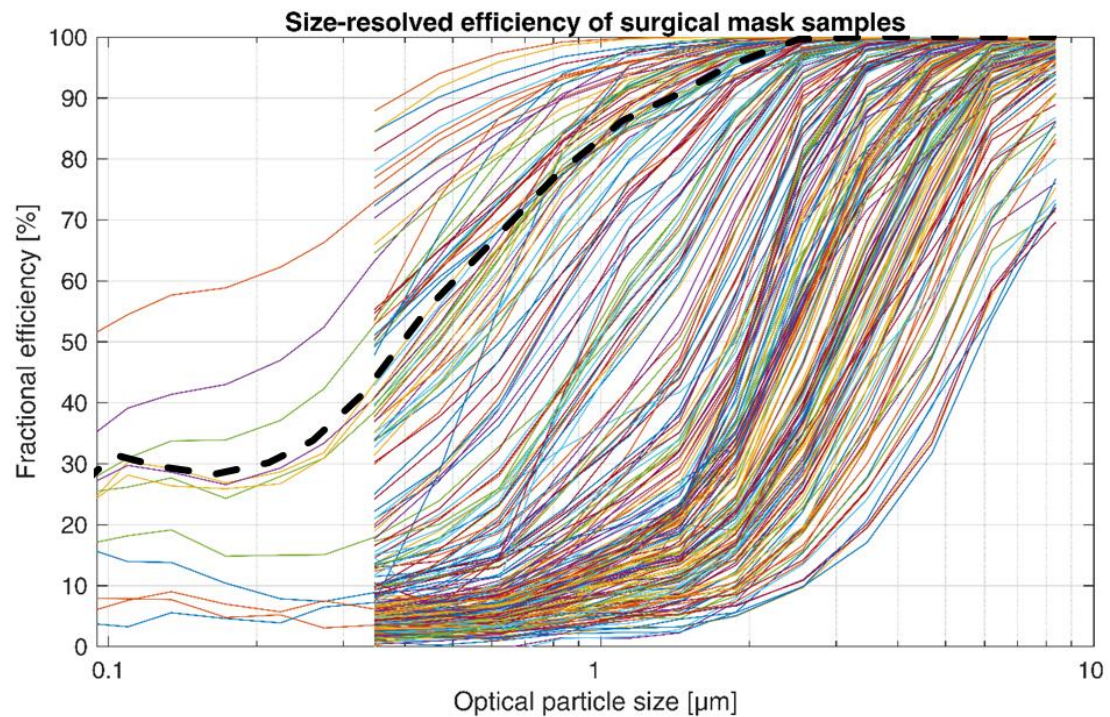


Figure 40. Fractional efficiency curves of tested surgical masks.

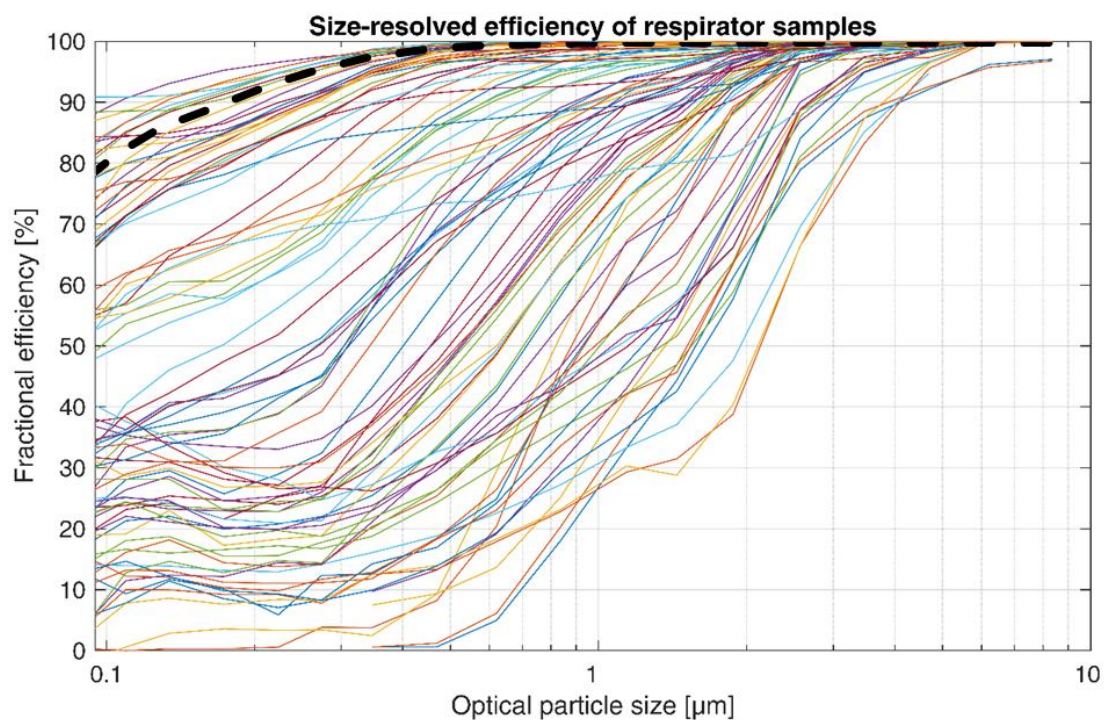


Figure 41. Fractional efficiency curves of tested respirators.

4.1. Comparison of performance of woven vs non-woven

Since face masks can be made up of woven and non-woven materials (or of a combination of these), we analyzed the performance of face masks made up of these materials. Figure 42 summarized the fractional efficiency data Table X shows SEM figures of each analyzed sample.

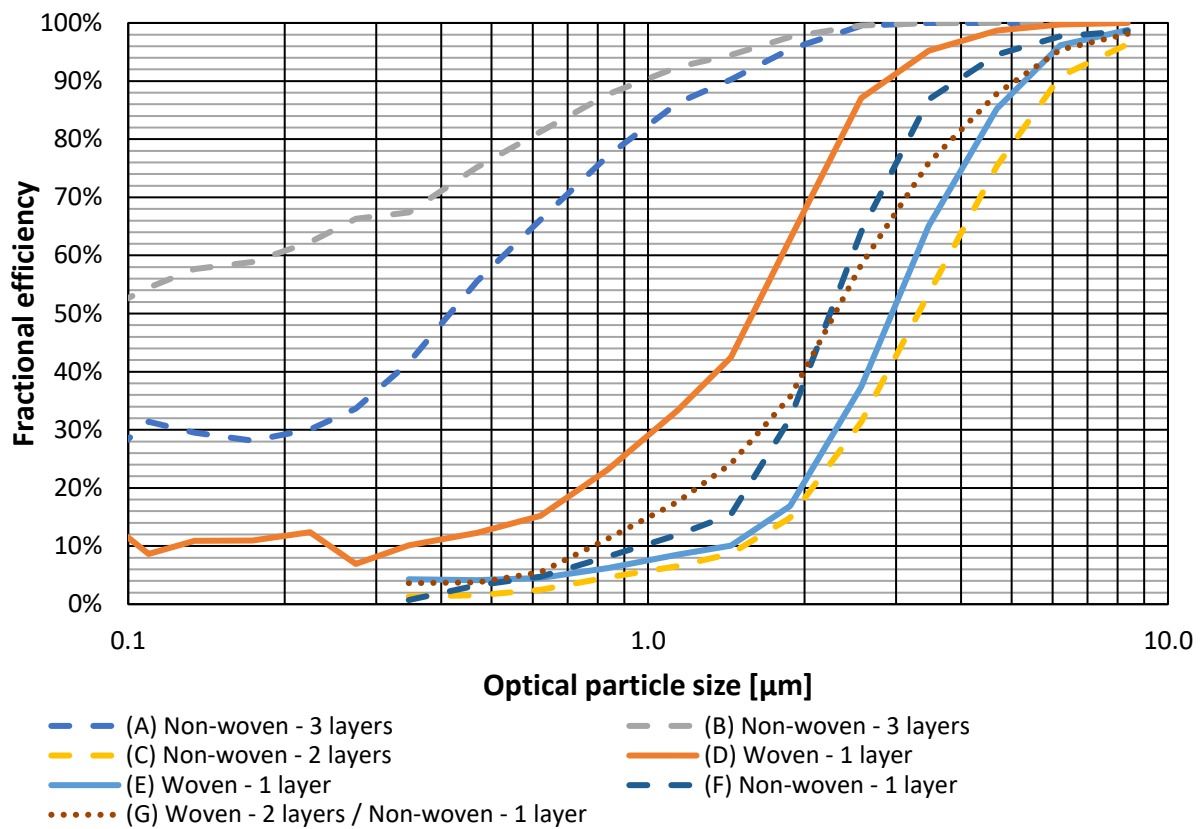
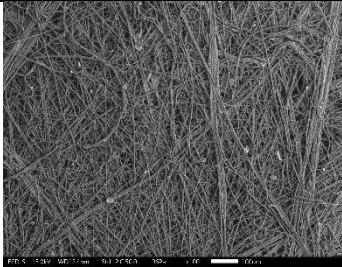
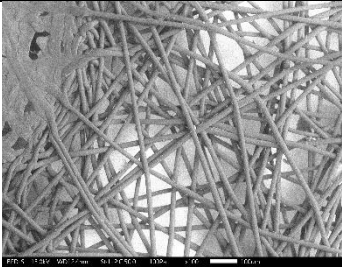
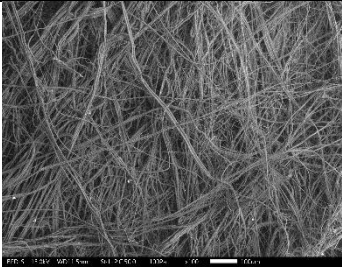


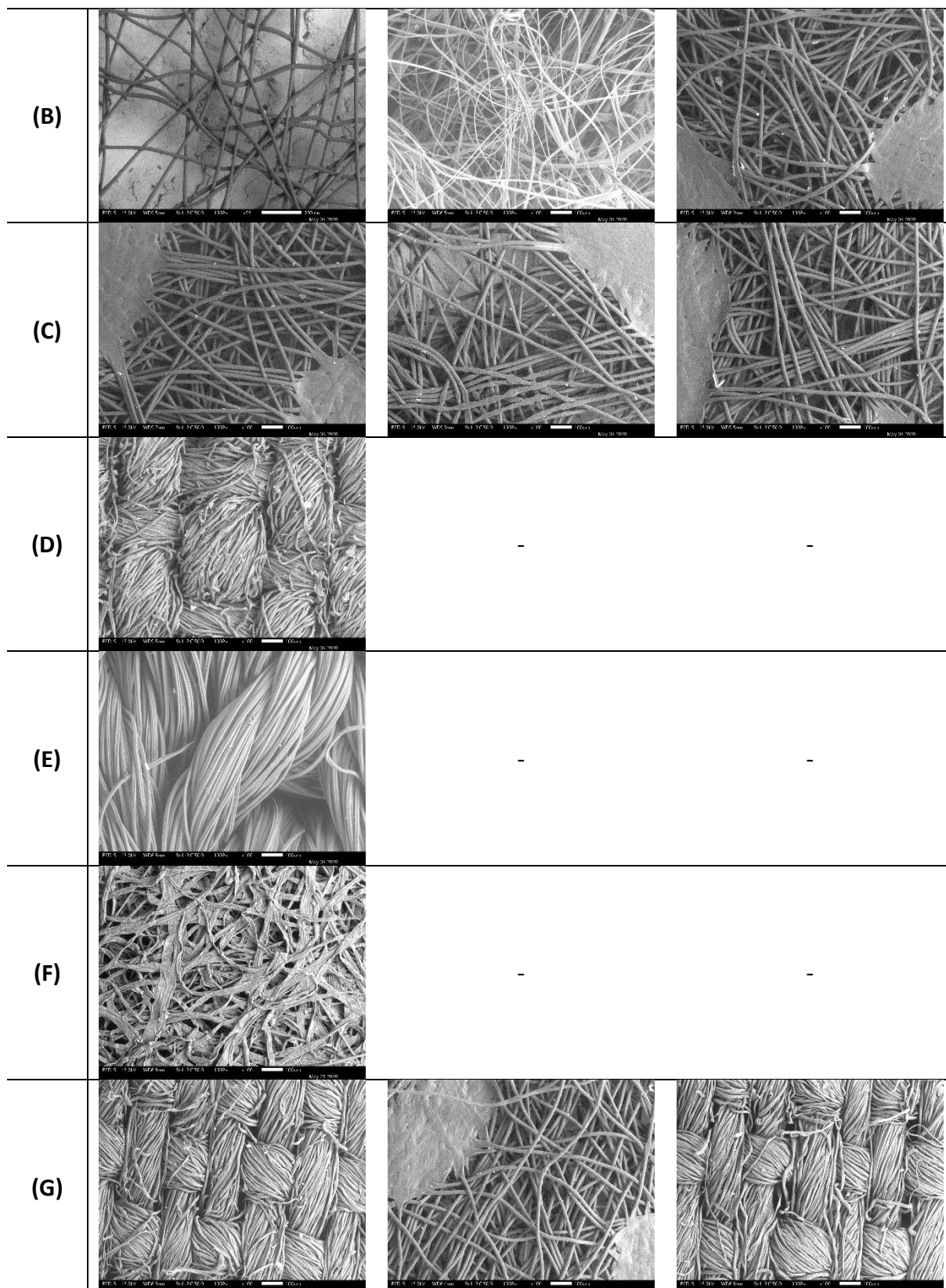
Figure 42. Fractional efficiency curve of samples made up of non-woven and woven materials.

The first thing to notice about Figure 42 is that performance of non-woven materials is not always better than the one of woven materials. For instance, in this chart, we can see that the best and the worst fractional efficiency curves correspond to non-woven materials. Furthermore, in some cases, woven materials are better than non-woven ones.

Another thing to notice is that above 10.0 μm filtration efficiency is almost 100% for all the samples, which means that to contain large droplets, both woven and non-woven materials can be used.

Table 4. SEM figures of tested samples at 100X.

ID	Layer 1	Layer 2	Layer 3
(A)			



4.2. Correlation between resistance to airflow and filtration efficiency

To properly evaluate the performance of a material, it is necessary to consider both filtration efficiency and resistance to airflow. A useful quantity to express performance by considering both parameters is the Quality Factor (Please, see C.2 of Appendix C for more information).

It is essential to mention that to compare the quality factors values between them; all the samples shall be tested at the same conditions during both fractional efficiency test and resistance to airflow test. Consequently, in this study, we cannot compare the quality factor values of surgical masks with the ones of respirators because these were tested under different conditions.

Figure 44 shows the quality factor values for surgical masks samples. These values were calculated by integrating the full fractional efficiency curve with the number particle size distribution showed in Figure 43 (Such particle size distribution is within prescribed limits of EN 14683) and by using the resistance to airflow at a face velocity of 27,2 cm/s.

Analyzing Figure 44, it is evident that there is a high-performance variability between the tested surgical masks, but almost all of them fall between 0.04 and 0.08 1/Pa. This behavior is by filtration theory because usually, a material with a high filtration capacity has a high resistance to airflow and the inverse.

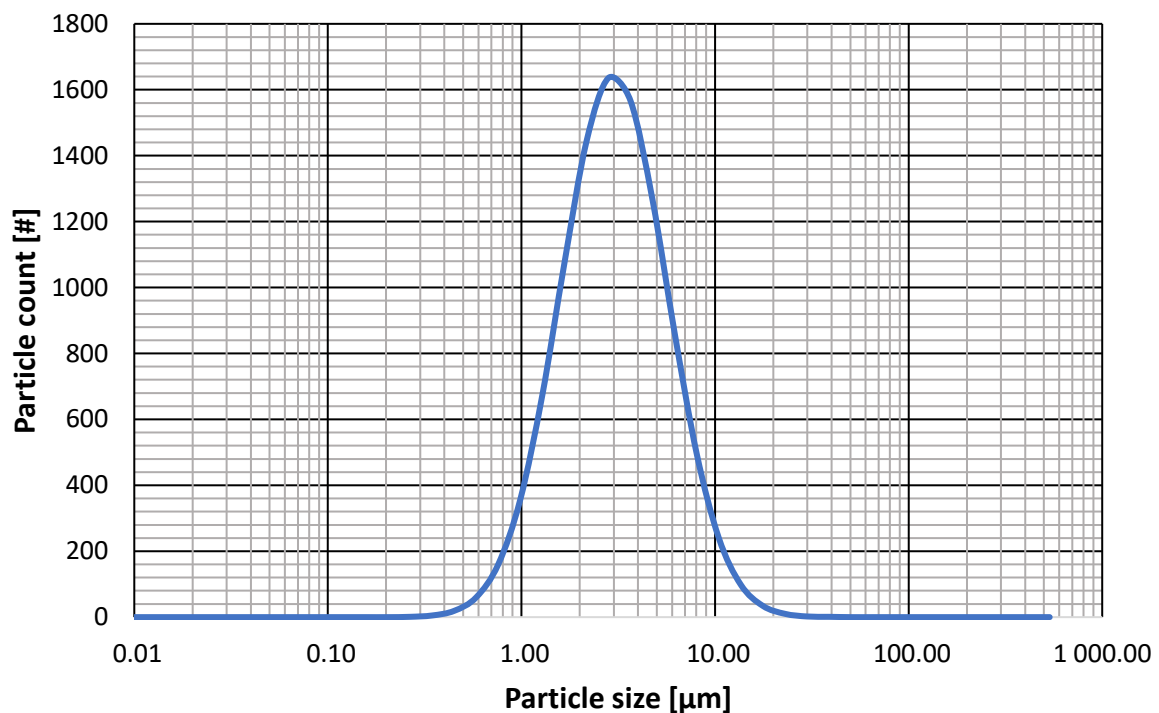


Figure 43. Reference number particle size distribution used to integrate surgical masks fractional efficiency curves. Count media diameter equal to 3.0 μm, geometric standard deviation equal to 1.89, and particle count equal to 10 000 particles.

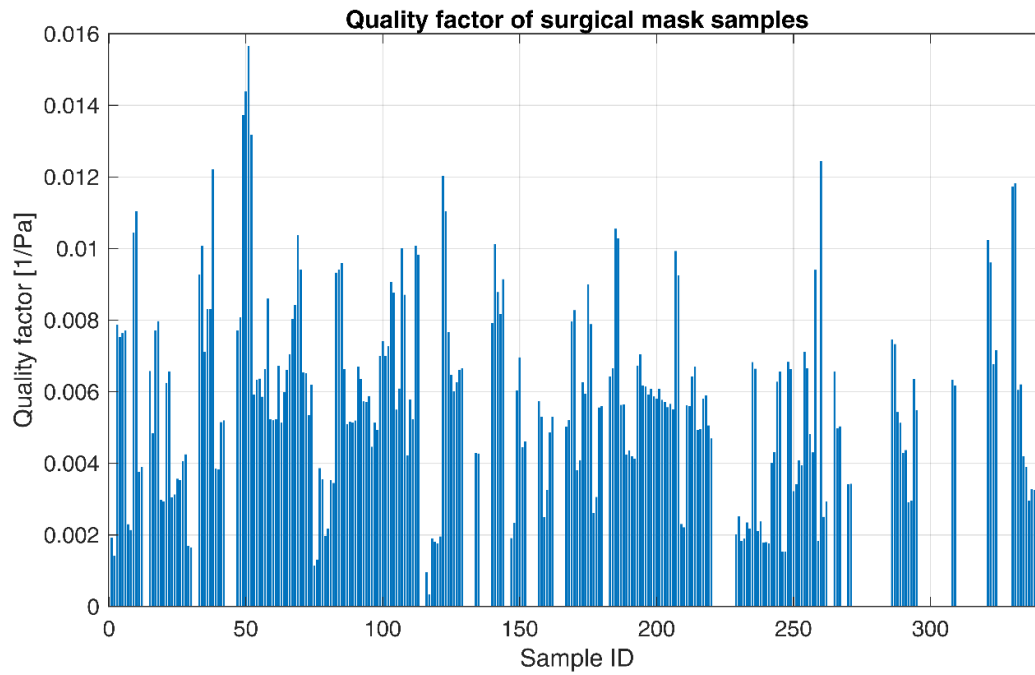


Figure 44. Quality factors of tested surgical masks.

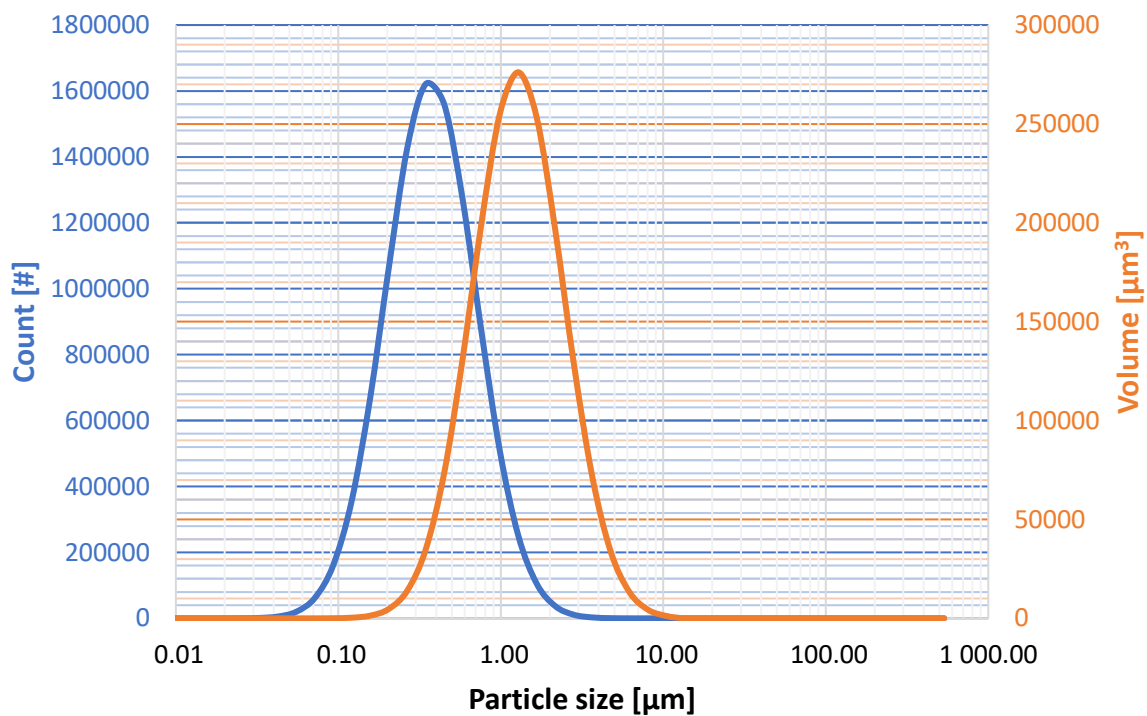


Figure 45. Number and volume particle size distribution used to integrate respirators fractional efficiency curves with paraffin oil aerosol. Count media diameter equal to $0.37 \mu\text{m}$ and geometric standard deviation equal to 1.9.

Figure 47 shows the quality factors of respirators. These values were calculated by integrating the full fractional efficiency curve with the volume particle size distributions showed in XX and XX and by using the resistance to airflow at 95 l/min.

Analyzing Figure 47, we can see that there is not an apparent behavior for the tested devices. Just a few samples have a high quality factor in comparison to others.

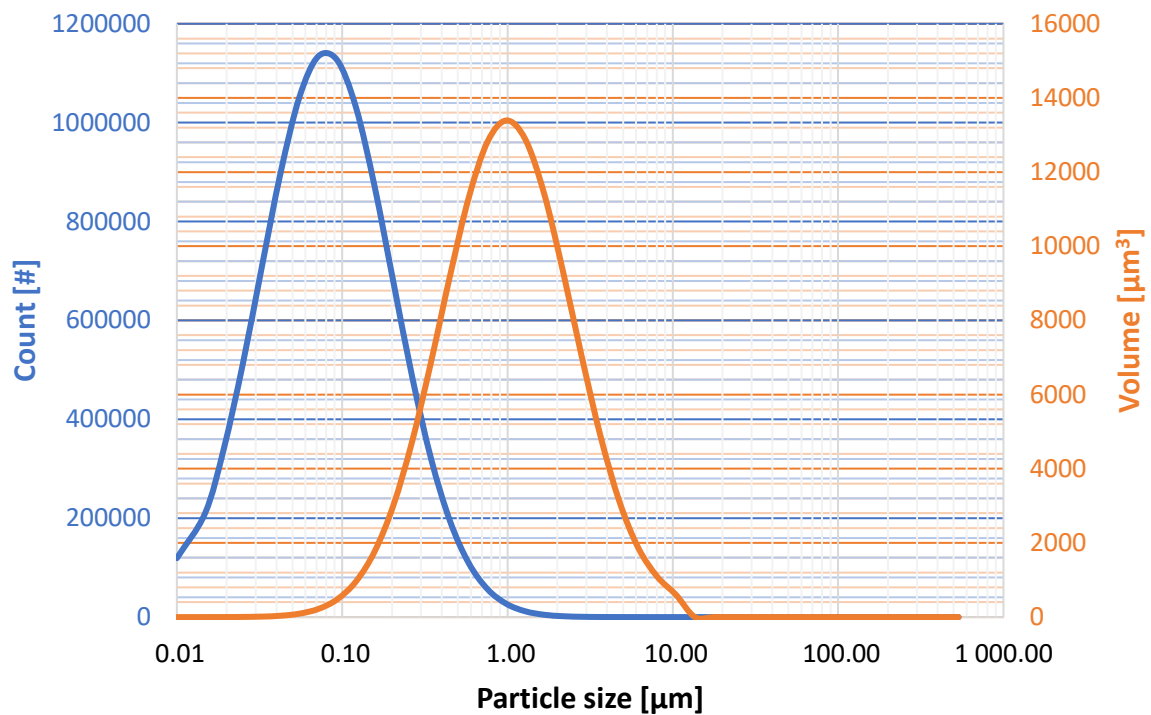


Figure 46. Number and volume particle size distribution used to integrate respirators fractional efficiency curves with NaCl aerosol. Count media diameter equal to 0.08 μm and geometric standard deviation equal to 2.5.

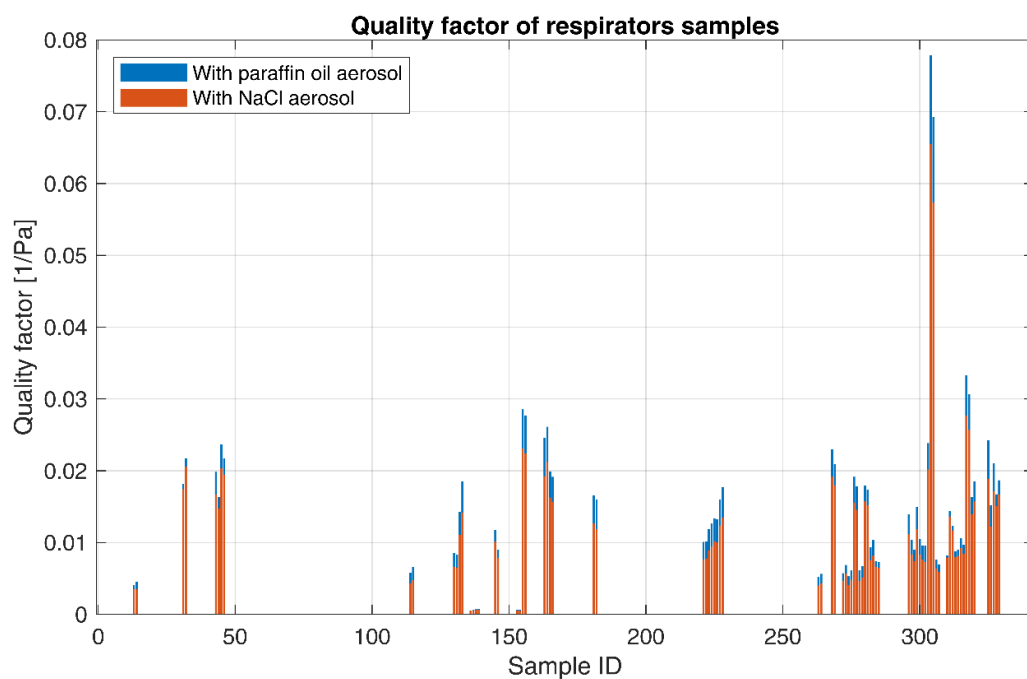


Figure 47. Quality factors of tested respirators.

4.3. Proposed classification

Since representing the performance of filtering materials as a curve is not convenient for rating them, it is necessary to transform the measured curve into a single value. There is not a clear opinion in which is the better way to do this, but the most fundamental approaches are:

- Studying a single size as a reference, for example, the filtration efficiency at 3.0 μm as suggested by CWA 17553:2020 (i.e., the European reference test method for community face coverings). The problem with this approach is that it does not consider the behavior above or below the reference size.
- It was integrating the fractional efficiency curve by using a reference particle size distribution. This is a much-complicated approach, but it considers either the full behavior of fractional efficiency curve in a specific particle size range and the characteristic of challenging aerosol that would be present at upstream of the tested device. This is the approach proposed by UNI PdR 90:2020. From a mathematical point of view, this approach is very similar to calculate a weighted average by averaging fractional efficiency values and weighting with a reference particle size distribution.

The second approach seems to be the most proper to be used. However, it is necessary to define two essential parameters: (1) The particle size range and the (2) characteristics and type of particle size distribution.

Regarding particle size range, the UNI PdR 90:2020 defines boundaries between 1.0 μm and 3.0 μm because. Regarding particle size distribution, UNI PdR 90:2020 prescribes the use of a mass integration by having a uniform number particle size distribution. Figure 48 shows a graphical representation of this distribution.

Having such distribution means that larger particles have a higher impact than smaller ones because of the mass increase with a third-grade moment. This is much more evident in Figure 49, where the height at 3.0 μm is around 30 times higher than the one at 1.0 μm . Therefore, this approach could obtain data very similar that the one would be obtained by applying CWA 17553:2020, but by considering the fractional efficiency curve and by using a reference particle size distribution.

Another advantage of this approach is that reference particle size distribution can be changed for a most proper one (for example, using the particle size distribution of aerosol generated by humans), but without changing the test method.

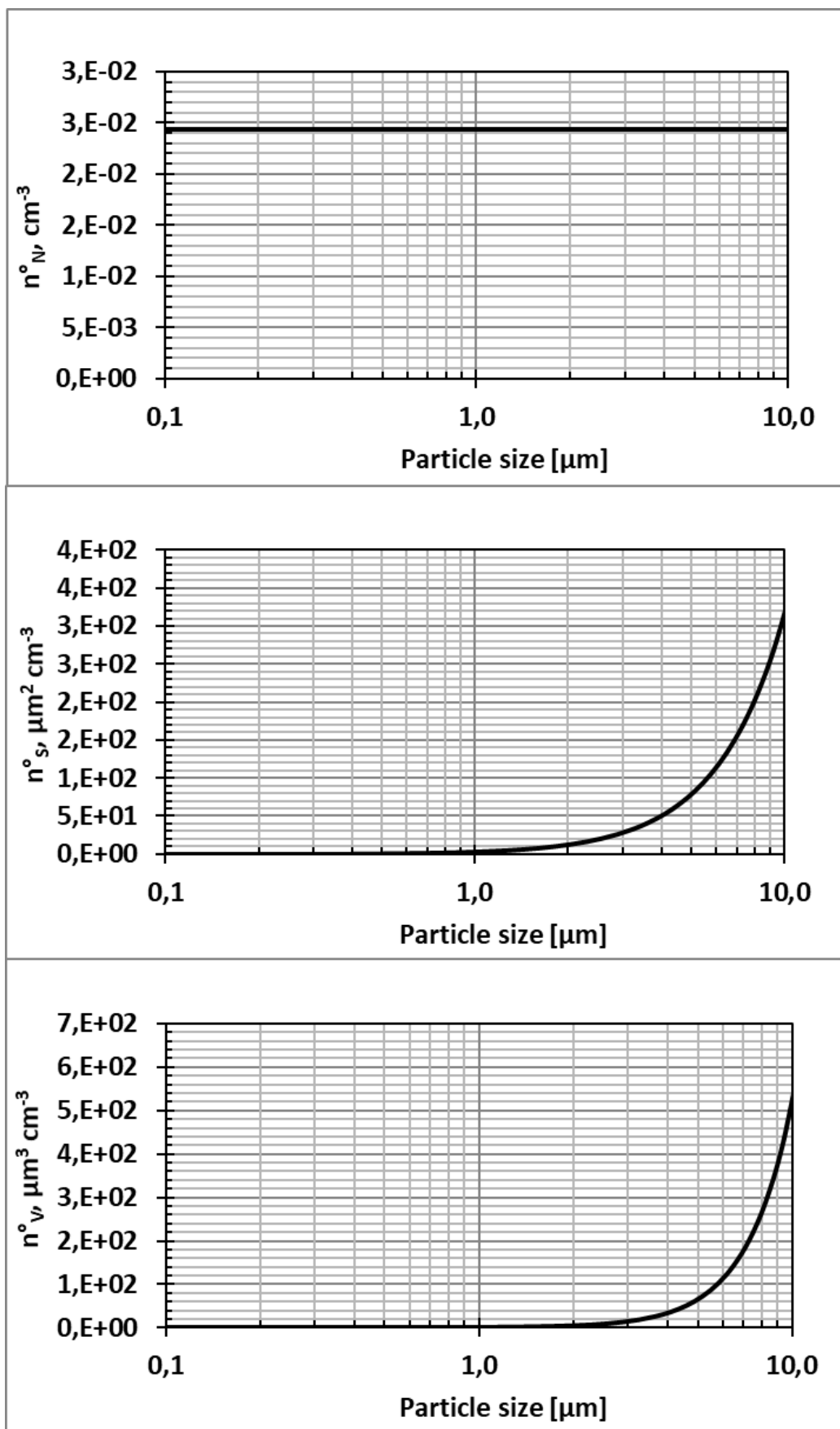


Figure 48. From top to bottom number, surface, and volume reference particle size distribution of UNI PdR 90:2020.

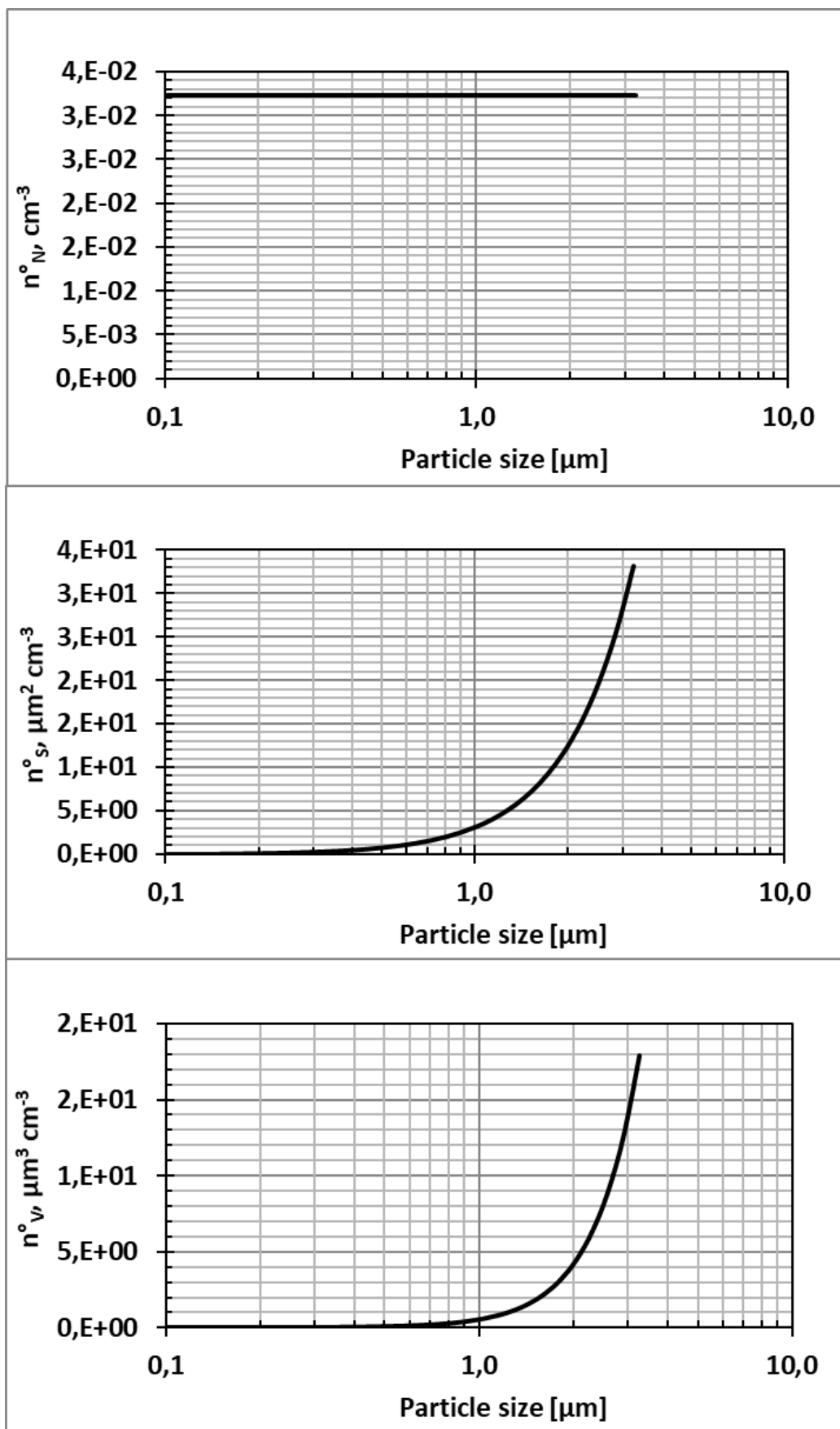


Figure 49. From top to bottom number, surface, and volume reference particle size distribution of UNI PdR 90:2020 represented till 3.0 μm .

4.4. Rating by using a reference particle size distribution

By using the procedure described in Section 4.3, we calculated the eCommunityFaceCovering rating (eCFC rating) for each sample by using its fractional efficiency curves. The results are summarized in Figure 50.

The first thing to notice is that the eCFC rating can vary in a wide range, as expected from the results showed in Figure 39.

We subdivided each sample by following the legend of Figure 51. In this case, the green bars represent the samples that cannot be classified as surgical masks neither as respirators by current European standards, but that could be classified as community face coverings per UNI PdR 90:2020. Please, notice that samples that would pass European standards (orange and yellow bars) are above the threshold of UNI PdR 90:2020. Therefore it could also be classified as a community face coverings.

Hence, this confirms that the new type of face coverings is a step below surgical masks and respirators, as expected.

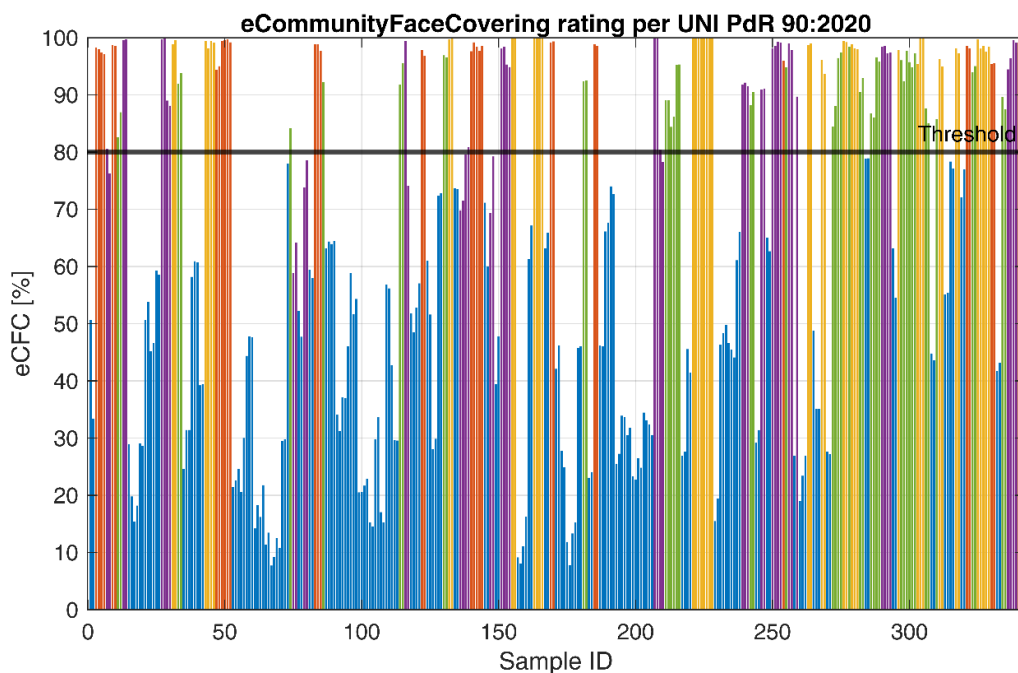


Figure 50. eCFC rating for all tested samples.

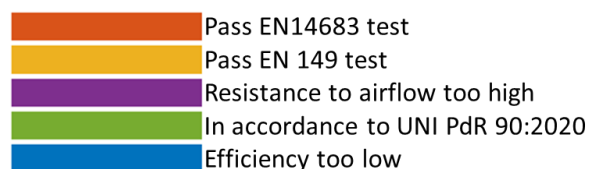


Figure 51. Legend of Figure 50.

5. CONCLUSIONS

As shown by the experimental results, face masks (i.e., surgical masks, respirators, and community face coverings) have an extensive range of filtering performance. We have found that in some cases, filtration efficiency can vary from almost zero to almost 100%.

The comparison of filtering performance of non-woven vs woven materials provided results that do not suggest any clear trend. In some cases, non-woven materials were both the best and the worst material in terms of fractional efficiency.

From SEM images, we have noticed that fibers of woven materials are very much larger than the ones of non-woven materials. Furthermore, by studying tested samples (i.e., samples challenged by aerosol), we have found that the former removes particles by sieving (a.k.a. surface filtration) and the latter by depth filtration.

Our innovative test method demonstrated to be a valid approach to screen face masks with lower efficiency than standardized face masks (i.e., surgical masks and respirators). We were able to differentiate in a specific way which face masks could be classified as community face coverings and which shall not.

Furthermore, this test method has many advantages in comparison with current standardized test methods for face masks. The most important are:

- The use of an inert liquid aerosol that could be used by any laboratory, and that can simulate the droplets of saliva properly.
- In contrast to photometer, proposed instrumentation to determine particle concentration is readily available on the market and represents the current state-of-art of current.
- It can provide removal efficiency by particle size in less than 30 minutes and providing data with specific statistical uncertainty. Furthermore, providing the fractional efficiency data, we can compare the performance of different materials in an improved way.
- It can be performed in a typical laboratory by using instrumentation commonly used for assessing the performance of air filtering media and devices (EN ISO 16890 and EN ISO 21083 series).
- The rating system can be adapted easily, just changing the reference particle size distribution, but without changing the test method. For example, someone could use as reference the particle size generated by humans when coughing, but the test methods to obtain a fractional efficiency curve could be the same.

The proposed test methods can be applied to any face mask (i.e., surgical masks, respirators, and community masks), allowing the comparison of their performance. This means that a manufacturer would be able to assess the possibility of face masks to fulfill prescribed requirements for different European standards by performing a single test.

6. ACKNOWLEDGMENTS

I would like to especially thank my tutor and boss, Prof. Paolo Tronville, for his support during the last years. He inspired my interest in the Aerosol Technology field, and he was instrumental in defining the path of my research.

I would like to thank my tutor, Prof. Valeria Chiono, for her guidance through each stage of the process. Even if this is her job, I would like to express thanks because she made a great effort to help me to conclude this phase of my professional career.

Furthermore, I would like to pay my special regards to the Aerosol Technology Research Group of the Energy Department, especially to Luis Medina, Geraldine Torres, and Emanuele Norata. Their help was fundamental to achieve the goals of this thesis.

7. REFERENCES

- [1] G. Renu, C. Andrew Barnett, and F. Ralph D., "Infectious disease," *Encyclopædia Britannica, inc.*, 2020. <https://www.britannica.com/science/infectious-disease> (accessed Jun. 19, 2020).
- [2] R. O. for S.-E. A. World Health Organization, "A brief guide to emerging infectious diseases and zoonoses," 2014. [Online]. Available: <https://apps.who.int/iris/bitstream/handle/10665/204722/B5123.pdf?sequence=1&isAllowed=y>.
- [3] E. Ka-Wai Hui, "Reasons for the increase in emerging and re-emerging viral infectious diseases," *Microbes Infect.*, vol. 8, no. 3, pp. 905–916, Mar. 2006, doi: 10.1016/j.micinf.2005.06.032.
- [4] V. Gaspar and G. Gopinath, "Fiscal Policies for a Transformed World – IMF Blog," *International Monetary Fund (IMF)*, 2020. <https://blogs.imf.org/2020/07/10/fiscal-policies-for-a-transformed-world/> (accessed Jul. 12, 2020).
- [5] World Health Organization (WHO), "WHO Coronavirus Disease (COVID-19) Dashboard," Jul. 12, 2020. <https://covid19.who.int/> (accessed Jul. 12, 2020).
- [6] Centers for Disease Control and Prevention (CDC), "SARS-CoV-2 Viral Culturing at CDC | CDC," May 05, 2020. <https://www.cdc.gov/coronavirus/2019-ncov/lab/grows-virus-cell-culture.html> (accessed Jul. 12, 2020).
- [7] J. Adda, "Economic activity and the spread of viral diseases: Evidence from high frequency data," *Q. J. Econ.*, vol. 131, no. 2, pp. 891–941, May 2016, doi: 10.1093/qje/qjw005.
- [8] C. Hedges, "What Every Person Should Know About War," *The New York Times*, Jul. 06, 2003.
- [9] R. Planning, "Influenza Pandemic Plan. The Role of WHO and Guidelines for National and Regional Planning," *World Heal. Organ.*, no. April 1999, pp. 1–66, 1999, Accessed: Jun. 25, 2020. [Online]. Available: <http://www.who.int/emc>.
- [10] M. Moriyama, W. J. Hugentobler, and A. Iwasaki, "Seasonality of Respiratory Viral Infections," *Annu. Rev. Virol.*, vol. 7, no. 1, p. annurev-virology-012420-022445, Sep. 2020, doi: 10.1146/annurev-virology-012420-022445.
- [11] J. Bedford *et al.*, "COVID-19: towards controlling of a pandemic," *Lancet*, vol. 395, no. 10229, pp. 1015–1018, Mar. 2020, doi: 10.1016/S0140-6736(20)30673-5.
- [12] C. Schweizer *et al.*, "Indoor time–microenvironment–activity patterns in seven regions of Europe," *J. Expo. Sci. Environ. Epidemiol.*, vol. 17, no. 2, pp. 170–181, Mar. 2007, doi: 10.1038/sj.jes.7500490.
- [13] N. E. KLEPEIS *et al.*, "The National Human Activity Pattern Survey (NHAPS): a resource for assessing exposure to environmental pollutants," *J. Expo. Sci. Environ. Epidemiol.*, vol. 11, no. 3, pp. 231–252, Jul. 2001, doi: 10.1038/sj.jea.7500165.
- [14] J. Wei and Y. Li, "Airborne spread of infectious agents in the indoor environment," *Am. J. Infect. Control*, vol. 44, no. 9, pp. S102–S108, Sep. 2016, doi:

10.1016/j.ajic.2016.06.003.

- [15] J. D. Siegel, E. Rhinehart, M. Jackson, and L. Chiarello, "2007 Guideline for Isolation Precautions: Preventing Transmission of Infectious Agents in Health Care Settings," *Am. J. Infect. Control*, vol. 35, no. 10, pp. S65–S164, Dec. 2007, doi: 10.1016/j.ajic.2007.10.007.
- [16] L. Morawska, "Droplet fate in indoor environments, or can we prevent the spread of infection?," in *Indoor Air*, Oct. 2006, vol. 16, no. 5, pp. 335–347, doi: 10.1111/j.1600-0668.2006.00432.x.
- [17] R. Tellier, Y. Li, B. J. Cowling, and J. W. Tang, "Recognition of aerosol transmission of infectious agents: A commentary," *BMC Infectious Diseases*, vol. 19, no. 1. BioMed Central Ltd., p. 101, Dec. 31, 2019, doi: 10.1186/s12879-019-3707-y.
- [18] R. Cammack *et al.*, Eds., *Oxford Dictionary of Biochemistry and Molecular Biology*. Oxford University Press, 2006.
- [19] G. Brankston, L. Gitterman, Z. Hirji, C. Lemieux, and M. Gardam, "Transmission of influenza A in human beings," *Lancet Infect. Dis.*, vol. 7, no. 4, pp. 257–265, Apr. 2007, doi: 10.1016/S1473-3099(07)70029-4.
- [20] M. Porta, Ed., *A Dictionary of Epidemiology*. Oxford University Press, 2014.
- [21] J. Lu *et al.*, "COVID-19 Outbreak Associated with Air Conditioning in Restaurant, Guangzhou, China, 2020," *Emerg. Infect. Dis.*, vol. 26, no. 7, pp. 1628–1631, Jul. 2020, doi: 10.3201/eid2607.200764.
- [22] J. Gralton, E. Tovey, M. L. McLaws, and W. D. Rawlinson, "The role of particle size in aerosolised pathogen transmission: A review," *Journal of Infection*, vol. 62, no. 1. Elsevier, pp. 1–13, Jan. 2011, doi: 10.1016/j.jinf.2010.11.010.
- [23] J. P. Duguid, "The size and the duration of air-carriage of respiratory droplets and droplet-nuclei," *Epidemiol. Infect.*, vol. 44, no. 6, pp. 471–479, Sep. 1946, doi: 10.1017/S0022172400019288.
- [24] S. Froum and M. Strange, "COVID-19 and the problem with dental aerosols _ Perio-Implant Advisory," Apr. 07, 2020.
- [25] E. A. Nardell and R. R. Nathavitharana, "Airborne Spread of SARS-CoV-2 and a Potential Role for Air Disinfection," *JAMA - Journal of the American Medical Association*. American Medical Association, Jun. 01, 2020, doi: 10.1001/jama.2020.7603.
- [26] World Health Organization (WHO), "Transmission of SARS-CoV-2: implications for infection prevention precautions," Jul. 09, 2020. <https://www.who.int/news-room/commentaries/detail/transmission-of-sars-cov-2-implications-for-infection-prevention-precautions> (accessed Jul. 12, 2020).
- [27] J. Paul A., "Guidelines for Preventing the Transmission of Mycobacterium tuberculosis in Health-Care Settings, 2005," Atlanta, 2005. [Online]. Available: <https://www.cdc.gov/mmwr/preview/mmwrhtml/rr5417a1.htm>.
- [28] World Health Organization, "Natural Ventilation for Infection Control in Health-Care Settings," World Health Organization, 2009. Accessed: Jun. 28, 2020. [Online].

Available: <https://www.ncbi.nlm.nih.gov/books/NBK143284/>.

- [29] A. Lowen and P. Palese, "Transmission of influenza virus in temperate zones is predominantly by aerosol, in the tropics by contactA hypothesis," *PLoS Curr.*, vol. 1, no. AUG, p. RRN1002, Aug. 2009, doi: 10.1371/currents.RRN1002.
- [30] W. Yang, S. Elankumaran, and L. C. Marr, "Relationship between Humidity and Influenza A Viability in Droplets and Implications for Influenza's Seasonality," *PLoS One*, vol. 7, no. 10, p. e46789, Oct. 2012, doi: 10.1371/journal.pone.0046789.
- [31] A. C. Lowen, S. Mubareka, J. Steel, and P. Palese, "Influenza virus transmission is dependent on relative humidity and temperature," *PLoS Pathog.*, vol. 3, no. 10, pp. 1470–1476, Oct. 2007, doi: 10.1371/journal.ppat.0030151.
- [32] Department of Molecular Virology and Microbiology - Baylor College of Medicine, "Introduction to Infectious Diseases." <https://www.bcm.edu/departments/molecular-virology-and-microbiology/emerging-infections-and-biodefense/introduction-to-infectious-diseases> (accessed Jul. 12, 2020).
- [33] S. S. Perdue and J. H. Humphrey, "Immune system | Description, Function, & Facts | Britannica," *Encyclopædia Britannica, inc.*, 2020. <https://www.britannica.com/science/immune-system> (accessed Jun. 25, 2020).
- [34] World Health Organization (WHO), "Infectious diseases." https://www.who.int/topics/infectious_diseases/en/.
- [35] G. Zayas *et al.*, "Effectiveness of cough etiquette maneuvers in disrupting the chain of transmission of infectious respiratory diseases," *BMC Public Health*, vol. 13, no. 1, pp. 1–11, Sep. 2013, doi: 10.1186/1471-2458-13-811.
- [36] R. B. Patel, S. D. Skaria, M. M. Mansour, and G. C. Smaldone, "Respiratory source control using a surgical mask: An in vitro study," *J. Occup. Environ. Hyg.*, vol. 13, no. 7, pp. 569–576, 2016, doi: 10.1080/15459624.2015.1043050.
- [37] T. Svoboda *et al.*, "Public health measures to control the spread of the severe acute respiratory syndrome during the outbreak in Toronto," *N. Engl. J. Med.*, vol. 350, no. 23, pp. 2352–2361, Jun. 2004, doi: 10.1056/NEJMoa032111.
- [38] Centers for Disease Control and Prevention (CDC), "Use of quarantine to prevent transmission of severe acute respiratory syndrome--Taiwan, 2003.," *MMWR. Morb. Mortal. Wkly. Rep.*, vol. 52, no. 29, pp. 680–3, Jul. 2003, doi: 10.1001/jama.290.8.1021.
- [39] A. Nicoll, "Personal (non-pharmaceutical) protective measures for reducing transmission of influenza--ECDC interim recommendations.," *Euro Surveill.*, vol. 11, no. 10, p. 3061, Oct. 2006, doi: 10.2807/esw.11.41.03061-en.
- [40] World Health Organization (WHO), "Tuberculosis control in prisons. A manual for programme managers," *WHO Doc.*, vol. WHO/CDS/TB, pp. 1–176, 2001.
- [41] D. Bell *et al.*, "Nonpharmaceutical Interventions for Pandemic Influenza, International Measures," *Emerg. Infect. Dis.*, vol. 12, no. 1, pp. 81–87, Jan. 2006, doi: 10.3201/eid1201.051370.
- [42] L. Canini *et al.*, "Surgical Mask to Prevent Influenza Transmission in Households: A

- Cluster Randomized Trial,” *PLoS One*, vol. 5, no. 11, p. e13998, Nov. 2010, doi: 10.1371/journal.pone.0013998.
- [43] E. Pistacchio, “Flügge’s droplets,” *Le Infez. Med.*, vol. 7, no. 2, pp. 129–132, 1999, Accessed: Jul. 12, 2020. [Online]. Available: <http://www.ncbi.nlm.nih.gov/pubmed/12759594>.
- [44] S. D. Judson and V. J. Munster, “Nosocomial transmission of emerging viruses via aerosol-generating medical procedures,” *Viruses*, vol. 11, no. 10. MDPI AG, p. 940, Oct. 12, 2019, doi: 10.3390/v11100940.
- [45] World Health Organization (WHO), “Advice on the use of masks in the context of COVID-19: interim guidance-2,” *Intern. Guid. WHO*, no. April, pp. 1–5, 2020, doi: 10.1093/jiaa077.
- [46] K. H. Chan and K. Y. Yuen, “COVID-19 epidemic: disentangling the re-emerging controversy about medical facemasks from an epidemiological perspective,” *Int. J. Epidemiol.*, 2020, doi: 10.1093/ije/dyaa044.
- [47] K. A. Prather, C. C. Wang, and R. T. Schooley, “Reducing transmission of SARS-CoV-2,” *Science (80-.)*, vol. 368, no. 6498, p. eabc6197, Jun. 2020, doi: 10.1126/science.abc6197.
- [48] J. T. F. Lau, H. Tsui, M. Lau, and X. Yang, “SARS Transmission, Risk Factors, and Prevention in Hong Kong,” *Emerg. Infect. Dis.*, vol. 10, no. 4, pp. 587–592, Apr. 2004, doi: 10.3201/eid1004.030628.
- [49] J. Wu *et al.*, “Risk Factors for SARS among Persons without Known Contact with SARS Patients, Beijing, China,” *Emerg. Infect. Dis.*, vol. 10, no. 2, pp. 210–216, Feb. 2004, doi: 10.3201/eid1002.030730.
- [50] D. F. Johnson, J. D. Druce, C. Birch, and M. L. Grayson, “A Quantitative Assessment of the Efficacy of Surgical and N95 Masks to Filter Influenza Virus in Patients with Acute Influenza Infection,” *Clin. Infect. Dis.*, vol. 49, no. 2, pp. 275–277, Jul. 2009, doi: 10.1086/600041.
- [51] B. J. Cowling, Y. Zhou, D. K. M. Ip, G. M. Leung, and A. E. Aiello, “Face masks to prevent transmission of influenza virus: a systematic review,” *Epidemiology and Infection*, vol. 138, no. 4. pp. 449–456, 2010, doi: 10.1017/S0950268809991658.
- [52] S. E. Eikenberry *et al.*, “To mask or not to mask: Modeling the potential for face mask use by the general public to curtail the COVID-19 pandemic,” *Infect. Dis. Model.*, vol. 5, pp. 293–308, Jan. 2020, doi: 10.1016/j.idm.2020.04.001.
- [53] L. Liao *et al.*, “Can N95 Respirators Be Reused after Disinfection? How Many Times?,” *ACS Nano*, vol. 14, no. 5, pp. 6348–6356, May 2020, doi: 10.1021/acsnano.0c03597.
- [54] S. A. Angadjivand, M. E. Jones, and D. E. Meyer, “Electret Filter Media,” US6119691A, May 29, 1994.
- [55] L. W. Barrett and A. D. Rousseau, “Aerosol loading performance of electret filter media,” *Am. Ind. Hyg. Assoc. J.*, vol. 59, no. 8, pp. 532–539, 1998, doi: 10.1080/15428119891010703.

- [56] M. Shields, C. O. Donnell, R. Liu, and A. Deutsch, "As virus explodes, world races to mask up," pp. 1–13, 2020.
- [57] F. Chaib, "Shortage of personal protective equipment endangering health workers worldwide," *World Heal. Organ.*, pp. 1–3, 2020, [Online]. Available: <https://www.who.int/news-room/detail/03-03-2020-shortage-of-personal-protective-equipment-endangering-health-workers-worldwide>.
- [58] EN, "EN 14683:2019+AC:2019 Medical face masks - Requirements and test methods." 2009.
- [59] V. Offeddu, C. F. Yung, M. S. F. Low, and C. C. Tam, "Effectiveness of Masks and Respirators Against Respiratory Infections in Healthcare Workers: A Systematic Review and Meta-Analysis," *Clin. Infect. Dis.*, vol. 65, no. 11, pp. 1934–1942, Nov. 2017, doi: 10.1093/cid/cix681.
- [60] C. Da Zhou, P. Sivathondan, and A. Handa, "Unmasking the surgeons: the evidence base behind the use of facemasks in surgery," *Journal of the Royal Society of Medicine*, vol. 108, no. 6, pp. 223–228, 2015, doi: 10.1177/0141076815583167.
- [61] S. A. Lee, D. C. Hwang, H. Y. Li, C. F. Tsai, C. W. Chen, and J. K. Chen, "Particle size-selective assessment of protection of european standard FFP respirators and surgical masks against particles-tested with human subjects," *J. Healthc. Eng.*, vol. 2016, 2016, doi: 10.1155/2016/8572493.
- [62] CEN, "CEN Workshop Agreement 17553:2020 Community face coverings – Guide to minimum requirements, methods of testing and use." 2020.
- [63] H. Jung *et al.*, "Comparison of filtration efficiency and pressure drop in anti-yellow sandmasks, quarantine masks, medical masks, general masks, and handkerchiefs," *Aerosol Air Qual. Res.*, vol. 14, no. 3, pp. 991–1002, 2014, doi: 10.4209/aaqr.2013.06.0201.
- [64] K. M. Shakya, A. Noyes, R. Kallin, and R. E. Peltier, "Evaluating the efficacy of cloth facemasks in reducing particulate matter exposure," *J. Expo. Sci. Environ. Epidemiol.*, vol. 27, no. 3, pp. 352–357, 2017, doi: 10.1038/jes.2016.42.
- [65] J. Y. Jang and S. W. Kim, "Evaluation of Filtration Performance Efficiency of Commercial Cloth Masks," *Korean J. Environ. Heal. Sci.*, vol. 41, no. 3, pp. 203–215, Jun. 2015, doi: 10.5668/jehs.2015.41.3.203.
- [66] M. Hamburger and O. H. Robertson, "Expulsion of group a hemolytic streptococci in droplets and droplet nuclei by sneezing, coughing and talking," *Am. J. Med.*, vol. 4, no. 5, pp. 690–701, 1948, doi: 10.1016/S0002-9343(48)90392-1.
- [67] R. G. Loudon and R. M. Roberts, "Droplet expulsion from the respiratory tract," *Am. Rev. Respir. Dis.*, vol. 95, no. 3, pp. 435–442, Mar. 1967, doi: 10.1164/arrd.1967.95.3.435.
- [68] R. S. Papineni and F. S. Rosenthal, "The size distribution of droplets in the exhaled breath of healthy human subjects," *J. Aerosol Med. Depos. Clear. Eff. Lung*, vol. 10, no. 2, pp. 105–116, 1997, doi: 10.1089/jam.1997.10.105.

- [69] K. P. Fennelly, J. W. Martyny, K. E. Fulton, I. M. Orme, D. M. Cave, and L. B. Heifets, "Cough-generated Aerosols of *Mycobacterium tuberculosis*," *Am. J. Respir. Crit. Care Med.*, vol. 169, no. 5, pp. 604–609, Mar. 2004, doi: 10.1164/rccm.200308-1101OC.
- [70] M. Nicas, W. W. Nazaroff, and A. Hubbard, "Toward understanding the risk of secondary airborne infection: Emission of respirable pathogens," *J. Occup. Environ. Hyg.*, vol. 2, no. 3, pp. 143–154, Mar. 2005, doi: 10.1080/15459620590918466.
- [71] G. R. Johnson *et al.*, "Modality of human expired aerosol size distributions," *J. Aerosol Sci.*, vol. 42, no. 12, pp. 839–851, Dec. 2011, doi: 10.1016/j.jaerosci.2011.07.009.
- [72] L. Morawska *et al.*, "Size distribution and sites of origin of droplets expelled from the human respiratory tract during expiratory activities," *J. Aerosol Sci.*, vol. 40, no. 3, pp. 256–269, Mar. 2009, doi: 10.1016/j.jaerosci.2008.11.002.
- [73] W. F. WELLS, "ON AIR-BORNE INFECTION*," *Am. J. Epidemiol.*, vol. 20, no. 3, pp. 611–618, Nov. 1934, doi: 10.1093/oxfordjournals.aje.a118097.
- [74] J. P. DUGUID, "The numbers and the sites of origin of the droplets expelled during expiratory activities," *Edinb. Med. J.*, vol. 52, no. 11, pp. 385–401, Nov. 1945, Accessed: Jun. 29, 2020. [Online]. Available: <http://www.ncbi.nlm.nih.gov/pubmed/21009905>.
- [75] W. G. Lindsley *et al.*, "Quantity and Size Distribution of Cough-Generated Aerosol Particles Produced by Influenza Patients During and After Illness," *J. Occup. Environ. Hyg.*, vol. 9, no. 7, pp. 443–449, Jul. 2012, doi: 10.1080/15459624.2012.684582.
- [76] E. C. Cole and C. E. Cook, "Characterization of infectious aerosols in health care facilities: An aid to effective engineering controls and preventive strategies," *Am. J. Infect. Control*, vol. 26, no. 4, pp. 453–464, Aug. 1998, doi: 10.1016/S0196-6553(98)70046-X.
- [77] J. W. Tang, Y. Li, I. Eames, P. K. S. Chan, and G. L. Ridgway, "Factors involved in the aerosol transmission of infection and control of ventilation in healthcare premises," *J. Hosp. Infect.*, vol. 64, no. 2, pp. 100–114, Oct. 2006, doi: 10.1016/j.jhin.2006.05.022.
- [78] C. Spence, "Inhale, Exhale - Explore," May 22, 2020. <http://explore.research.ufl.edu/inhale-exhale.html> (accessed Jul. 12, 2020).
- [79] UNI, "UNI PdR 90:2020 'Community Face Covering - Part 1: Requirements, typology and marking.'" UNI, Ente Italiano di Normazione, 2020.
- [80] UNI, "UNI PdR 90:2020 'Community Face Covering - Part 2: Test methods.'" UNI, Ente Italiano di Normazione, 2020.
- [81] ASTM, "ASTM F2101 - 19 'Standard Test Method for Evaluating the Bacterial Filtration Efficiency (BFE) of Medical Face Mask Materials, Using a Biological Aerosol of *Staphylococcus aureus*.'" .
- [82] Centers for Disease Control and Prevention (CDC), "Do We Need to Challenge Respirator Filters With Biological Aerosols? | | Blogs | CDC," 2014. <https://blogs.cdc.gov/niosh-science-blog/2014/04/02/respirator-filter-testing/> (accessed Jul. 13, 2020).
- [83] EN, "EN 149:2001+A1:2009 - 'Respiratory protective devices. Filtering half masks to protect against particles. Requirements, testing, marking.'" 2009.

- [84] I. EN, "ISO EN 21083:2018 'Test method to measure the efficiency of air filtration media against spherical nanomaterials — Part 1: Size range from 20 nm to 500 nm.'" 2018.
- [85] ISO, "ISO 5167-1:2003 'Measurement of fluid flow by means of pressure differential devices inserted in circular cross-section conduits running full — Part 1: General principles and requirements.'" 2003.
- [86] Air Techniques International, "Laskin Nozzle Generators TDA-4B and TDA-4Blite Operation and Maintenance Manual," 2000. Accessed: Jun. 30, 2020. [Online]. Available: <https://www.atitest.com/wp-content/uploads/2016/05/4B-4B-lite.pdf>.
- [87] T. Incorporated, "ISO 16890-2 AIR FILTERS FOR GENERAL VENTILATION: DETERMINING FRACTIONAL EFFICIENCY," 2017. Accessed: Jun. 30, 2020. [Online]. Available: https://www.tsi.com/getmedia/8e668c17-c622-42ab-9b66-2d0c3c04c181/AFT-005_ISO16890_AppNote_A4-web?ext=.pdf.
- [88] I. EN, "ISO EN 16890-1:2016 'Air filters for general ventilation — Part 1: Technical specifications, requirements and classification system based upon particulate matter efficiency (ePM).'" 2016.
- [89] I. EN, "ISO EN 16890-2:2016 'Air filters for general ventilation — Part 2: Measurement of fractional efficiency and air flow resistance.'" 2016.
- [90] R. G. Pinnick, J. D. Pendleton, and G. Videen, "Response characteristics of the Particle Measuring Systems active scattering aerosol spectrometer probes," *Aerosol Sci. Technol.*, vol. 33, no. 4, pp. 334–352, Oct. 2000, doi: 10.1080/02786820050121530.
- [91] T. Incorporated, "Laser Aerosol Spectrometer 3340." <https://www.tsi.com/discontinued-products/laser-aerosol-spectrometer-3340/> (accessed Jul. 13, 2020).
- [92] T. Incorporated, "Optical Particle Sizer 3330." <https://tsi.com/products/particle-sizers/particle-size-spectrometers/optical-particle-sizer-3330/> (accessed Jul. 13, 2020).
- [93] TEXTTEST, "FX 3300 LabAir IV." <https://texttest.ch/en/portfolio-items/fx-3300-labair-iv/> (accessed Jul. 13, 2020).
- [94] W. Hinds, *Aerosol Technology: properties, behavior, and measurement of airborne particles*, 2nd ed. Cambridge: WILEY-INTERSCIENCE, 1999.

APPENDIX A. AIRBORNE PARTICLE CHARACTERIZATION

A.1. Particle size, shape, and density

Particle size is the most critical parameter to characterize the behavior of aerosols. All the properties of aerosols depend on the size of the particles; some of them very strongly. Additionally, most aerosols cover a wide range of sizes; a hundred times greater range between the smallest and largest particles in an aerosol is expected.

The properties of aerosols not only depend on the size of the particles, but the nature of the laws governing these properties can change with the size of the particles. This emphasizes the need to take a microscopic approach and characterize the properties on an individual particle basis. The mean properties can then be estimated by integrating over the size distribution. An appreciation of how aerosol properties vary with particle size is critical to understanding their properties.

In general, dust, ground material, and pollen are in the micron range or larger, and the fumes and mists are submicron. The smallest aerosol particles approach the size of large gas molecules and have many of their properties. Ultrafine particles cover the range of large gas molecules at approximately 100 nm (0.001 to 0.1 μm). Particles larger than 10 μm have limited stability in the air but can still be a significant source of occupational exposure because of the worker's proximity to the source. The most massive aerosol particles are visible grains that have properties described by the familiar Newtonian physics of baseballs and automobiles. The point above the letter "i" has a diameter of about 400 μm , and the smallest flour grains that can be seen under normal conditions are 50-100 μm . The finest wire mesh sieves have openings of approximately 20 μm . The wavelength of visible light is in the sub-micrometer size range, approximately 0.5 μm .

Liquid particles are almost always spherical. Solid aerosol particles often have complex shapes. In the development of the theory of aerosol properties, it is generally necessary to assume that the particles are spherical. Correction factors and the use of equivalent diameters enables these theories to be applied to non-spherical particles.

Particle density refers to the mass per unit volume of the particle itself, not of the aerosol. Liquid particles and crushed or crushed solid particles have a density equal to that of their original material. Smoke and smoke particles may have significantly lower bulk densities than predicted by their chemical composition. This is the result of the large amount of space in its highly agglomerated structure, which can resemble a bunch of grapes.

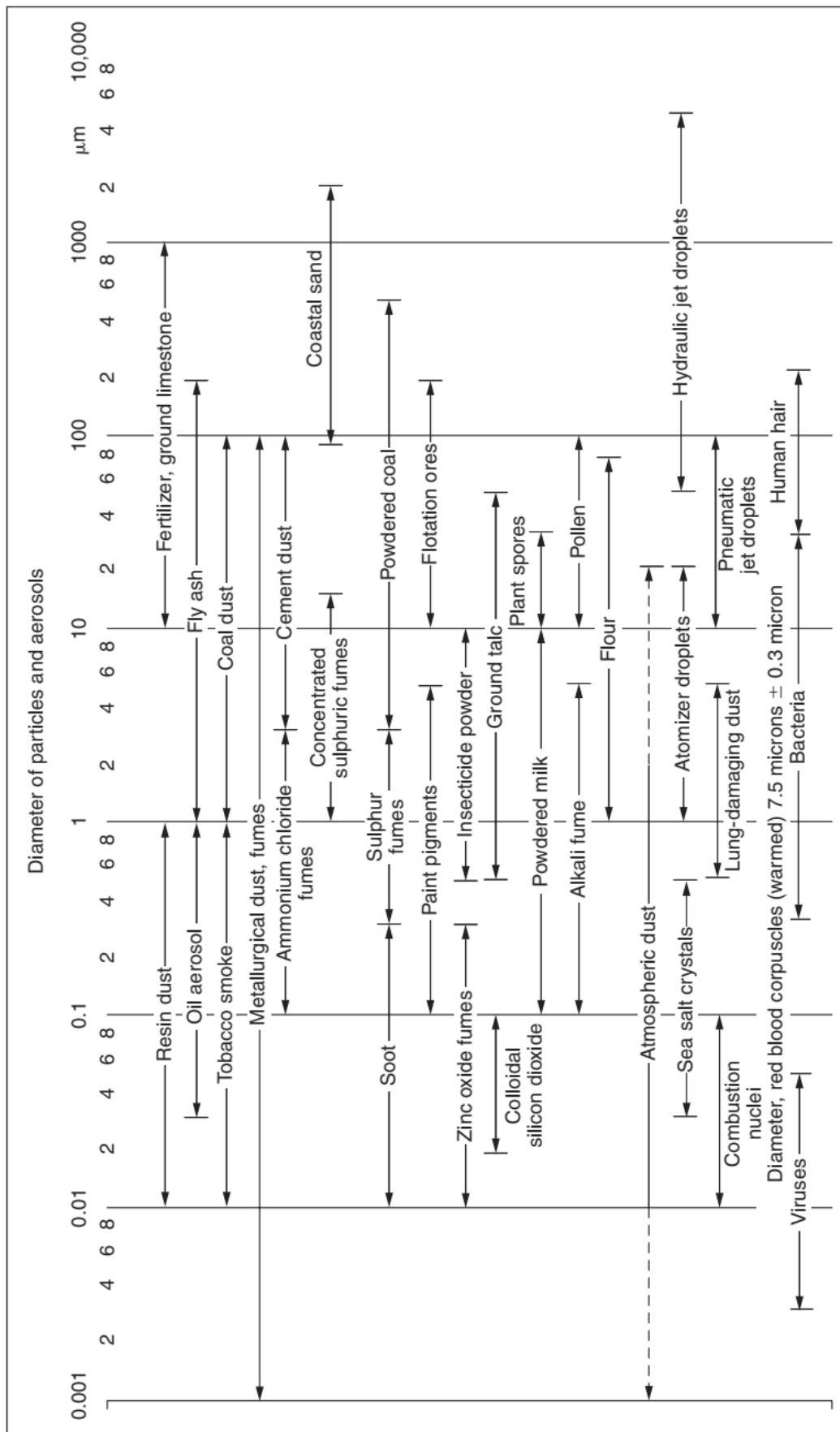


Figure 52. The particle size range of different substances [94]. Particle size expressed in μm .

A.2. Optical, aerodynamic, electrical diameter.

An equivalent diameter is the diameter of the sphere that has the same value of physical property as that of an irregular particle

A.3. Aerosol concentration

The most measured aerosol property, and the most important for health and environmental effects, is the mass concentration, the mass of particulate matter in a unit volume of aerosol. The mass concentration is equivalent to the density of the set of aerosol particles in the air.

Another standard measure of concentration is number concentration, the number of particles per unit volume of aerosol.

APPENDIX B. PARTICLE SIZE STATISTICS

The particle size of a monodisperse aerosol is entirely defined by a single parameter, the size of the particles. However, most aerosols are polydisperse and can have particle sizes that vary by two or more magnitude orders. Due to this wide size range and the fact that the physical properties of aerosols are strongly dependent on particle size, it is necessary to characterize these size distributions by statistical means.

B.1. Properties of size distributions

We would like to have a picture of how the particles are distributed among the different sizes and to be able to calculate several different types of statistics that describe the properties of the aerosol.

The first step in such a summary is to divide the entire size range into a series of successive particle size intervals and determine the number of particles in each interval. The intervals, also known as channels, should be contiguous and cover the entire size range so that no particles are left behind. The upper size limit of each interval coincides with the lower limit of the immediately higher interval. If a particle size falls precisely on the interval limit, it is grouped in the highest interval. These grouped data are much easier to process and give the first insight into the shape of the size distribution.

A graphical representation of grouped data is the histogram, shown in Figure 53, where the width of each rectangle represents the size range, and the height represents the number of particles in the range. Inappropriately, the figure gives a distorted picture of the size distribution because the height of any interval depends on the width of that interval. Therefore, doubling the width of an interval results in approximately twice as many particles falling into that interval, and the interval grows to twice its height. To avoid this distortion, the histogram is normalized for the interval width by dividing the number of particles in each interval by the width of that interval.

As shown in Figure 54, the height of each rectangle is now equal to the number of particles per unit size interval (particle count/ μm), and the heights of the intervals with different widths are comparable. Furthermore, the area of each rectangle is proportional to the number or frequency of particles in that size range.

Finally, using many rectangles and drawing a smooth curve through the tops, we obtain the particle size distribution curve, which is the graphical representation of the frequency function or probability density function. Figure 55 is an accurate picture of how particles are distributed among different sizes.

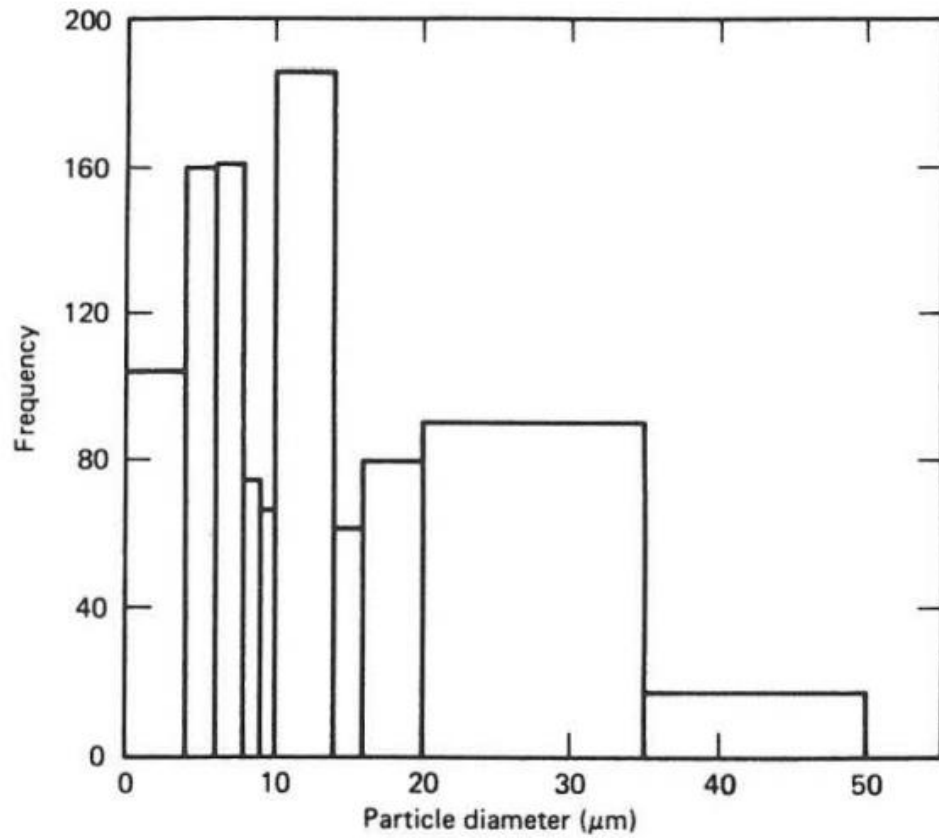


Figure 53. Histogram of frequency vs. particle size.

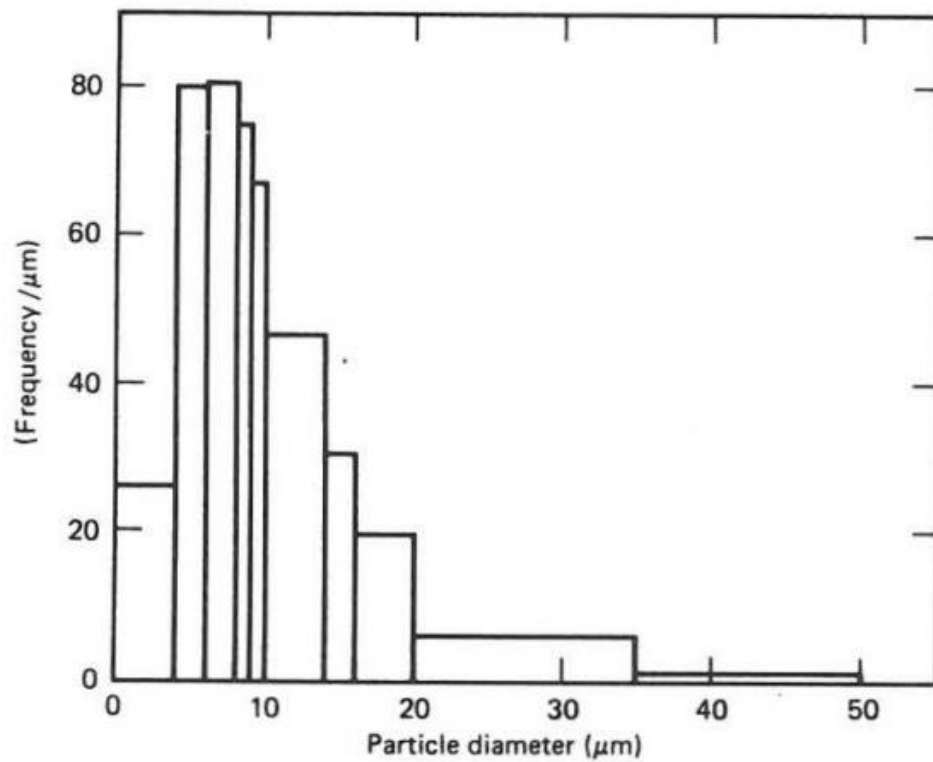


Figure 54. Histogram of frequency normalized by width of intervals vs. particle size.

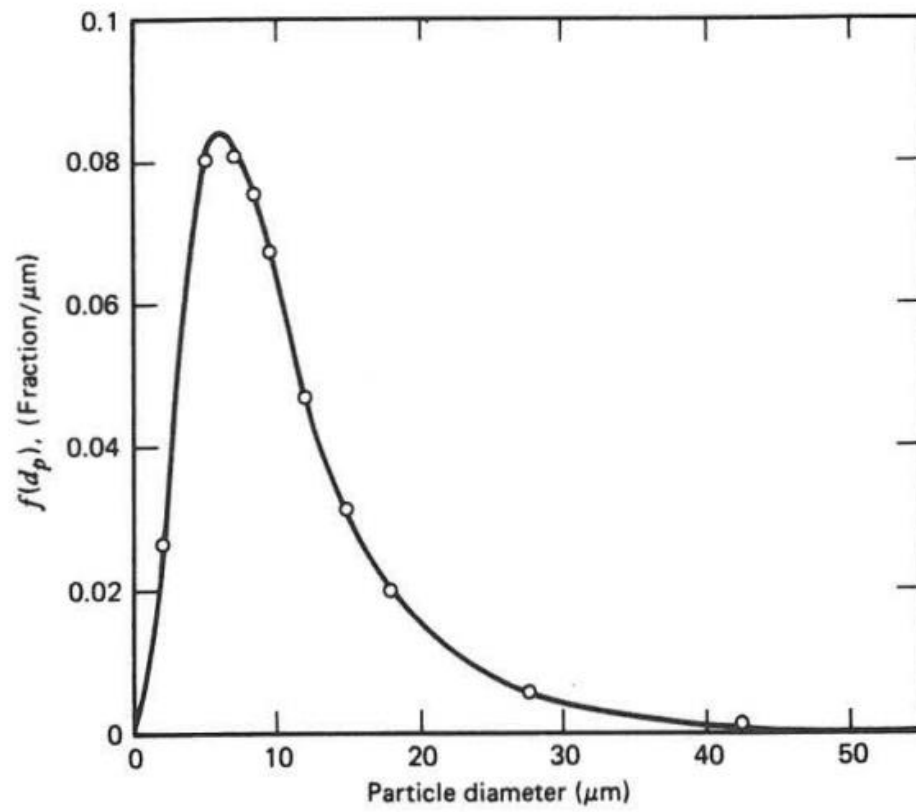


Figure 55. Probability density function.

APPENDIX C. AIR FILTRATION

C.1. Surface filtration vs. Deep filtration

Surface filtration implies that the particles are retained mainly on the surface of the medium, forming a layer of material that increases the efficiency or fineness of the retained particles. This type of filter media is known as having "nominal retention,"; perhaps initially being 60% to 70% efficient in retaining the target particle size and how the "cake layer" develops over time, becoming almost 100% efficient. Nominally rated media are the most common and are less expensive than depth media. The amount of surface area is directly correlated with the concrete load capacity and the related pressure drop.

Depth filtration refers to thicker media or multiple layers of media, forming a tortuous path to retain particles. This type of designed media ideally retains larger particles on the surface and progressively finer particles through-thickness or layers. Although there are nominal depth filter media, the more complex designs are often rated at 95-99% efficiency and therefore do not rely on a filter cake for efficiency. The effect of the surface on the filtration rate is only part of the overall filtration efficiency.

C.2. Quality factor

To properly evaluate the performance of a material, it is necessary to take into account both filtration efficiency and resistance to airflow through the medium.

The Quality Factor can represent a useful quantity to express performance. This value factor can be defined as:

$$Quality\ factor = - \frac{\log_{10}(1 - E)}{\Delta p} \quad (8)$$

A high quality factor is indicative of good combined capture and pressure drop performance. High efficiency is always desirable but keeping a low-pressure drop.

C.3. Deposition mechanisms

A deposition mechanism is a process by which particles in airflow hit the fibers, granular bodies, or porous walls of the filter medium. Important parameters of the gas for the filtration mechanisms include the velocity of the medium face, the viscosity, and the temperature.

These four deposition mechanisms form the basic set of mechanisms for all types of aerosol particle deposition, including deposition in a lung, in a sampling tube, or an air cleaner. The analysis and prediction method is different for each situation, but the deposition mechanisms are the same.

C.3.1. Interception

The interception effect is due to the finite size of the particles under the assumption that the particles follow flow streamlines. It is based on geometric interference caused by the size of the particles themselves. In their movement, the finest and lightest particles tend to follow the contour of the filter fibers and, due to their size, are retained when the distance between one fiber and the other is less than the radius of the same particle.

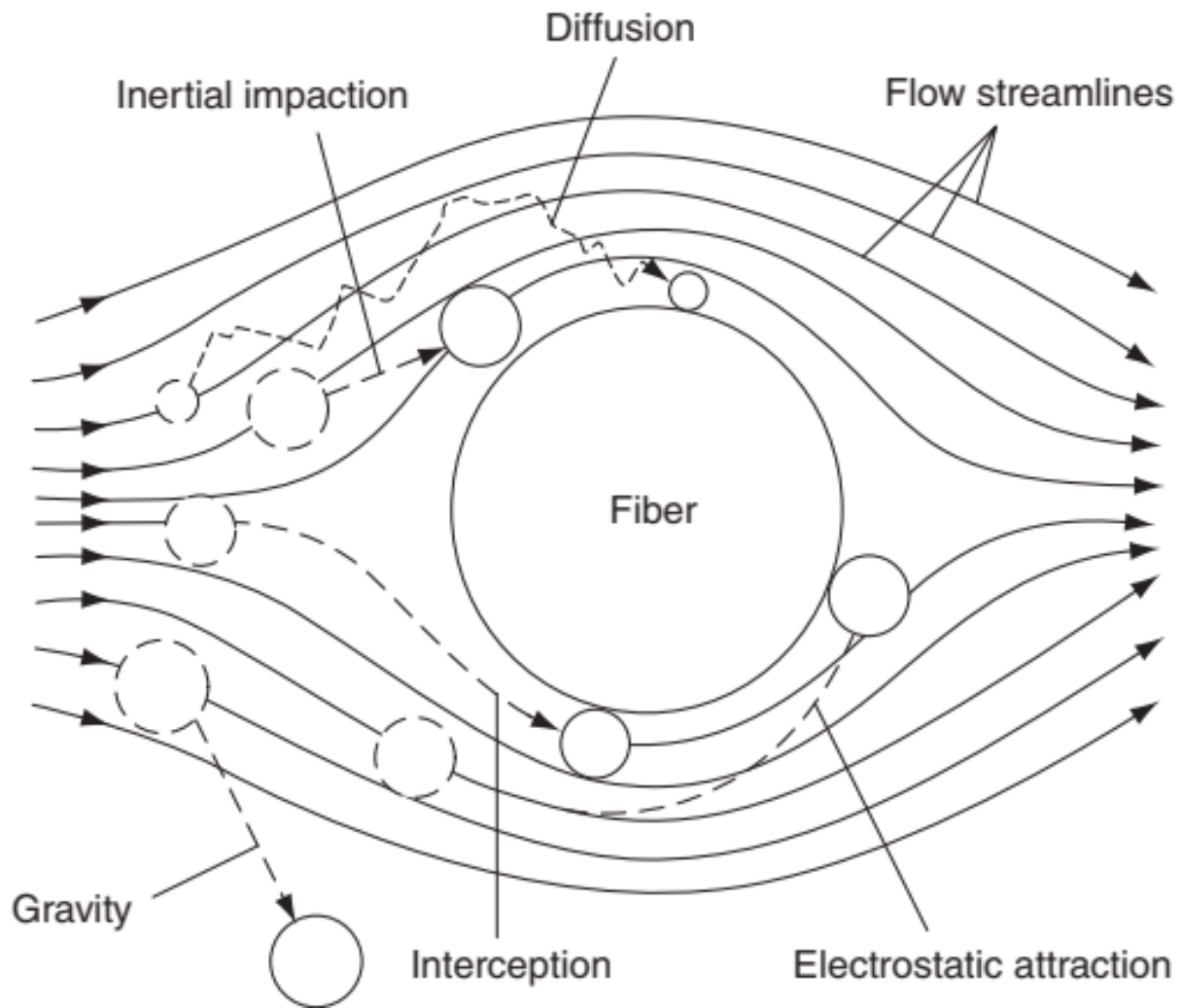


Figure 56. Scheme of deposition mechanism by representing the effect of a single fiber.

C.3.2. Inertial impaction

In the proximity of the filter, the airflow tends to follow the edge of the fiber, while the particle, due to its mass, continues its path and directly impacts the fiber. Particle adhesion to the fibers can be improved by coating the fibers with a viscous liquid.

C.3.3. Diffusion

The diffusion mechanism accounts for the particles that undergo Brownian motion that then hit the fibers and are captured. The probability of the particles colliding with the fiber increases both with decreasing particle and fiber diameters and with decreasing air face velocity. The particles adhere to the fibers because of the electrostatic and intermolecular forces. Diffusion may be the dominant mechanism for nanoparticle filtration (i.e., $<0.1 \mu\text{m}$).

C.3.4. Electrostatic attraction

When the particle size is small, the electrical forces can become more effective than the force of gravity. The particle is subjected to the non-uniform electric field generated by the fiber, and the result is a dielectric force that draws the particle into the fiber. Electret filters, with intentionally electrically charged fibers, take advantage of electrostatic attraction to improve

filtration efficiency, without affecting flow resistance. Brown analyzed the efficiency of a single fiber due to coulombic strength for fibers with uniform load distributions

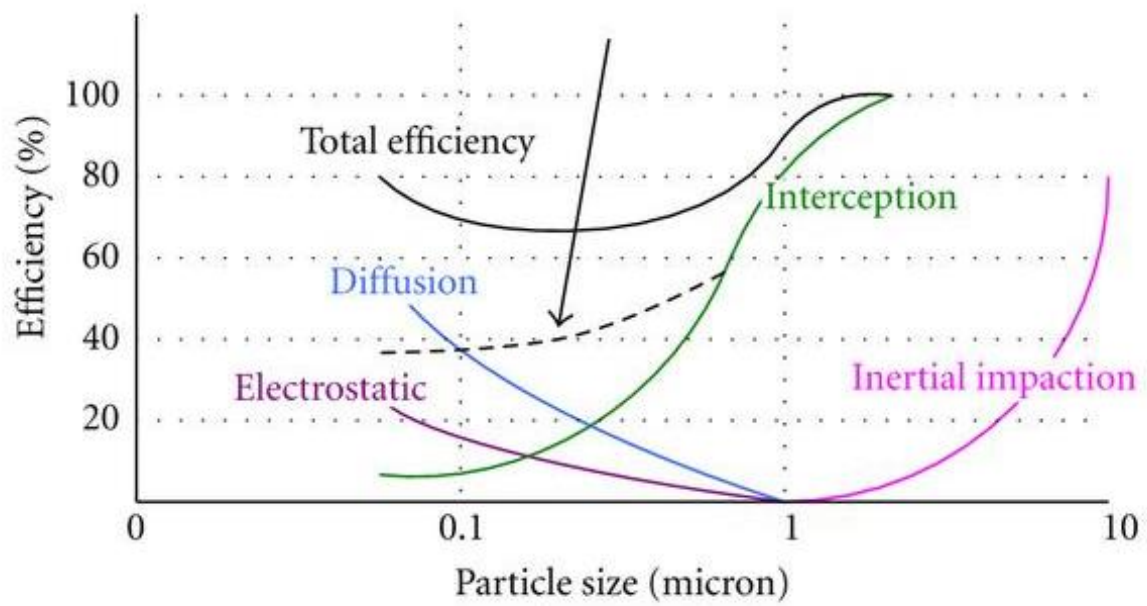


Figure 57. How the deposition mechanism impacts the fractional efficiency curve?

APPENDIX D. SCANNING ELECTRON MICROSCOPE FIGURES OF
LAYERS OF FACE MASKS MADE UP OF WOVEN AND NON-WOVEN
MATERIALS

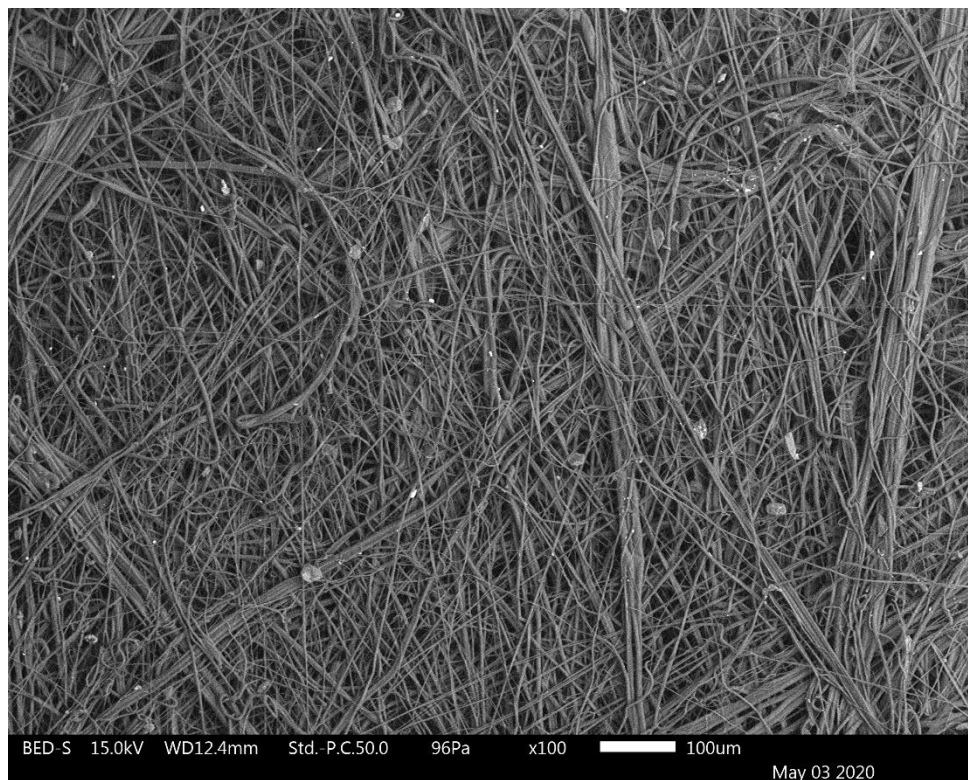


Figure 58. SEM figure of the first layer of the sample (A) at 100X.

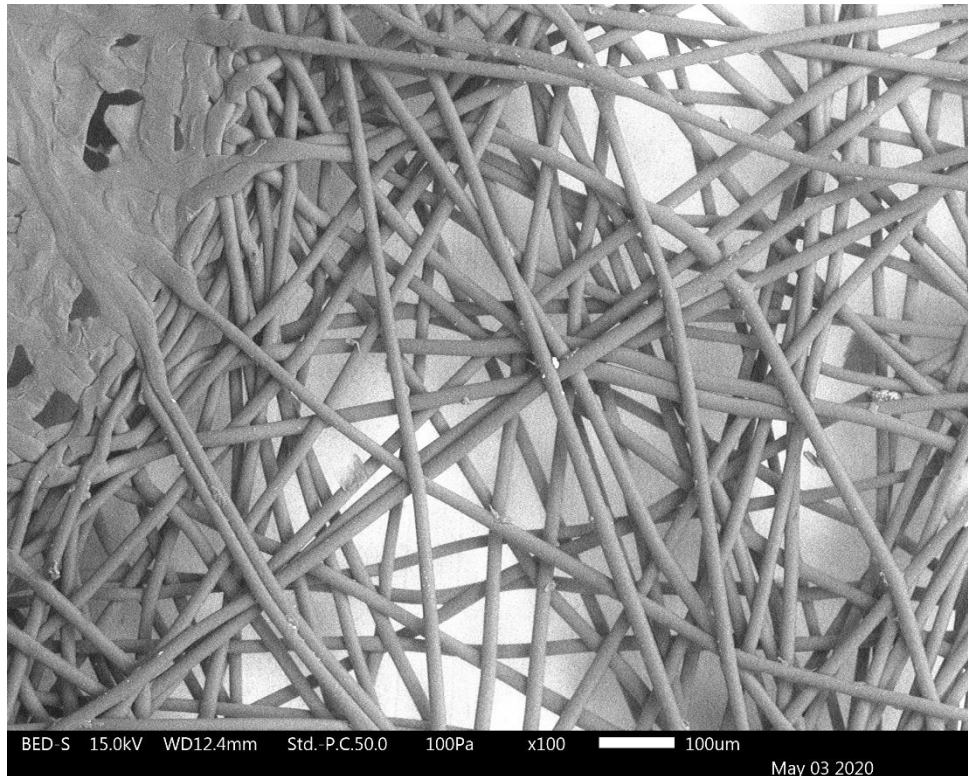


Figure 59. SEM figure of the second layer of the sample (A) at 100X.

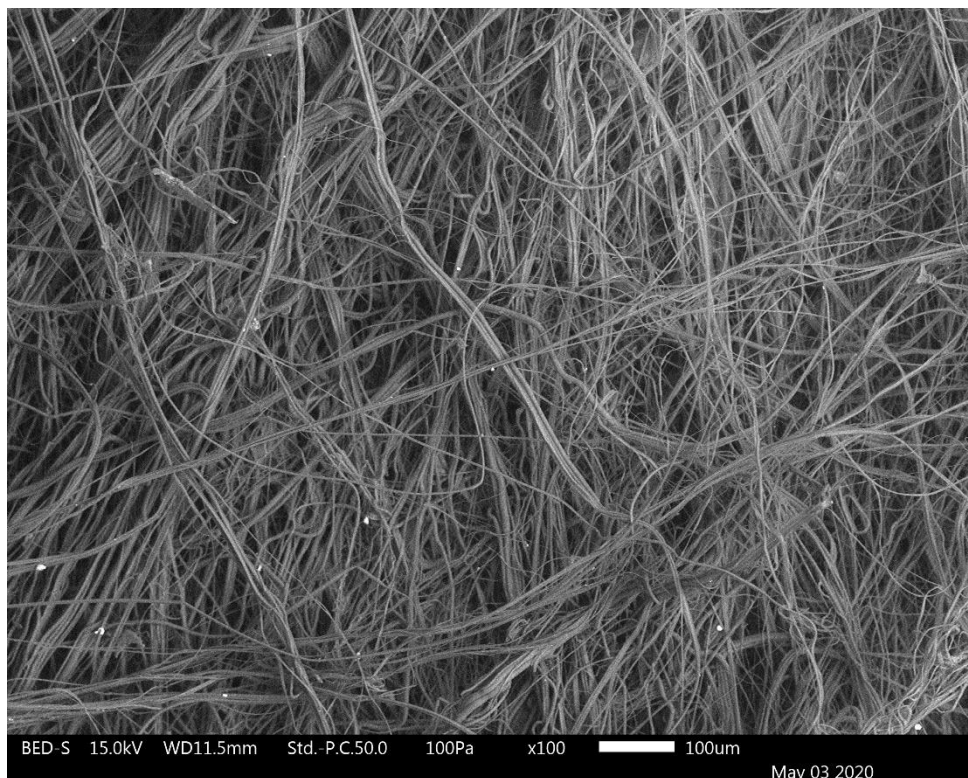


Figure 60. SEM figure of the third layer of the sample (A) at 100X.

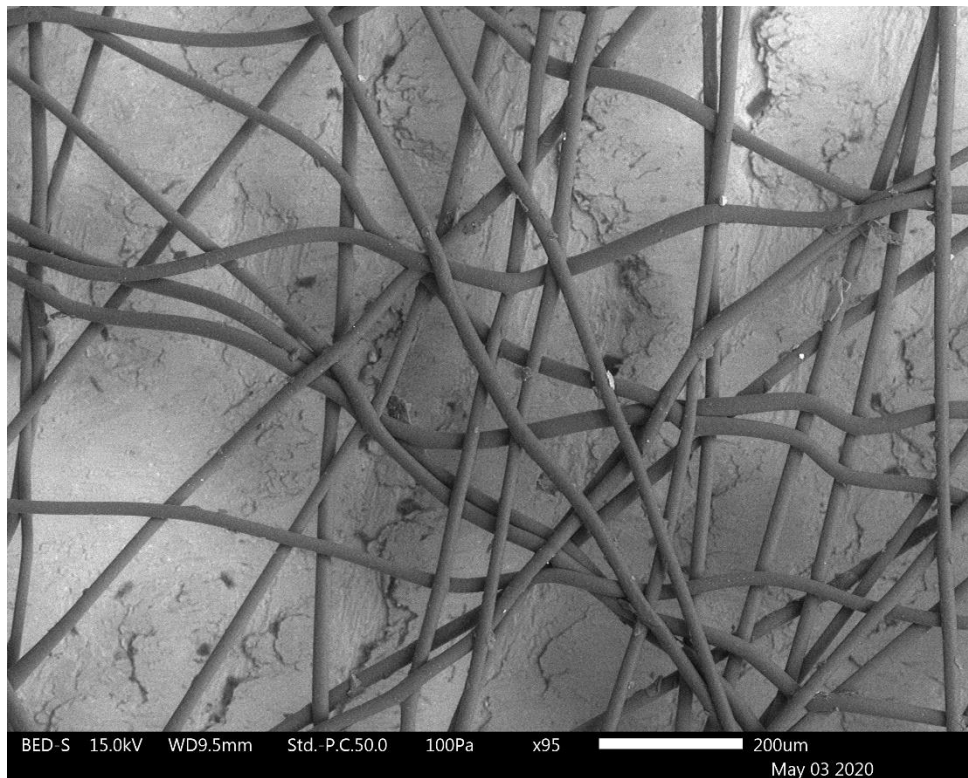


Figure 61. SEM figure of the first layer of the sample (B) at 100X.

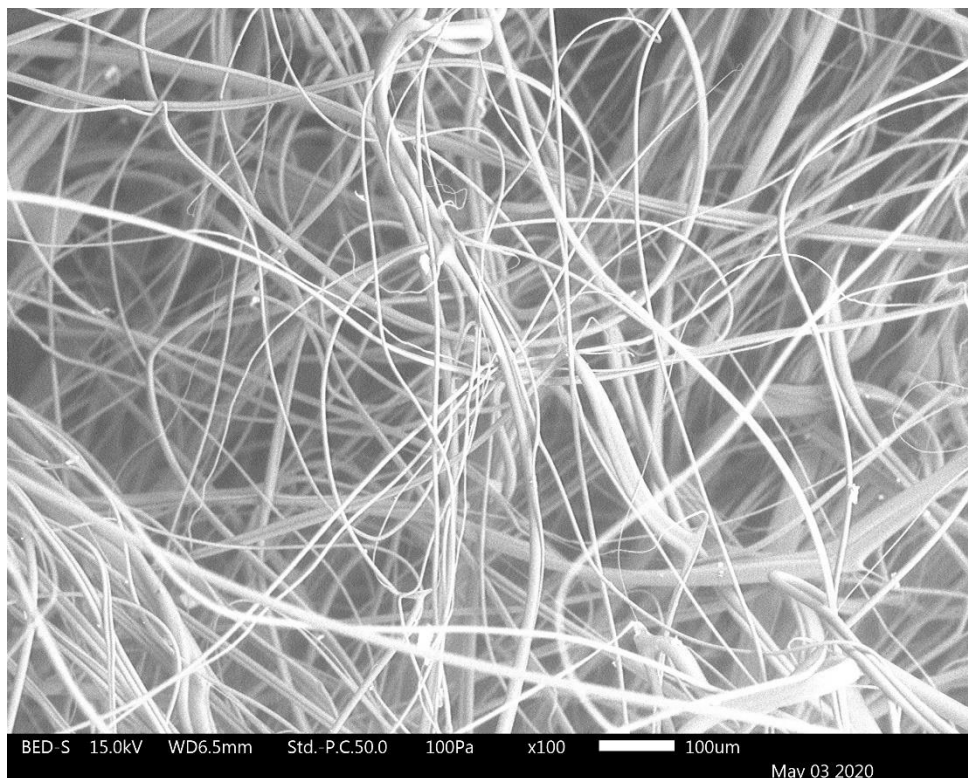


Figure 62. SEM figure of the second layer of the sample (B) at 100X.

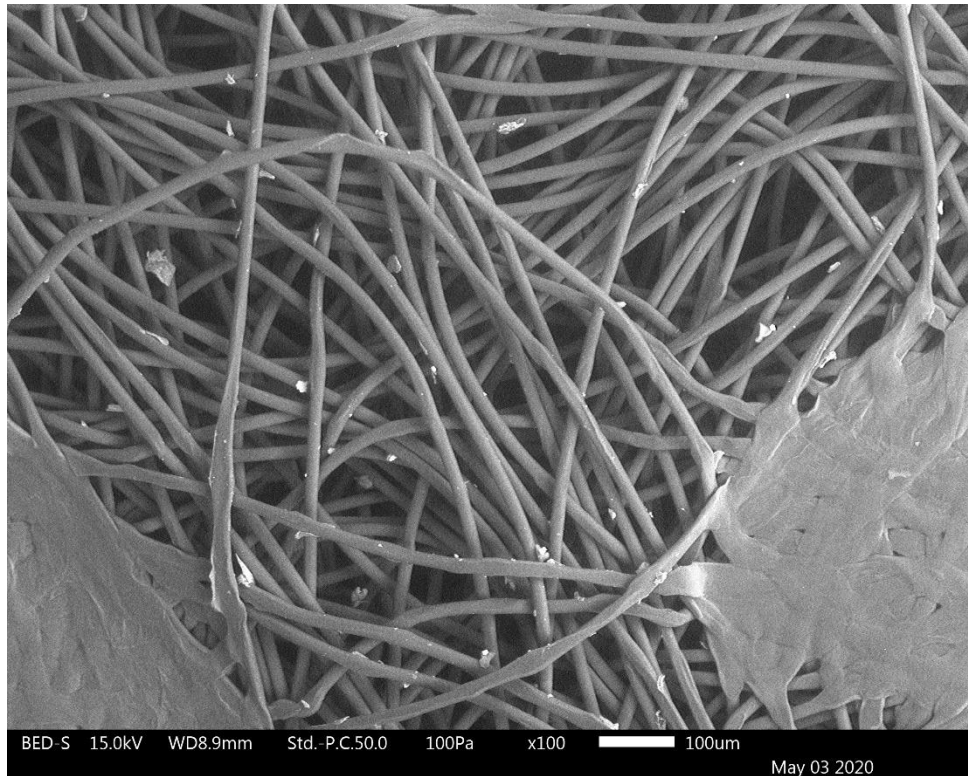


Figure 63. SEM figure of the third layer of the sample (B) at 100X.

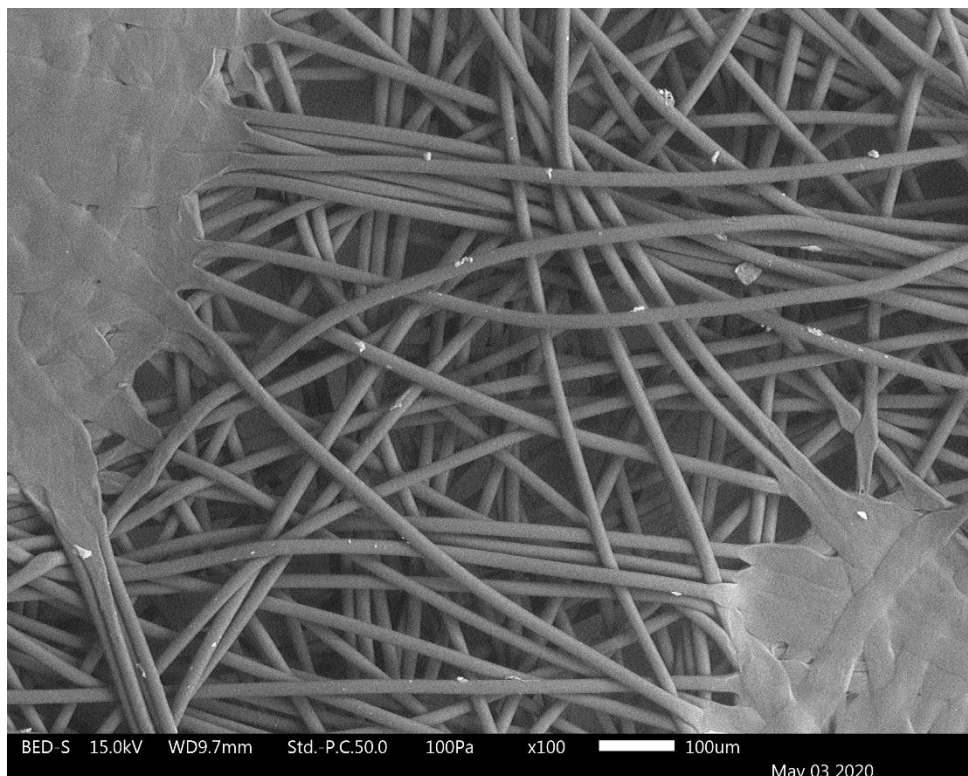


Figure 64. SEM figure of the first layer of the sample (C) at 100X.

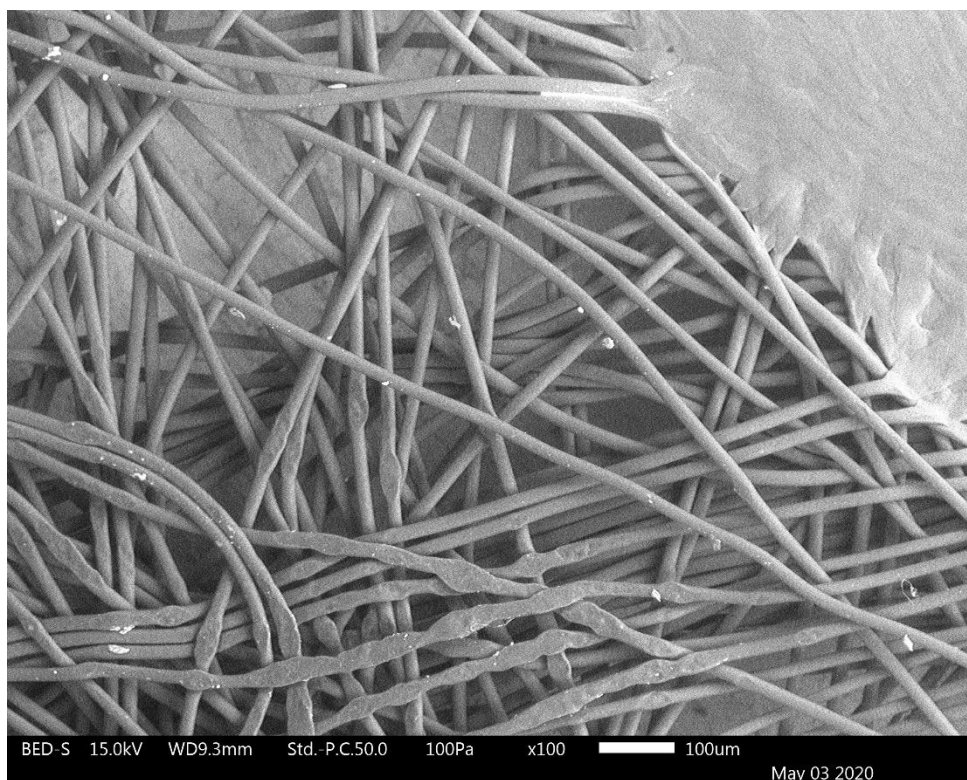


Figure 65. SEM figure of the second layer of the sample (C) at 100X.

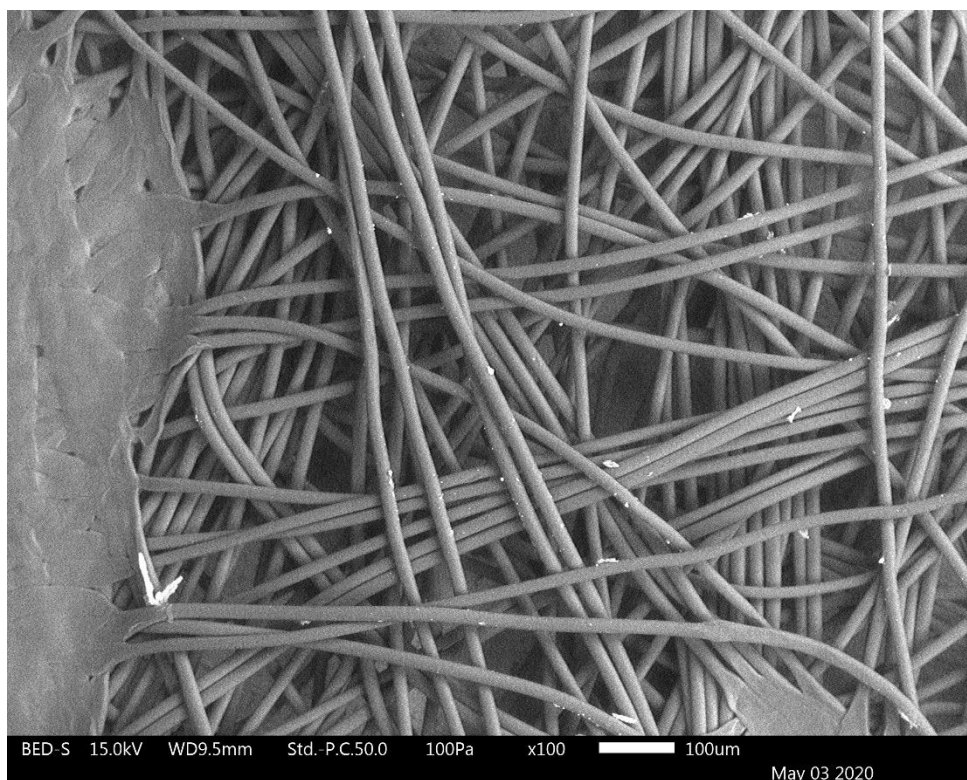


Figure 66. SEM figure of the third layer of the sample (C) at 100X.

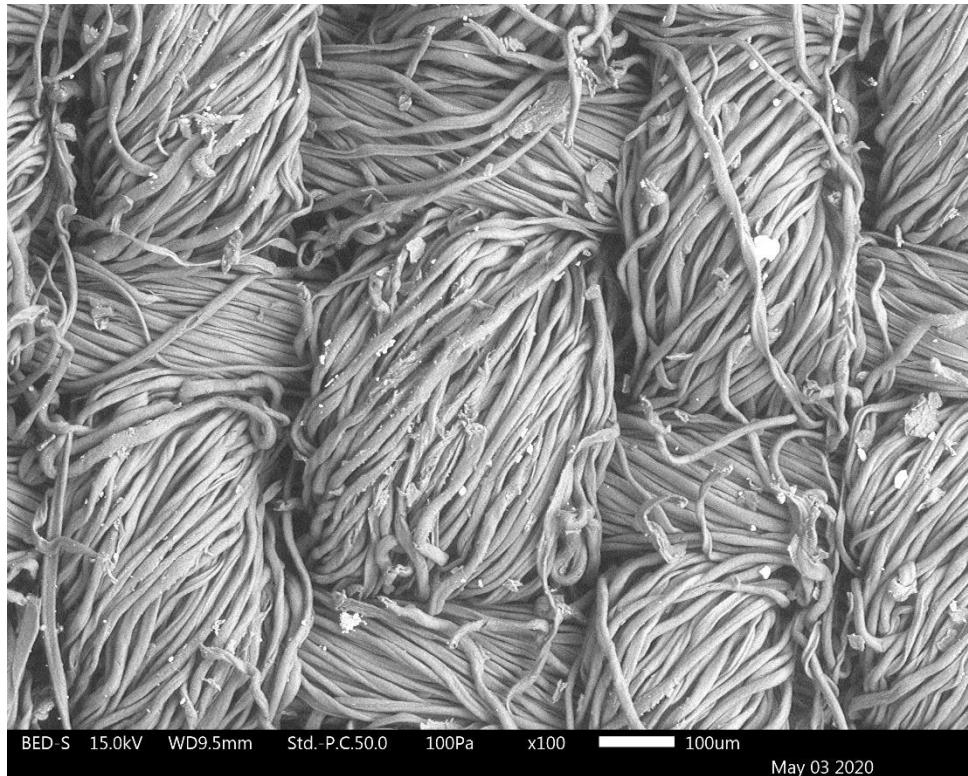


Figure 67. SEM figure of the sample (D) at 100X.

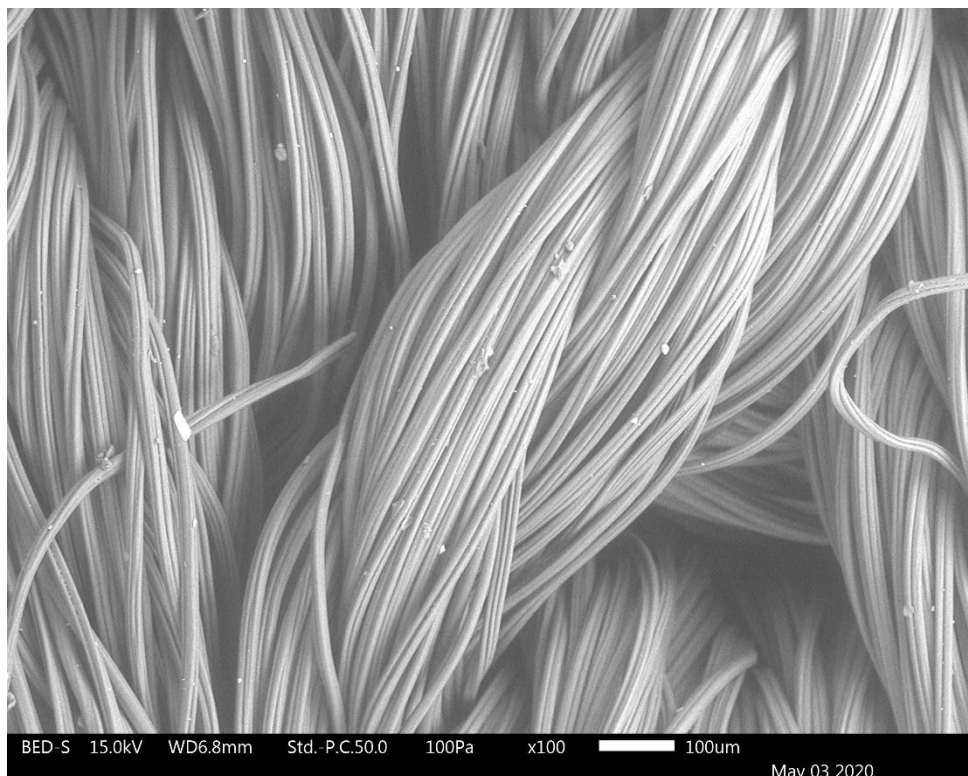


Figure 68. SEM figure of the sample (E) at 100X.

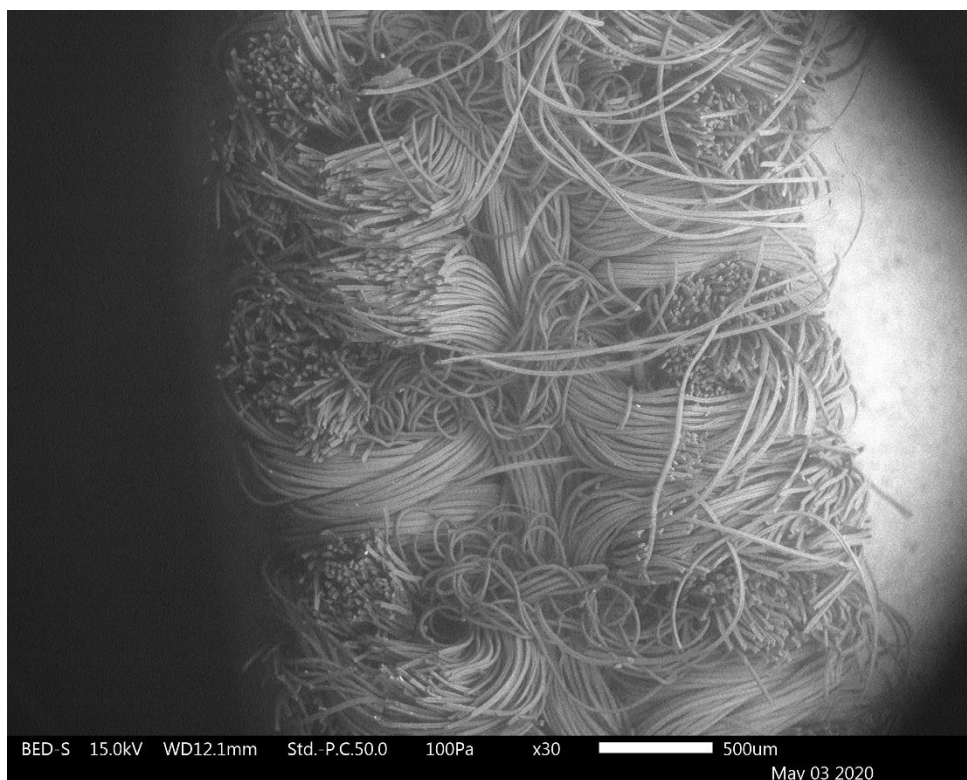


Figure 69. SEM figure of the transversal section of the sample (E) at 30X.

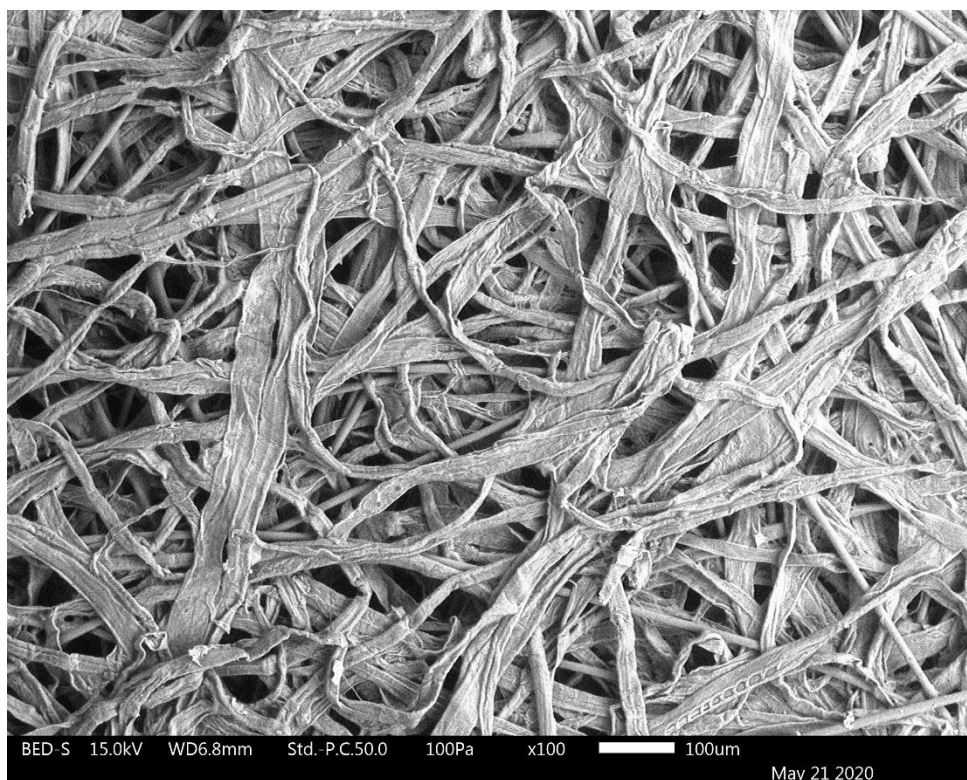


Figure 70. SEM figure of the sample (F) at 100X.

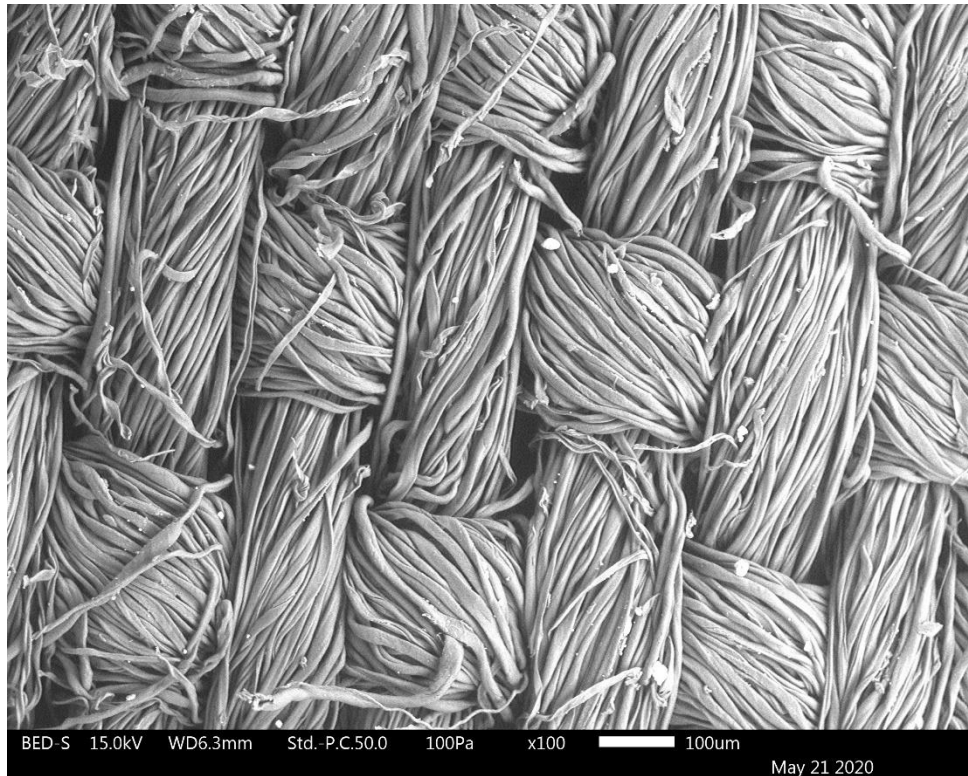


Figure 71. SEM figure of the first layer of sample (G) at 100X.

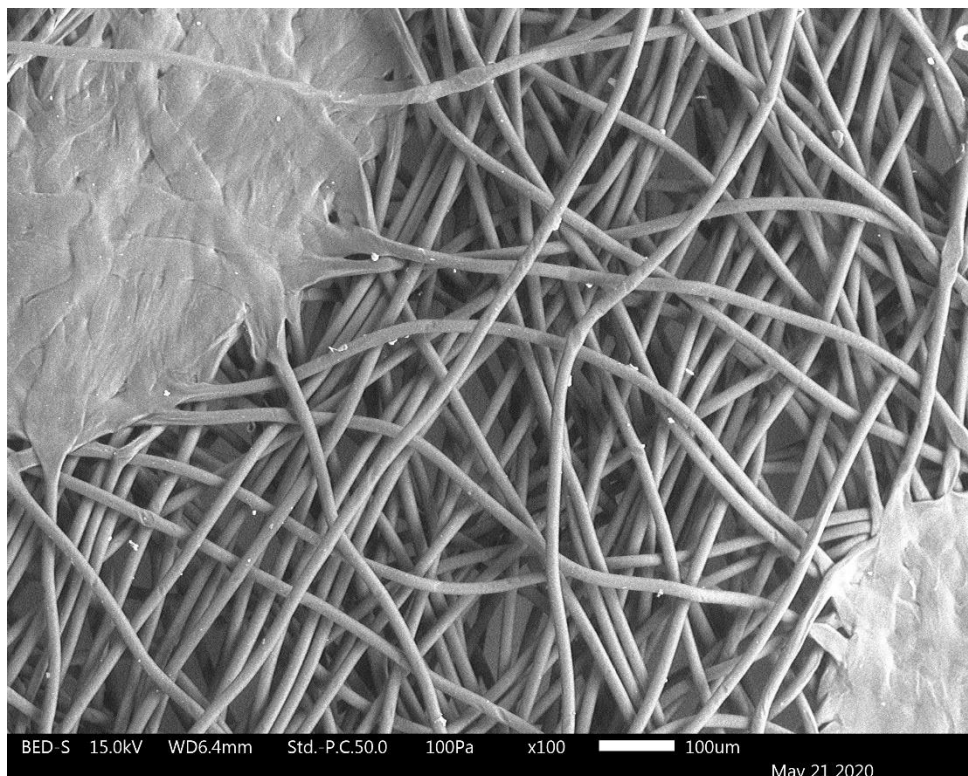


Figure 72. SEM figure of the second layer of the sample (G) at 100X.

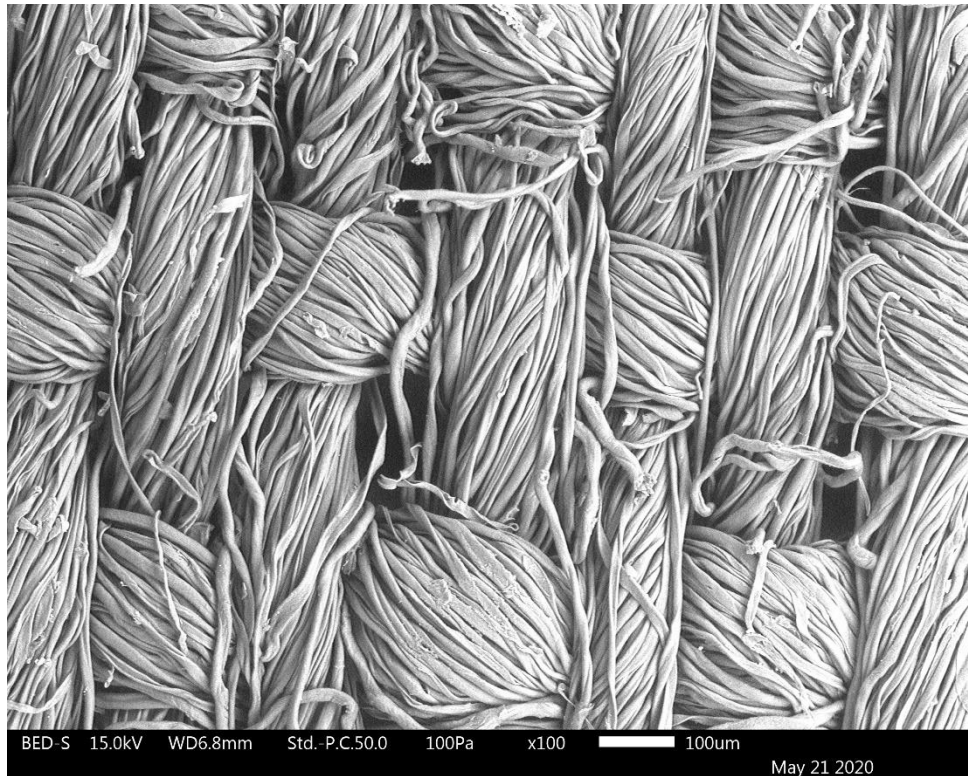


Figure 73. SEM figure of the third layer of the sample (G) at 100X.